

1-1-2014

Molecular Studies On The Anti-Tumor Effects Of Metal-Based Complexes: Involvement Of The Ubiquitin-Proteasome And Apoptotic Pathways

Sara M. Schmitt
Wayne State University,

Follow this and additional works at: http://digitalcommons.wayne.edu/oa_dissertations

 Part of the [Molecular Biology Commons](#), and the [Oncology Commons](#)

Recommended Citation

Schmitt, Sara M., "Molecular Studies On The Anti-Tumor Effects Of Metal-Based Complexes: Involvement Of The Ubiquitin-Proteasome And Apoptotic Pathways" (2014). *Wayne State University Dissertations*. Paper 915.

This Open Access Dissertation is brought to you for free and open access by DigitalCommons@WayneState. It has been accepted for inclusion in Wayne State University Dissertations by an authorized administrator of DigitalCommons@WayneState.

MOLECULAR STUDIES ON THE ANTI-TUMOR EFFECTS OF METAL-BASED COMPLEXES: INVOLVEMENT OF THE UBIQUITIN-PROTEASOME AND APOPTOTIC PATHWAYS

by

SARA M. SCHMITT

DISSERTATION

Submitted to the Graduate School

of Wayne State University,

Detroit, Michigan

in partial fulfillment of the requirements

for the degree of

DOCTOR OF PHILOSOPHY

2014

MAJOR: CANCER BIOLOGY

Approved by:

Advisor

Date

©COPYRIGHT BY

SARA M. SCHMITT

2014

All Rights Reserved

DEDICATION

For my family.

For my parents: Mom and Dad, thank you for your never-ending love and support. You have always inspired me to succeed and I would not be who or where I am today without you. I am lucky to have had parents that always let me try anything (within reason) at least once, and for letting me decide when I had taken on too much. Thank you for always being there to cheer me on or pick me up when I was down, even if it meant dropping everything else to be there. Thank you for always encouraging me and pushing me to succeed, especially in those times when I was ready to give up. Thank you for always believing in me and knowing that I could, and would, succeed if I put my mind to it. Words cannot express how grateful I am for all of the sacrifices you have made for me throughout my life.

To my sisters: Christa and Libbie, thank you for remaining the unique women that you are and for reminding me to have a little fun sometimes. Thank you for always cheering me on and for the little notes of encouragement when you couldn't be there in person. Finally, thank you for forcing me to be a better version of myself so that you had someone to look up to and be proud of.

For my husband: Curtis, you have been with me throughout this whole process and I never would have gotten through this without your love and support. I am so grateful for your patience and encouragement through all of my ups and downs. Thank you for always letting me follow my path and for pushing me to try new things. Your generally stress-free attitude towards life has grounded me and for that I am extremely grateful. Thank you for being you and for allowing me to be me.

ACKNOWLEDGEMENTS

This dissertation would not have been possible without the mentorship of Dr. Q. Ping Dou, who accepted me into his lab and gave me the guidance necessary to complete such a work. Thank you for giving me the many opportunities to participate in such a variety of projects as well as for trusting me to independently write research articles, reviews, editorials and book chapters. I know that these opportunities, as well as the collaborations that I have participated in, have expanded my skills and will be useful in the future.

Thank you to my committee members, Dr. Julie Boerner, Dr. Sreenivasa Chinni, Dr. Arun Rishi and Dr. Jeremy Kodanko, for all of your guidance in all matters of my graduate studies. Your questions and advice have been invaluable throughout this process. Thank you also to the Graduate Program in Cancer Biology, especially individually Dr. Larry Matherly, Dr. George Brush and Dr. Malathy Shekhar, for everything you've done for me. I know that my time in this program will afford me success in the future.

Thank you to Dajena Tomco and Dr. Claudio Verani, as well as Dr. Jai Prakash and Dr. Jeremy Kodanko, from the Department of Chemistry at Wayne State University and Dr. Chiara Nardon and Dr. Delores Fregona from the University of Padova for synthesizing the many compounds for me to work with. Our collaborations have been extremely productive and I am glad that I was given the opportunity to work with all of you. Thank you to Dr. Christine Neslund-Dudas and Dr. Bharati Mitra for formulating the ALAD project and for allowing me to contribute to the early discussions and final product.

I would be remiss if I did not thank all of the members of the Dou lab, both past and present. Special thanks to Dr. Min Shen and Dr. Daniela (Buac) Ventro for always discussing data and

offering suggestions, as well as to Dr. Di Chen and Cindy Cui for training and helping me with experiments when needed. Thank you also to Jian Zuo for your collaboration on the XIAP project.

Finally, thank you to the friends I've made here, without whom this experience would have lacked any sanity. Elizabeth Tovar, thank you for always being there for me no matter what, I am so lucky and grateful to have a wonderful friend like you. Thank you again to Daniela, for being not only a great colleague, but also a friend; your advice was always appreciated.

TABLE OF CONTENTS

Dedication _____	ii
Acknowledgements _____	iii
List of Tables _____	vii
List of Figures _____	viii
Chapter 1. Introduction _____	1
Ubiquitin-Proteasome Pathway _____	1
Apoptosis _____	8
Proteasome Inhibitors _____	10
δ -Aminolevulinic Acid Dehydratase _____	24
Metals in Cancer Development _____	28
Metal-based Complexes as Proteasome Inhibitors _____	29
Proteasome Inhibition via Metal Chelation _____	35
Chapter 2. Materials and Methods _____	39
Chapter 3. The Heme Synthesis Enzyme δ -Aminolevulinic Acid Dehydratase (ALAD) as an Endogenous Inhibitor of the Proteasome: Involvement of ALAD-20S Proteasome Complexes in Ubiquitination and Acetylation of Proteasomal α 2 Subunits _____	48
Results _____	49
Discussion _____	61
Chapter 4. Metal Complexes Targeting the Proteasomal Core _____	65
4.1 Effects of Tethered Ligands and of Metal Oxidation State on the Interactions of Cobalt Complexes with the 26S Proteasome	
Results _____	76
Discussion _____	84

4.2 Gold(III)-Dithiocarbamate Peptidomimetics in the Forefront of the Targeted Anticancer Therapy: Preclinical Studies against Human Breast Neoplasia	
Results _____	85
Discussion _____	101
4.3 Inhibition of the 26S Proteasome as a Possible Mechanism for Toxicity of Heavy Metal Species	
Results _____	103
Discussion _____	111
4.4 Differential Effects of Ga(III)- and Zn(II)-Tethered Ligands on Proteasome Activity and Apoptosis in Cultured Prostate Cancer Cells	
Results _____	113
Discussion _____	121
4.5 Nitroxoline Inhibits the Tumor Proteasome and Suppresses Tumor Growth	
Results _____	122
Discussion _____	132
Chapter 5. Metal Chelators Destabilize the E3 Ligase X-linked Inhibitor of Apoptosis (XIAP): Novel Polypyridyl Chelators Deplete Cellular Zinc and Destabilize the X-linked Inhibitor of Apoptosis Protein (XIAP) Prior to Induction of Apoptosis in Human Prostate and Breast Cancer Cells _____	133
Results _____	134
Discussion _____	147
References _____	150
Abstract _____	189
Publications _____	191
Autobiographical Statement _____	194

LIST OF TABLES

Table 1. Structures of Compounds Targeting Upstream Factors. _____	23
Table 2. AuD6 and 8 inhibit proteasome activity under cell-free conditions. _____	90

LIST OF FIGURES

Figure 1. Structure of the 26S Proteasome. _____	4
Figure 2. Ubiquitin-Proteasome Pathway. _____	7
Figure 3. The UPP and Apoptosis. _____	9
Figure 4. Structures of Peptide Aldehyde Proteasome Inhibitors. _____	11
Figure 5. Structures of Naturally Occurring Proteasome Inhibitors. _____	13
Figure 6. Structure of Bortezomib. _____	15
Figure 7. Structures of Next-Generation Proteasome Inhibitors. _____	20
Figure 8. Heme Biosynthesis and ALAD Structure. _____	26
Figure 9. Structures of Gallium Complexes. _____	32
Figure 10. Structures of Gold Complexes. _____	34
Figure 11. Structures of Metal Chelators Used as Proteasome Inhibitors. _____	38
Figure 12. ALAD binds the 20S proteasome in place of the 19S regulatory cap and is associated with ubiquitinated forms of $\alpha 2$ in cultured prostate cancer cells. _____	51
Figure 13. ALAD binds the 20S proteasome and is associated with ubiquitinated forms of $\alpha 2$ in human erythrocytes. _____	52
Figure 14. ALAD is both an inhibitor and a target of the proteasome. _____	54
Figure 15. SAHA treatment enhances the ALAD-proteasome interaction, associated with acetylation of ubiquitinated $\alpha 2$ subunits. _____	56
Figure 16. SAHA-treatment promotes nuclear localization of ALAD and modified $\alpha 2$. _____	58
Figure 17. Purified ALAD promotes ubiquitination of proteasomal $\alpha 2$ under cell free conditions. _____	60
Figure 18. Proposed Mechanism of ALAD-Proteasome Binding. _____	64
Figure 19. Structures of Cobalt Compounds. _____	67
Figure 20. Structures of New Gold(III) Complexes. _____	69

Figure 21. Structures of Heavy Metal Complexes. _____	71
Figure 22. Structures of Tethered Ga(III) and Zn(II) Complexes. _____	73
Figure 23. Structures of Nitroxoline and Clioquinol. _____	75
Figure 24. Complex 3, the Co(III) species, inhibits PC-3 cell proliferation. _____	77
Figure 25. Complex 3 inhibits purified 20S proteasome activity. _____	79
Figure 26. Complex 3 inhibits cellular proteasome activity. _____	81
Figure 27. Complex 3 induces apoptosis in PC-3 cells. _____	83
Figure 28. AuD6 and AuD8 are potent inhibitors of cellular proliferation. _____	86
Figure 29. Trolox enhances the anti-proliferative ability of AuD6. _____	88
Figure 30. AuD6 and 8 inhibit intact cellular proteasome in MDA-MB-231 cells. _____	92
Figure 31. AuD6 and 8 inhibit intact cellular proteasome and induce apoptosis in MDA-MB-231 cells. _____	94
Figure 32. AuD6 and 8 induce apoptosis in MDA-MB-231 cells. _____	96
Figure 33. AuD8 inhibits the proteasome and tumor growth <i>in vivo</i> . _____	98
Figure 34. AuD8 inhibits the proteasome and induces apoptosis <i>in vivo</i> . _____	100
Figure 35. Heavy metal complexes suppress cell proliferation in CRL2221 cells. _____	104
Figure 36. Heavy metal complexes inhibit purified proteasome activity. _____	106
Figure 37. Heavy metal complexes inhibit cellular proteasome activity. _____	108
Figure 38. Heavy metal complexes inhibit proteasome activity in cell extracts. _____	110
Figure 39. Tethered Ga(III) inhibits purified proteasome activity. _____	114
Figure 40. Tethered Ga(III) inhibits cellular proteasome activity and cell proliferation. _____	116
Figure 41. Tethered Ga(III) inhibits cellular proteasome activity and induces apoptosis. _____	118
Figure 42. Tethered Ga(III) and Zn(II) complexes have no effect on proteasome activity in CRL2221 cells. _____	120

Figure 43. Nitroxoline complexes with copper and inhibits purified 20S proteasome. _____	123
Figure 44. 5NHQ-Cu inhibits proteasome activity and induces apoptosis in human leukemia cells. _____	125
Figure 45. 5NHQ-Cu suppresses cell proliferation and proteasome activity and induces apoptosis in prostate cancer cells. _____	127
Figure 46. 5NHQ-Cu inhibits cell proliferation and proteasome activity and causes apoptosis in breast cancer cells. _____	129
Figure 47. 5NHQ suppresses tumor growth <i>in vivo</i> . _____	131
Figure 48. Structures and Zn-binding affinities (Zn^{II} K_d) of tested chelators. _____	135
Figure 49. Polypyridyl chelators inhibit cell proliferation and induce apoptosis in prostate cancer cells associated with XIAP depletion and dependent on Zn-binding. _____	138
Figure 50. Polypyridyl chelators inhibit cell proliferation and induce apoptosis in breast cancer cells associated with XIAP depletion and dependent on Zn-binding. _____	140
Figure 51. Addition of Zn and Fe has differential effects on BnTPEN- and N4Py-induced cell viability inhibition and apoptosis. _____	142
Figure 52. Effects of N4Py and BnTPEN in PC-3 cells are reversed by pre-treatment with Zn. _____	144
Figure 53. Effects of N4Py are reversible by treatment with NAC. _____	146
Figure 54. Proposed mechanism by which Zn-chelators BnTPEN and N4Py induce cellular death. _____	148

CHAPTER 1

INTRODUCTION

Cancer is described as a disease of uncontrolled proliferation, which can be caused by a number of internal or external factors. The acquisition of tumors has been attributed to ten “hallmarks of cancer” (Hanahan and Weinberg 2000, 2011), characteristics common to cells which have progressed to a malignant state. These hallmarks include self-sufficiency in growth signals, insensitivity to anti-growth signals, evasion of apoptosis, limitless replicative potential, sustained angiogenesis, tissue invasion and metastasis (Hanahan and Weinberg 2000), deregulated metabolism, evasion of immune signals, DNA instability and inflammation (Hanahan and Weinberg 2011). These traits have served as the backdrop for the design of new cancer treatments, with the goal of targeting multiple characteristics to increase toxicity.

The American Cancer Society estimates that approximately 1,666,000 new cases of cancer will be diagnosed in 2014, with an estimated 586,000 deaths. Between 2006 and 2010, cancer death rates decreased on average 1.6% per year, a trend that has existed for nearly twenty years. The almost 20% decline in cancer-related deaths may be attributed to a variety of factors, including earlier diagnosis and better treatment options (Siegel 2014). However, there remains no cure and treatment options are still extremely limited, oftentimes progressing to resistance. Therefore, the search for novel therapeutic targets with decreased toxicities continues. One target that has been proposed, and proven viable, is the ubiquitin-proteasome pathway.

Ubiquitin-Proteasome Pathway

The ubiquitin-proteasome pathway (UPP) is the major mechanism for protein processing within cells, responsible for the selective proteolytic degradation of about 90% of cellular proteins (Ciechanover, et al. 1978; Hershko, et al. 1980). Proteins degraded by the UPP play roles in a variety

of biological processes including development, differentiation, proliferation, signal transduction and apoptosis (Nalepa, et al. 2006). While its major role is regulation of protein turnover, the proteasome also functions in several non-proteolytic processes, such as transcription-coupled nucleotide excision repair (Krogan, et al. 2004), transcription initiation and elongation (Baker and Grant 2005), and regulation of gene expression (Collins and Tansey 2006). These processes are so critical to normal cellular homeostasis that the 2004 Nobel Prize in Chemistry was awarded to the discoverers of the UPP.

UPP-mediated protein degradation is carried out via two critical steps: 1) conjugation of multiple ubiquitin molecules to the protein substrate, and 2) degradation of the ubiquitin-tagged substrate by the 26S proteasome (Ciechanover 1998). The 26S proteasome is a large (2.5 MDa), multi-subunit complex, comprised of a catalytic 20S core, and one or two 19S regulatory caps (Figure 1) (Adams 2004b; Peters, et al. 1993), that is localized both in the cytosol and nucleus of cells (Hirsch and Ploegh 2000; Rivett 1998; Wojcik and DeMartino 2003). The 20S core was initially referred to as the conjugate-degrading factor-3 (CF-3), and the 19S regulatory cap as CF-1 and inhibitory CF-2 (Ganoth, et al. 1988). The 20S core consists of 28 subunits that form a barrel-like structure of four alternately stacked rings: two α rings surrounding two β rings, containing seven subunits each (Figure 1) (Baumeister, et al. 1998; Groll, et al. 1997; Groll, et al. 1999). The α subunits block direct access to the catalytic sites by allowing access only to unfolded proteins, while the role of the β subunits is to carry out the proteolytic activities of the proteasome, which are dependent on an amino-terminal nucleophilic Thr1 residue (Groll et al. 1999). There are three active β subunits: β 1, β 2 and β 5, responsible for caspase or peptidyl-glutamyl peptide-hydrolyzing (PGPH)-like, trypsin-like and chymotrypsin (CT)-like activities, respectively (Figure 1) (DeMartino and Slaughter 1999; Goldberg, et al. 2002; Groll et al. 1999). The 19S regulatory

cap(s) (700 kDa) can be divided into base and lid components: with the base responsible for recognition and unfolding of ubiquitinated protein substrates, as well as opening of the 20S core and transport of substrates into the core, and the lid deubiquitinating substrates prior to degradation. The base is comprised of six ATPase subunits, Rpt1-6, which form a hexameric ring (da Fonseca and Morris 2008; Hartmann-Petersen, et al. 2001; Nickell, et al. 2009), as well as two non-ATPase subunits Rpn-1 and -2 (Fu, et al. 1999; Rubin, et al. 1998) and the lid consists of at least six non-ATPases, including Rpn-10/S5a and Rpn-13/Adrm1, which contain ubiquitin interacting motifs (UIMs) (Finley 2009). Rpn-10/S5a has two UIMs that bind preferentially to poly-ubiquitinated substrates (Deveraux, et al. 1994) and Rpn-13/Adrm1 binds to the non-ATPase Rpn-2, promoting recruitment of deubiquitinating enzymes (DUBs) to the proteasome (Hamazaki, et al. 2006; Qiu, et al. 2006; Yao, et al. 2006). Like the rest of the pathway, deubiquitination is highly regulated and very important for recycling of ubiquitin molecules and controlling the rate of degradation (Yao et al. 2006).

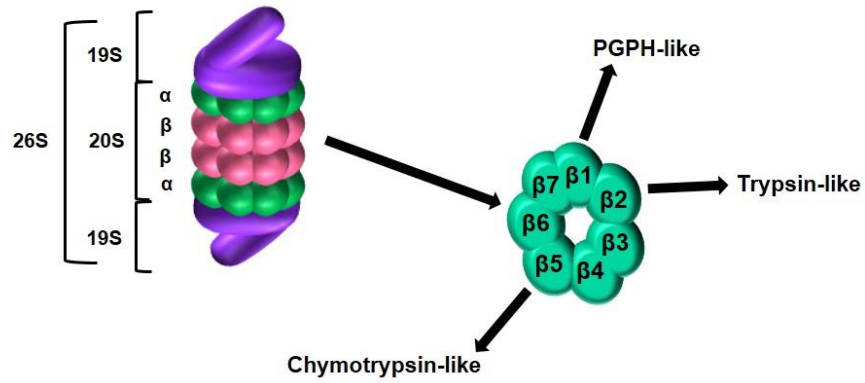


Figure 1. Structure of the 26S Proteasome. The 26S proteasome is made up of the 20S catalytic core and one or two 19S regulatory caps. The 20S core contains two β rings surrounded by two α rings. The catalytic activity is carried out by three β subunits: 1 (PGPH-like), 2 (trypsin-like) and 5 (CT-like).

The ubiquitination step of the UPP is executed by three distinct types of enzymes, E1, E2s and E3s (Figure 2). The pathway is initiated by ATP-dependent E1-mediated activation of ubiquitin, a small 76 amino acid protein that is expressed ubiquitously throughout cells and serves as a tag for protein substrates destined for UPP-mediated degradation as well as various other fates, including membrane-trafficking, protein kinase activation, DNA repair and chromatin remodeling (Chen and Sun 2009). Activated ubiquitin is then transferred from E1 to one of several ubiquitin-conjugating E2 enzymes, and then to an E3 ubiquitin-ligating enzyme, which aid in the transfer of active ubiquitin to lysine residues within the target protein (Figure 2) (Adams 2003; Ciechanover, et al. 2000). Following the conjugation of a sufficiently sized ubiquitin chain, usually four, except in the case of proteins like mODC and HIF-1 α , which require no ubiquitination for proteasome-mediated degradation (Hoyt and Coffino 2004; Hoyt, et al. 2003; Jariel-Encontre, et al. 2008), the ubiquitinated protein substrate is then recognized, deubiquitinated and translocated to the 26S proteasome by components of the 19S regulatory cap (Coux, et al. 1996; Nandi, et al. 2006). Finally, the substrate is degraded into short peptide fragments and the ubiquitin is recycled (Figure 2) (Ciechanover 2006). This process is tightly regulated and critical to the regulation of a number of cellular processes, including those involved in tumorigenesis (Adams 2004a), making it a promising target for anti-cancer agents.

The essential role of unbalanced protein homeostasis in development, growth and survival of various cancers (Smith, et al. 2007), has led to intensive investigation into the targeting of factors involved in the synthesis and degradation of proteins, including the UPP, as a potential anticancer strategy (Dou and Li 1999). Increased proteasome activity has been reported in several types of human cancer, including colon (Loda, et al. 1997), prostate (Li and Dou 2000) and leukemia (Kumatori, et al. 1990), suggesting that malignant cells are more dependent on the UPP

than non-malignant cells and indicating that targeting the UPP is a viable strategy in the treatment of cancer. Indeed, inhibition of the $\beta 5$ subunit (chymotrypsin-like activity) by as little as 25% has been shown to be associated with cell cycle arrest and apoptosis induction (An, et al. 1998; LeBlanc, et al. 2002; Lopes, et al. 1997). Thus, proteasome inhibition may selectively induce apoptosis in cancer cells with minimal effects on healthy cells, but may also effectively sensitize resistant cancer cells to chemo- and/or radiotherapeutics (Orlowski and Kuhn 2008). Furthermore, the clinical use of proteasome inhibitors was validated by the USFDA approval of bortezomib for the treatment of relapsed/refractory multiple myeloma and mantle cell lymphoma (Kane, et al. 2003).

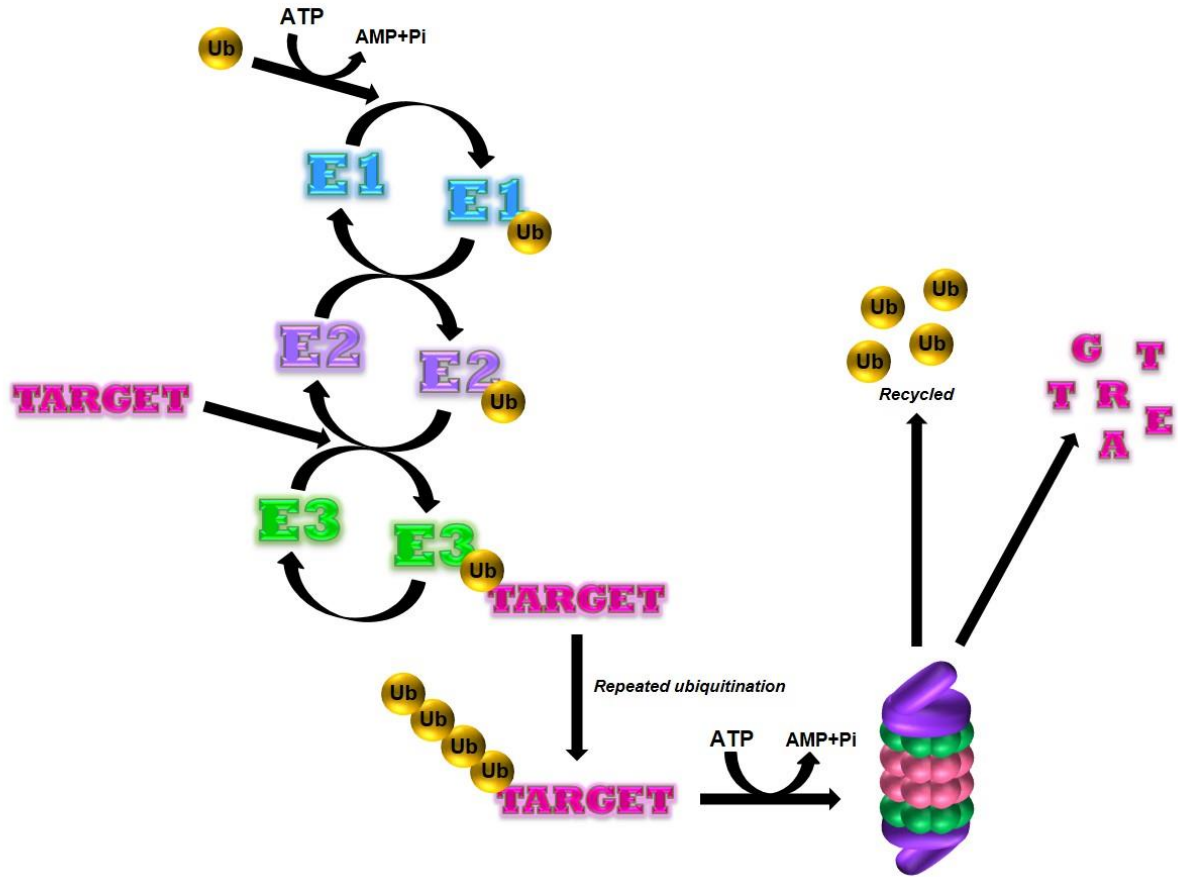


Figure 2. Ubiquitin-Proteasome Pathway. Ubiquitin is first activated by an E1 ubiquitin-activating enzyme, is transferred to an E2 ubiquitin-conjugating enzyme, followed by transfer from the E2- to the E3 ubiquitin ligase-bound substrate. Finally, the poly-ubiquitinated protein target is directed to the 26S proteasome where components of the 19S regulatory cap deubiquitinate and unfold the target before it is ultimately degraded. Ub = ubiquitin.

Apoptosis

One major pathway that is an established target of the UPP is the apoptosis cascade. There are several checkpoints for which ubiquitination-dependent degradation is responsible, including degradation of transcription factors and enzymes necessary for cell proliferation, such as NF- κ B and ODC (Grassilli, et al. 1998; He, et al. 1998; Ivanov and Nikolic-Zugic 1998), cell cycle regulators like p27 (Gil-Gomez, et al. 1998) and pro- and anti-apoptotic proteins like caspases and IAPs (Figure 3) (Morizane, et al. 2005; Salvesen and Duckett 2002; Schile, et al. 2008; Vaux and Silke 2005; Wilson, et al. 2002; Yang, et al. 2000). The IAPs (inhibitor of apoptosis) are perhaps the most important of these apoptosis-related proteasome substrates. The IAP family of proteins, including c-IAP and XIAP, serve as endogenous inhibitors of apoptosis, whose major role is binding and inhibiting caspase proteins (Eckelman, et al. 2006). All members of the IAP family contain 1-3 BIR (baculoviral IAP repeat) domains, which are critical to their function (Liston, et al. 2003; Morizane et al. 2005; Vaux and Silke 2005). Importantly, many IAPs also contain RING finger domains, which, in addition to their E3 ligase activity, activate and recruit caspases through their CARD domains (Schimmer and Dalili 2005; Yang et al. 2000), ultimately leading to caspase degradation (Figure 3). Additionally, IAPs, in response to apoptotic stimuli, are auto-ubiquitinated and degraded by the proteasome (Figure 3) (Yang et al. 2000; Yang and Li 2000). Therefore, in addition to targeting the UPP, targeting inhibitory factors, like XIAP, within the apoptosis cascade, is also a promising strategy in the treatment of human cancers.

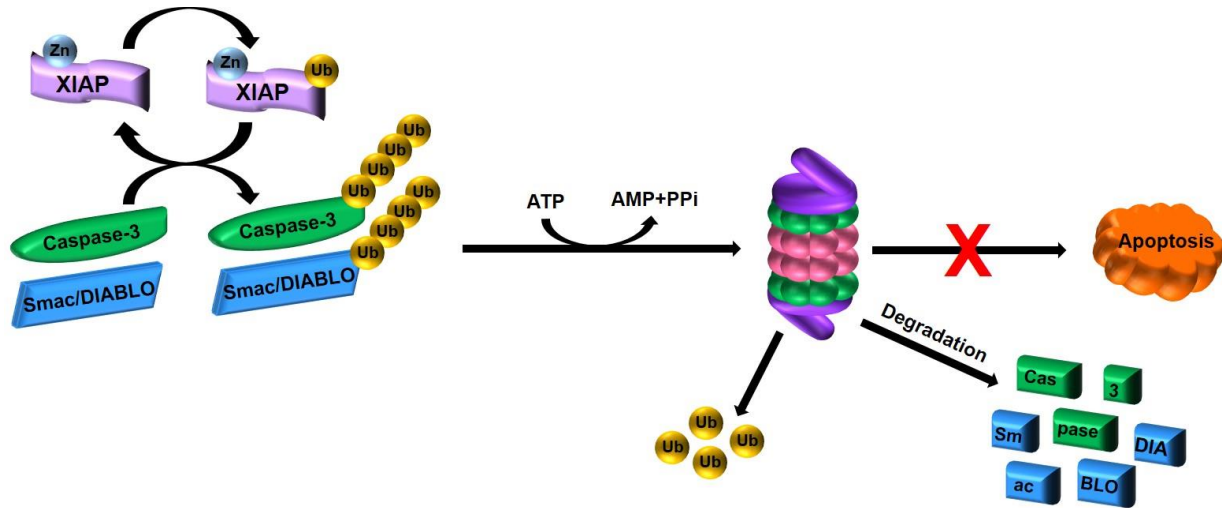


Figure 3. The UPP and Apoptosis. Many apoptotic proteins are degraded by the proteasome, including various caspases, as well as most IAPs, like XIAP. In this case, XIAP is an E3 ligase that ubiquitinates caspase-3 and Smac/DIABLO, as well as autoubiquitinating itself, eventually resulting in degradation of these pro-apoptotic proteins and inhibition of apoptosis. Ub = ubiquitin; Cas-3 = caspase-3.

Proteasome Inhibitors

Early Inhibitors

Leading up to the development and approval of bortezomib, several preclinical studies validated the UPP as a viable druggable target. Among the early proteasome inhibitors, peptide aldehydes, which are analogs of proteasome substrates that inhibit the CT-like activity of the proteasome and include MG-132 (Cbz-leu-leu-leucinal), MG-115 (Cbz-leu-leu-norvalinal) and ALLN (acetyl-leu-leu-norleucinal) (Figure 4) (Lee and Goldberg 1996; Rock, et al. 1994), are perhaps the most widely studied. X-ray diffraction revealed that ALLN forms a hemiacetyl complex with the N-terminal threonine hydroxyl groups of the catalytic β subunits (Groll et al. 1997; Lowe, et al. 1995), thus elucidating the active site for compounds in this class. PSI (Cbz-ile-glu(O-t-Bu)-ala-leucinal; Figure 4), another peptide inhibitor, has been shown to selectively inhibit proteasome-mediated proteolysis without affecting isopeptidase or ATPase activities (Figueiredo-Pereira, et al. 1994). These inhibitors are extremely potent (MG-132 K_i = low nanomolar in purified proteasome; IC_{50} = low micromolar in cultured cells), as well as reversible by their removal from the system (Lee and Goldberg 1996; Rock et al. 1994). Additionally, because peptide aldehydes also inhibit calpains and some lysosomal cysteine proteases, some degradative processes originally believed to be mediated by calpains are now attributed to the proteasome.

Another class of potent proteasome inhibitors is the vinyl sulfone peptides (Bogyo, et al. 1997), which exert their proteasome inhibitory activity through covalent binding to the hydroxyl groups of the active site threonine within the catalytic β subunits. Their use in human lymphoma cells has been shown to result in proteasome inhibition followed by the appearance of distinct cell variants expressing a compensatory proteolytic system, which has not yet been clearly identified (Glas, et al. 1998).

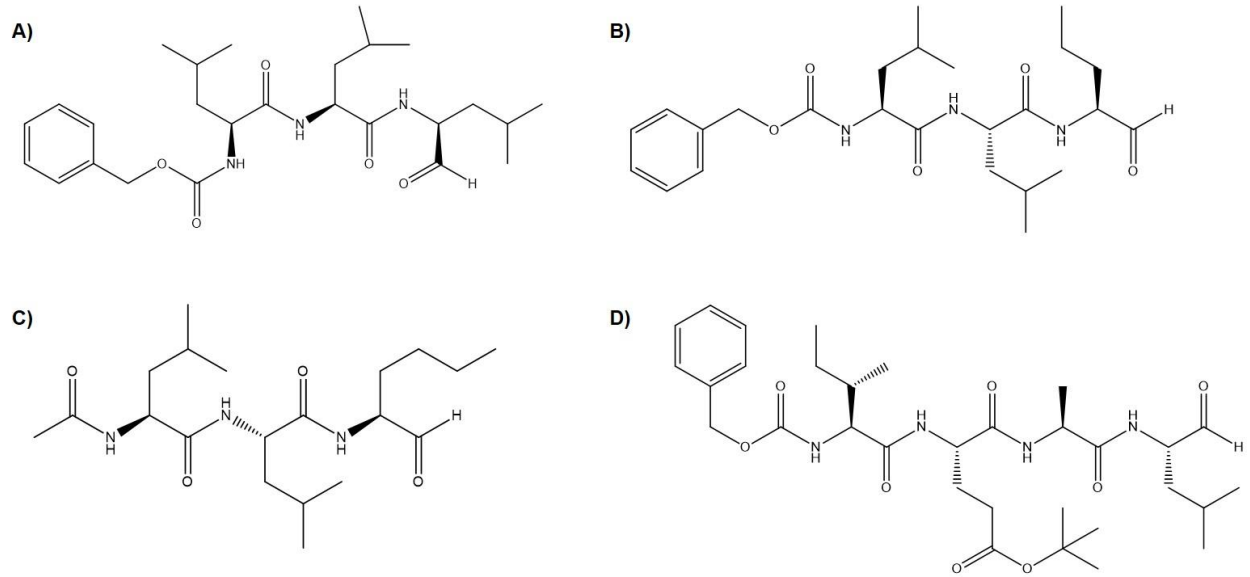


Figure 4. Structures of Peptide Aldehyde Proteasome Inhibitors. A) MG-132 B) MG-115 C) ALLN D) PSI

Several naturally occurring metabolites have also been investigated as inhibitors of the proteasome. One example is lactacystin and its derivative *clasto*-lactacystin β -lactone (Figure 5), the active form to which it is converted in aqueous solution (Dick, et al. 1996). Lactacystin was first isolated from actinomycetes because of the discovery that it could promote neurite outgrowth and block cell division in cultured neurons (Omura, et al. 1991). Importantly, these compounds differ structurally and are much more specific than the peptide aldehydes, with a mode of action similar to that of the vinyl sulfones (Craiu, et al. 1997; Fenteany, et al. 1995).

Other naturally occurring products that have been used as proteasome inhibitors in the preclinical setting include TMC-95A and argyrin A (Figure 5). TMC-95A is a cyclic triterpide, originally isolated from *Apiospora montagnei*, that specifically binds to all three catalytic β subunits via hydrogen bonds, causing inhibition in the low nanomolar range (Groll, et al. 2001; Koguchi, et al. 2000). Finally, argyrin A, a cyclic octapeptide derived from *Archangium gephyra*, has been shown to suppress tumor cell growth through inhibition of proteasomal degradation of the CDK inhibitor p27^{kip1} (Nickeleit, et al. 2008; Sasse, et al. 2002). The identification of these inhibitors led to the discovery and design of many other compounds specifically targeting the tumor proteasome, culminating in the 2003 USFDA approval of bortezomib for the treatment of relapsed and refractory multiple myeloma and mantle cell lymphoma (Kane et al. 2003).

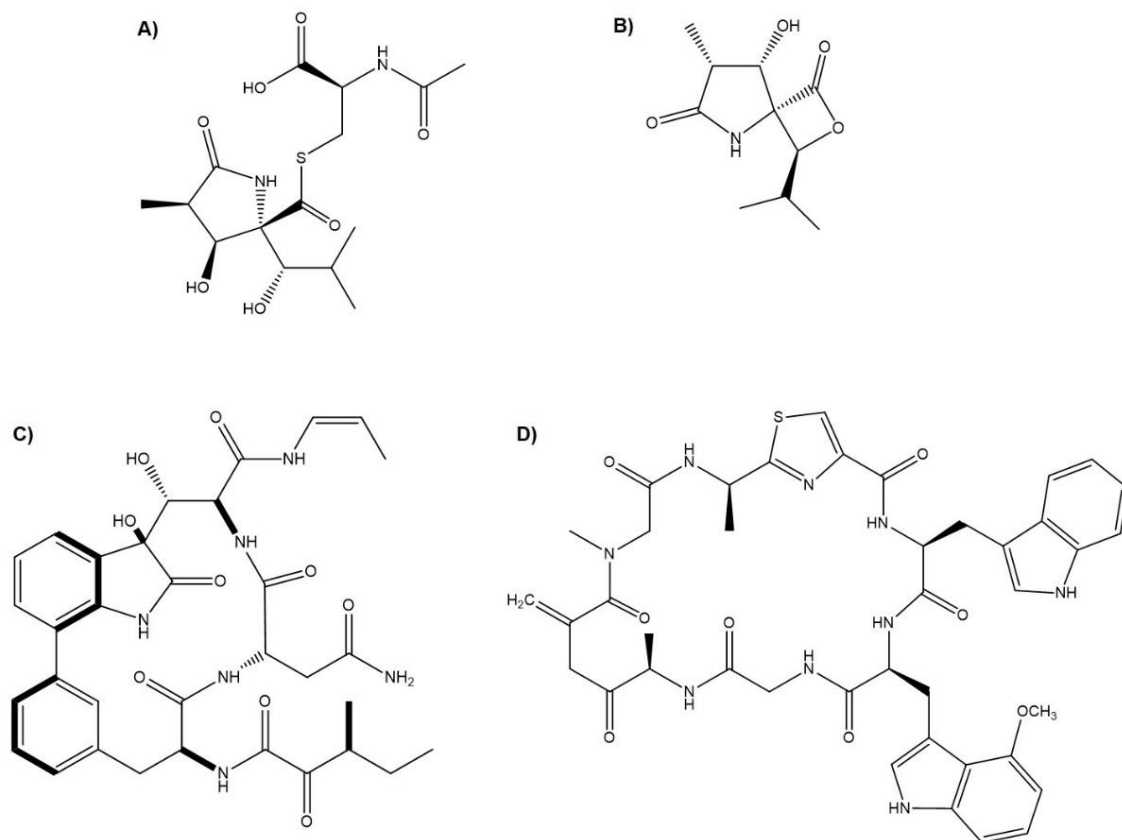


Figure 5. Structures of Naturally Occurring Proteasome Inhibitors. A) Lactacystin B) Clasto-lactacystin β lactone C) TMC-95 D) Argyrin A

Bortezomib as a Proof of Concept

Bortezomib (Velcade®; Figure 6), a dipeptide boronic acid derivative containing pyrazinoic acid, phenylalanine and leucine in its structure, was first synthesized in 1995 by Myogenics Company and after demonstrating potent apoptosis-inducing activity in a variety of tumor cell lines and animal models (Adams, et al. 1999; Frankel, et al. 2000; Hideshima, et al. 2001), it was approved by the USFDA for the treatment of relapsed or refractory multiple myeloma and mantle cell lymphoma (Kane et al. 2003). Bortezomib enters nearly all tissues except brain and adipose, and is metabolized through intracellular cytochrome p450-mediated oxidative deboronation (Kane et al. 2003). Furthermore, bortezomib distributes to the plasma within ten minutes of IV injection and has a half-life of more than 40 hours (Ryan, et al. 2006a; Ryan, et al. 2006b).

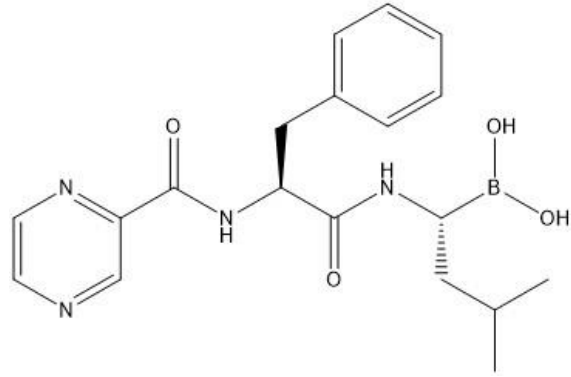


Figure 6. Structure of Bortezomib.

Bortezomib is a slowly reversible inhibitor of the 26S proteasome, with proteasome activity generally recovering within 72 hours of administration (Groll et al. 1999). Bortezomib-mediated cell death has been shown to occur via direct inhibition of the $\beta 5$ -subunit (Adams and Cory 1998; Crawford, et al. 2006; Gross, et al. 1999; Oda, et al. 2000). Several preclinical studies have demonstrated the activity of bortezomib against tumor cells *in vitro*. A standard NCI-60 screen revealed that bortezomib potently inhibited cellular growth and induced apoptosis in various malignant cell lines, including multiple myeloma, pancreatic and squamous cell carcinomas (Adams 2002; Adams et al. 1999; Shah, et al. 2001; Sunwoo, et al. 2001). Importantly, bortezomib toxicity was evident in both chemoresistant and chemosensitive myeloma cells and a sublethal dose of bortezomib significantly increased the sensitivity of resistant cells to chemotherapy with no effect on normal hematopoietic cells (Berenson, et al. 2001; Ma, et al. 2003). Additionally, an *in vitro* study of four ovarian and three prostate cancer cell lines indicated comparable effects of bortezomib on cells derived from solid tumors and hematological malignancies (Frankel et al. 2000). Finally, a series of animal studies showed that bortezomib could inhibit tumor growth and angiogenesis *in vivo* in multiple myeloma (LeBlanc et al. 2002) as well as various solid tumors, including prostate (Williams, et al. 2003), lung, breast (Teicher, et al. 1999), mesothelioma (Sartore-Bianchi, et al. 2007), and neuroblastoma (Michaelis, et al. 2006).

Multiple targets of bortezomib have been identified in malignant cells, most notably, the NF- κ B signaling pathway. NF- κ B is a p50/p65 heterodimer that is constitutively inactive in the cytoplasm due to its binding with the inhibitory protein, I κ B. Upon degradation of I κ B, NF- κ B is activated and translocated into the nucleus where it triggers transcription of cytokines (IL-6, TNF- α), survival factors (IAPs, Bcl-X_L) and insulin-like growth factor-I (IGF-I), resulting in proliferation, resistance to apoptosis and drug-resistance in cancer cells (Chauhan and Anderson

2003). Bortezomib acts to prevent degradation of I κ B, which blocks activation of NF- κ B and suppresses expression of related cytokines and survival factors (Feinman, et al. 1999; Ma et al. 2003). In contrast, a study of mice bearing human multiple myeloma cells showed that treatment with bortezomib was associated with NF- κ B activation, rather than inhibition (Hideshima, et al. 2009), suggesting that the NF- κ B pathway may play a biphasic role in bortezomib-mediated tumor cell death.

Still other mechanisms of bortezomib-mediated apoptosis include induction of the proapoptotic protein NOXA (Nikiforov, et al. 2007; Qin, et al. 2005); induction of extrinsic and intrinsic apoptotic pathways via activation of caspases-8 and -9 (Mitsiades, et al. 2002; Strauss, et al. 2007); inhibition of angiogenesis (Nawrocki, et al. 2002; Sunwoo et al. 2001); activation of the p38 mitogen-activated protein kinase (MAPK) pathway (Lioni, et al. 2008); disruption of the interaction between tumor cells and dendritic cells (Kukreja, et al. 2007); and induction of endoplasmic reticulum (ER) stress resulting in generation of reactive oxygen species (ROS) (Fribley and Wang 2006; Fribley, et al. 2004). Multiple targets generally play important roles in bortezomib-mediated apoptosis in some cancer cells, while others may be critical in other cells.

While bortezomib has proven successful in the treatment of some hematological malignancies, it is much less potent in solid tumors. This, coupled with the adverse effects, including peripheral neuropathy and cardiac toxicities, associated with bortezomib, has prompted the development of a new generation of proteasome inhibitors with a more favorable therapeutic profile and broader spectrum of activity. In addition to the next generation inhibitors with similar structures, inhibitors with different structures employing various metal centers, as well as some targeting factors outside the catalytic core, have been designed and investigated.

Next-Generation Proteasome Inhibitors

Following the success of, and because of resistance associated with bortezomib, several second generation proteasome inhibitors have been developed. Carfilzomib (Figure 7A), an irreversible inhibitor of the $\beta 5$ subunit, was approved by the FDA for the treatment of previously treated multiple myeloma in 2012. Because protein synthesis is necessary for recovery of proteasome activity (Radhakrishnan, et al. 2010), carfilzomib is a more potent inhibitor, with fewer off-target effects, than bortezomib. Additionally, carfilzomib has been shown to target the immunoproteasome-associated $\beta 5i$ subunit, which is preferentially expressed in multiple myeloma (Ruschak, et al. 2011).

Marizomib (NPI-0052; Figure 7B) is another irreversible inhibitor of the proteasome that has been shown to induce prolonged, rapid inhibition of all three catalytic 20S subunits. A phase I trial of marizomib reported responses in patients with bortezomib-refractory multiple myeloma; with no significant treatment-associated peripheral neuropathy, thrombocytopenia or myelosuppression reported. Marizomib also possesses interesting tissue distribution properties and pharmacokinetic and pharmacodynamic profiles, indicating a possible role in patients with different disease characteristics, such as extramedullary spread (Moreau, et al. 2012).

Two next-generation boronate-based reversible inhibitors, ixazomib (MLN-9708; Figure 7C) and delanzomib (CEP-18770; Figure 7D) have also been investigated in clinical trials. Ixazomib is the first oral proteasome inhibitor, which not only makes the treatment more convenient for patients, but also produces fewer and milder adverse effects. Single-agent ixazomib has been shown to be effective and well-tolerated in a phase I trial of heavily pretreated relapsed/refractory multiple myeloma patients (Moreau et al. 2012). Delanzomib activity is comparable to that of bortezomib in both hematologic and solid tumor cell lines, as well as in

primary patient-derived multiple myeloma cells (Molineaux 2012). Finally, the irreversible epoxyketone-based inhibitor oprozomib (ONX-0912; Figure 7E) has been shown in preclinical human xenograft and mouse syngeneic studies to have oral activity equivalent to that of intravenous carfilzomib (Chauhan, et al. 2010). Promisingly, oral oprozomib is currently under investigation in early clinical trials.

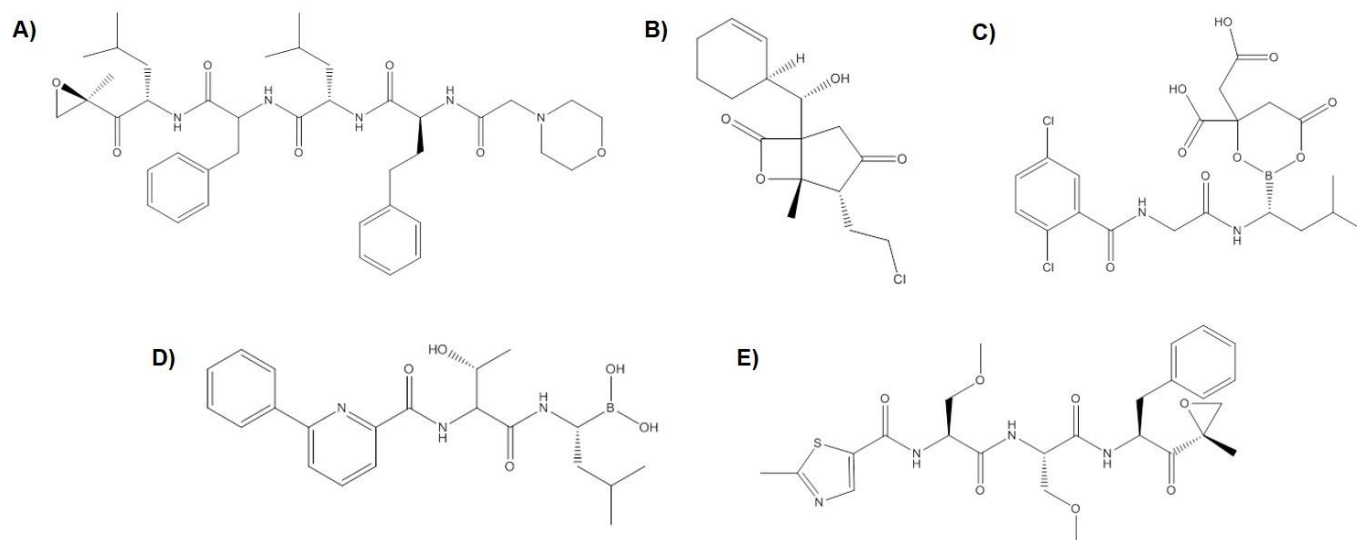


Figure 7. Structures of Next-Generation Proteasome Inhibitors. A) Carfilzomib B) Marizomib; NPI-0052 C) Ixazomib; MLN-9708 D) Delanzomib; CEP-18770 E) Oprozomib; ONX-0912

Targeting Sites Outside the Catalytic Core

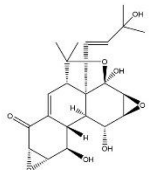
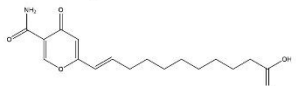
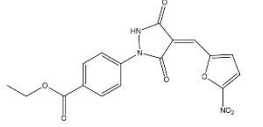
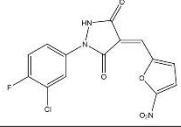
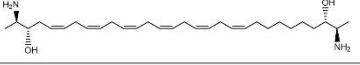
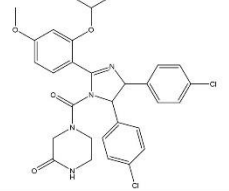
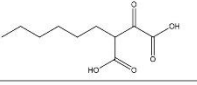
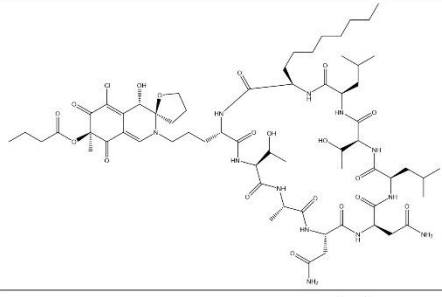
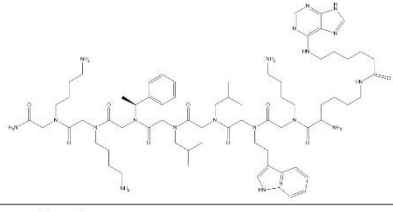
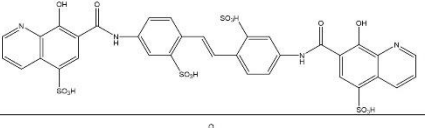
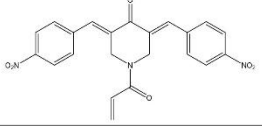
E1, E2s, and E3s: Inhibiting the ubiquitin E1 enzyme was initially disregarded due to a lack of specificity and related potential toxicity. However, the identification of two natural E1 inhibitors, panepophenanthrin and himeic acid (Table 1), has indicated that this may indeed be a viable strategy. Both inhibitors specifically target the formation of E1-ubiquitin thioester intermediates (Sekizawa, et al. 2002; Tsukamoto, et al. 2005). In addition, a synthetic pyrazone derivative, PYR-41 (Table 1), has also been developed and shown to inhibit E1 activity, preventing protein degradation and cytokine-mediated activation of NF- κ B (Yang, et al. 2007). Another compound, PYZD-4409 (Table 1) caused cell death in cultured tumor cells as well as in a leukemia mouse model, potentially by a mechanism similar to ER stress induced by classical proteasome inhibitors (Xu, et al. 2010). Additionally, inhibition of the E2 enzymes has also been explored, especially following the finding that functional knockdown of the E2 Ubc13 results in increased p53 activity (Laine, et al. 2006). Indeed, a natural compound, leucettamol A (Table 1), has been shown to inhibit the interaction between the E2 Ubc13 and the inactive conjugating enzyme variant Uev1A, which is required for efficient poly-ubiquitin chain formation (Tsukamoto, et al. 2008).

Perhaps one of the most widely researched strategies for targeting factors upstream of the proteasomal catalytic core is inhibition of E3 ubiquitin ligases, likely due to their important role in identifying target proteins for ubiquitination. The p53-specific RING-type E3 MDM2/HDM2, for example, is a popular target for inhibition, due to its tendency toward overexpression in human cancers (Vassilev 2007). Indeed, nutlin-3 (Table 1), a MDM2 small molecule inhibitor, has been shown to suppress tumor growth in mouse xenograft models (Vassilev, et al. 2004), indicating that MDM2 is a promising target. Additionally, nutlin-3 in combination with bortezomib resulted in additive and synergistic cytotoxic effects in bortezomib-sensitive multiple myeloma and epithelial carcinoma cells, respectively (Ooi, et al. 2009). Some natural products, including chlorofusin and

(-)-hexylitaconic acid (Table 1), have also been identified as inhibitors of MDM2-p53 binding (Clark, et al. 2008; Duncan, et al. 2001; Nakahashi, et al. 2009; Tsukamoto, et al. 2006). Therefore, inhibition of upstream factors of the UPP may be a viable strategy in the treatment of human cancers, a strategy that is further explored in this dissertation (Chapter 5).

19S Regulatory Subunit: Inhibition of proteasomal regulators may also be an effective strategy, as inhibition of these factors should hinder only certain proteasomal functions. In fact, screening of a purine analog-capped peptoid library identified RIP-1 (Regulatory Particle Inhibitor Peptoid-1; Table 1) as an inhibitor of protein unfolding via the ATPase Rpt4 (Lim, et al. 2007a; Lim, et al. 2007b). Other studies have also indicated that ubistatin A (Table 1) is able to suppress proteasome-mediated proteolysis by blocking the recruitment of ubiquitinated proteins to the 26S proteasome by binding with ubiquitin chains (Verma, et al. 2004), indicating that ubiquitin-chain receptors may also be worthwhile drug targets. Furthermore, inhibition of deubiquitinase activity of the 19S regulatory particle could be another useful strategy. Indeed, a small molecular weight compound, b-AP15 (Table 1), has demonstrated anticancer activity through inhibition of specific deubiquitinases, like USP14 and UCHL5, but not POH1, in solid tumor models (D'Arcy and Linder 2012). Thus, it is evident that factors regulating the 20S catalytic core are promising drug targets that should be further explored.

Table 1. Structures of Compounds Targeting Upstream Factors.

Name	Structure	Target
Panepophenanthrin		E1
Himeic Acid		E1
PYR-41		E1
PYZD-4409		E1
Leucettamol A		E2 (Ubc13)
Nutlin-3		E3 (MDM2)
(-)-Hexylitaconic Acid		E3 (MDM2)
Chlorofusin		E3 (MDM2)
RIP-1		Protein Unfolding (ATPase Rpt4)
Ubistatin A		Substrate Recruitment
b-AP15		Deubiquitinases (USP14; UCHL5)

δ -Aminolevulinic Acid Dehydratase

Shortly after the discovery of the UPP, several reports suggested the presence of a potential endogenous inhibitor of the proteasome (Li, et al. 1991; Speiser and Etlinger 1983), which was later identified as δ -aminolevulinic acid dehydratase (ALAD) (Guo, et al. 1994). The gene for ALAD is found on chromosome 9q32, and encodes a 330 amino acid protein (Figure 8B), of which three isoforms (ALAD 1-1, 1-2 and 2-2) have been reported.

ALAD is a critical component of the heme biosynthetic pathway, responsible for catalyzing the second step, condensation of two δ -aminolevulinic acid (ALA) molecules into porphobilinogen (PBG; Figure 8A). ALAD is a cytosolic protein that functions as an octomer consisting of eight identical subunits, with dimerization occurring in a “hugging” conformation where the α/β barrel of each monomer is bound by the N-terminal branch of the adjacent monomer (Figure 8C) (Breinig, et al. 2003). Each ALAD monomer is bound by two or three zinc molecules, which are necessary for the activity of the enzyme. Additionally, many studies have shown that lead binding is inhibitory, and therefore, it is not surprising that the gene polymorphism is now known to cause defects in lead uptake and binding within the blood and tissue (Hernberg, et al. 1970; Jaffe, et al. 2001; Kelada, et al. 2001; Thompson, et al. 1977; Tsukamoto, et al. 1979). In fact, measurement of ALAD activity is the current standard test for determining lead poisoning in the clinic (Berlin and Schaller 1974; Hernberg et al. 1970). Although rare, ALAD deficiency is well-defined as a cause of acute porphyria (Jaffe and Stith 2007); its role in cancer, however, has not been fully characterized. In fact, very few studies have demonstrated a clear link between ALAD expression of activity and any form of human malignancy, with the majority correlating the two based solely on the role of lead poisoning in cancer (Grover, et al. 2010; Rajaraman, et al. 2005; Rajaraman, et al. 2006; Shaik, et al. 2009; van Bommel, et al. 2011). Interestingly, according to The Human

Protein Atlas, ALAD mRNA and protein levels are moderate to low in normal prostate tissue, and very low in prostate cancer tissues (Uhlen, et al. 2010), while the canSAR database provides evidence of differential expression in various cancers, including prostate, with the highest mRNA levels reported in HCT116 colon cancer and OVCAR.8 ovarian cancer cells (Halling-Brown, et al. 2012).

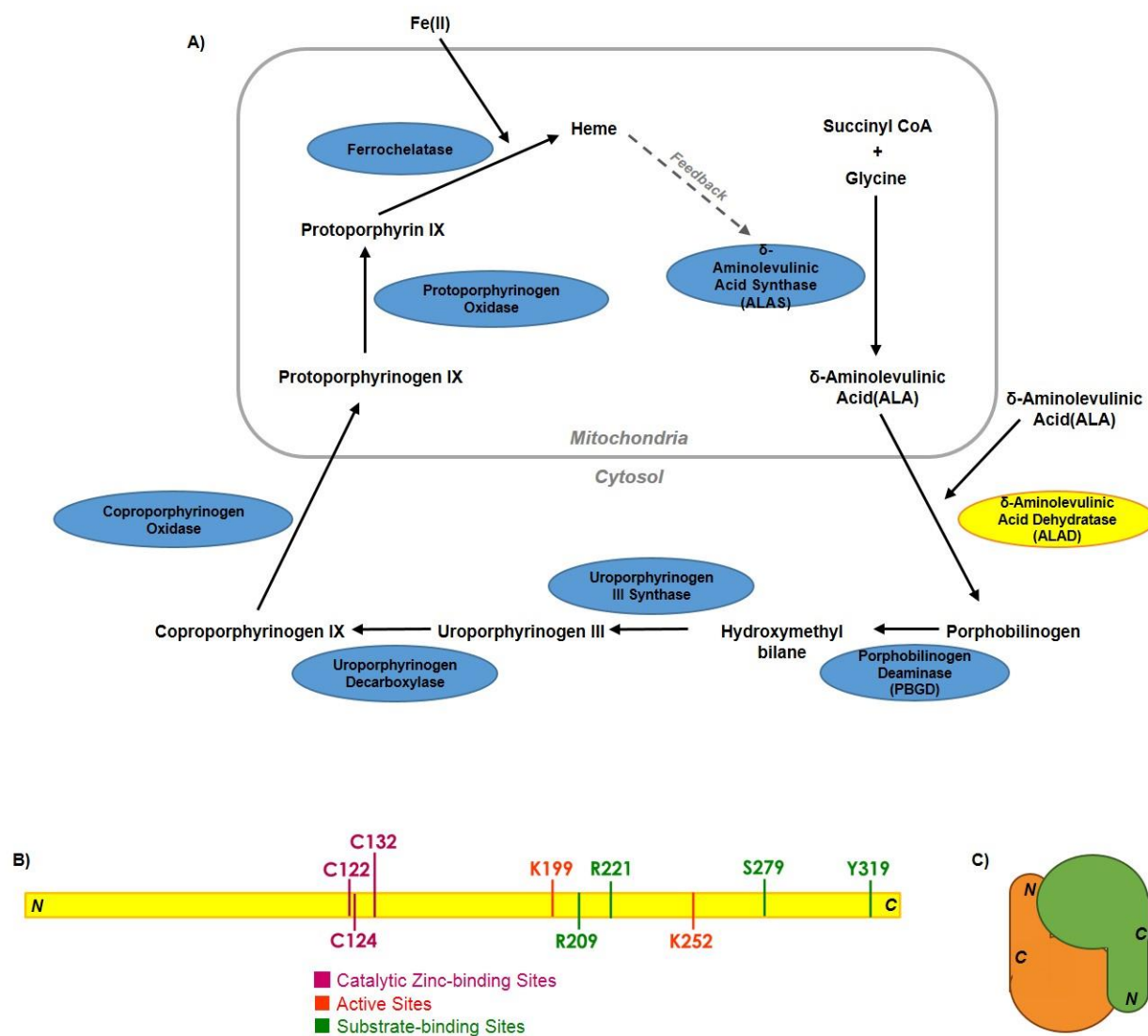


Figure 8. Heme Biosynthesis and ALAD Structure. A) Heme Biosynthesis Pathway; ALAD (highlighted in yellow) catalyzes the condensation of two molecules of ALA into PBG. B) ALAD Protein Structure: ALAD contains three catalytic zinc-binding sites, two active sites and four substrate-binding sites. C) ALAD Dimerization: The N-terminal arm of one ALAD monomer wraps around the α/β barrel of the other.

Upon the discovery that ALAD is an endogenous proteasome inhibitor, ALAD was shown to be identical to the inhibitory CF-2 component of the proteasome (Guo et al. 1994) due to their common N-terminal amino acid sequences and isoelectric points, specific antibody cross-reactivity, similar proteasome inhibitory and dehydratase activities, and identical migration on native and SDS-PAGE gels (Guo et al. 1994). ALAD was also shown to possess calpain inhibitory ability (Murakami and Etlinger 1986), and the CF-2 inhibitory subunits were shown to exist in a ubiquitinated form within the proteasome complex (Li and Etlinger 1992). However, ubiquitination of the inhibitor/ALAD caused a 90% loss of ALAD and proteasome inhibitory activity (Etlinger, et al. 1993). Importantly, a recent report has demonstrated that ALAD is, in fact, a proteasome-interacting protein rather than a component of the proteasome (Bardag-Gorce and French 2011). The relationship of ALAD to the proteasome and its role in human malignancies must be further investigated, as the relationship could present a novel strategy for treatment of human cancers, as well as other diseases involving the proteasome. The data presented herein explore this relationship, and suggest a previously unreported post-translational proteasomal modification (Chapter 3).

Metals in Cancer Development

Just as proteasome activity is altered in cancer, so too are levels of metals like copper and zinc, a discovery which has led to extensive investigation into the roles of these metals in the development of human cancers, as well as their potential use in anticancer therapeutics.

Copper

High serum and tissue levels of copper have been reported in a variety of human tumors including brain (Turecky, et al. 1984), breast (Kuo, et al. 2002; Rizk and Sky-Peck 1984), colon (Nayak, et al. 2003), lung (Diez, et al. 1989) and prostate (Habib, et al. 1980; Nayak et al. 2003) and in 1980, copper was shown to play an important role in angiogenesis (McAuslan and Reilly 1980). In fact, copper, but not other metals, is a cofactor required for several angiogenic mediators including VEGF (Frangoulis, et al. 2007; Sen, et al. 2002), basic fibroblast growth factor (bFGF) (Nasulewicz, et al. 2004) and interleukins-1 and -8 (Moriguchi, et al. 2002), all of which are involved in the regulation of angiogenesis (Brem 1999; Brewer 2001; Lowndes and Harris 2005; Theophanides and Anastassopoulou 2002). Additional cell culture studies also revealed that copper stimulates proliferation and migration of human endothelial cells (Hu 1998). Thus, due to the importance of angiogenesis and copper to tumor development, the use of copper chelators has emerged as an interesting strategy in cancer therapeutics (Pan, et al. 2002; Yoshii, et al. 2001).

Zinc

Like copper, zinc levels have also been shown to be altered in cancer patients, although a firm relationship between cancer development and zinc has not been proven, and seems dependent on tumor type (Chakravarty, et al. 1986; Margalioth, et al. 1983; Schwartz, et al. 1974). For instance, low levels of zinc have been reported in liver, gallbladder, digestive tract, and prostate cancers (Costello and Franklin 2006; Zhao and Eide 1996), while both high and low levels of zinc

have been observed in breast cancers (Manning, et al. 1994; Taylor, et al. 2007; Zhao and Eide 1996). Zinc is also structurally important to various proteins and enzymes such as DNA repair enzymes, cell signaling proteins and transcription factors (Murakami and Hirano 2008; Provinciali, et al. 1995), as well as playing an important role in many cellular processes, including apoptosis, proliferation, differentiation and defense against free radicals (Chakravarty et al. 1986; Chang, et al. 2006; Federico, et al. 2001; Franklin and Costello 2009; Prasad, et al. 1998). Interestingly, the role of zinc in apoptosis is complex, and appears to be cell-type specific. For example, in breast, cervical, renal, and lung epithelial cells, as well as macrophages, zinc is anti-apoptotic, while in prostate, ovarian epithelial and glial cells, zinc is pro-apoptotic (Chakravarty et al. 1986; Franklin and Costello 2007). Not surprisingly, an association between zinc transporter levels and cancer progression has also been proposed (Christiansen and Rajasekaran 2006; Gupta, et al. 2005). Indeed, ZIP4 has been shown to increase cell proliferation through zinc transport, specifically in pancreatic cancer (Franklin and Costello 2009; Li, et al. 2007) and both ZIP6 and ZIP10 have roles in the progression and metastasis of breast cancer (Manning et al. 1994; Murakami and Hirano 2008; Taylor et al. 2007). Conversely, ZIP1 has been suggested as a tumor suppressor of prostate cancer (Costello and Franklin 2006). Thus, by disrupting the distribution of zinc in tissues, altered levels of zinc transporters may enhance the development of various tumors, indicating the potential of zinc as an anticancer agent.

Metal-Based Complexes as Proteasome Inhibitors

The discovery that some metal-based compounds, like cisplatin, possess potent anticancer properties, coupled with the importance of copper and zinc to essential biological processes like tumorigenesis, has led to the investigation into copper and zinc, as well as other metals like cobalt, gallium and gold, as metal centers in anticancer drugs. Since its discovery over four decades ago,

cisplatin has cured over 90% of testicular cancer cases, as well as playing a critical role in the treatment of various other cancers, including bladder, cervical, ovarian, lymphoma and melanoma (Wong and Giandomenico 1999). Extensive studies have shown that the cytotoxicity of cisplatin is due to its interactions with DNA, which results in the formation of adducts that interfere with replication and transcription (Eckhardt 2002). Unfortunately, though cisplatin has proven extremely effective, it is also associated with toxicity and resistance, which has hampered its clinical use (Galanski, et al. 2003; Galanski, et al. 2005) and prompted the search for less-toxic metal-based drugs.

Gallium Complexes

Although there is no known biological role for gallium, its use in therapeutic applications has been explored, partially due to its ability to function as an iron mimetic, which disturbs iron-mediated processes within cells. In fact, preclinical studies have shown that gallium nitrate, a group IIIa metal salt, inhibits proliferation of tumor cells *in vitro* and *in vivo*, and clinical trials have reported on the anti-tumor activity of gallium nitrate in non-Hodgkin's lymphoma and bladder cancer (Chitambar 2004; Collery, et al. 2002; Foster, et al. 1986). As a result of these positive results, the antitumor activities of various other gallium species, including gallium chloride (Collery et al. 2002), gallium maltolate (Figure 9A) (Chua, et al. 2006), *tris*(8-quinolonato)gallium(III) (Figure 9B) (Collery, et al. 2000) and gallium thiosemicarbazones (Arion, et al. 2002), as well as gallium-containing asymmetric [NN'O] tridentate ligands (Figure 9C) (Chen, et al. 2007b; Shakya, et al. 2006), have been investigated. Few studies have reported on the mechanisms of action of these gallium complexes, but the proteasome has been implicated as a target of the gallium-containing asymmetric [NN'O] tridentate ligands (Chen et al. 2007b;

Shakya et al. 2006). The proteasome-inhibitory and apoptosis-inducing abilities of a new gallium species is explored in this dissertation (Chapter 4).

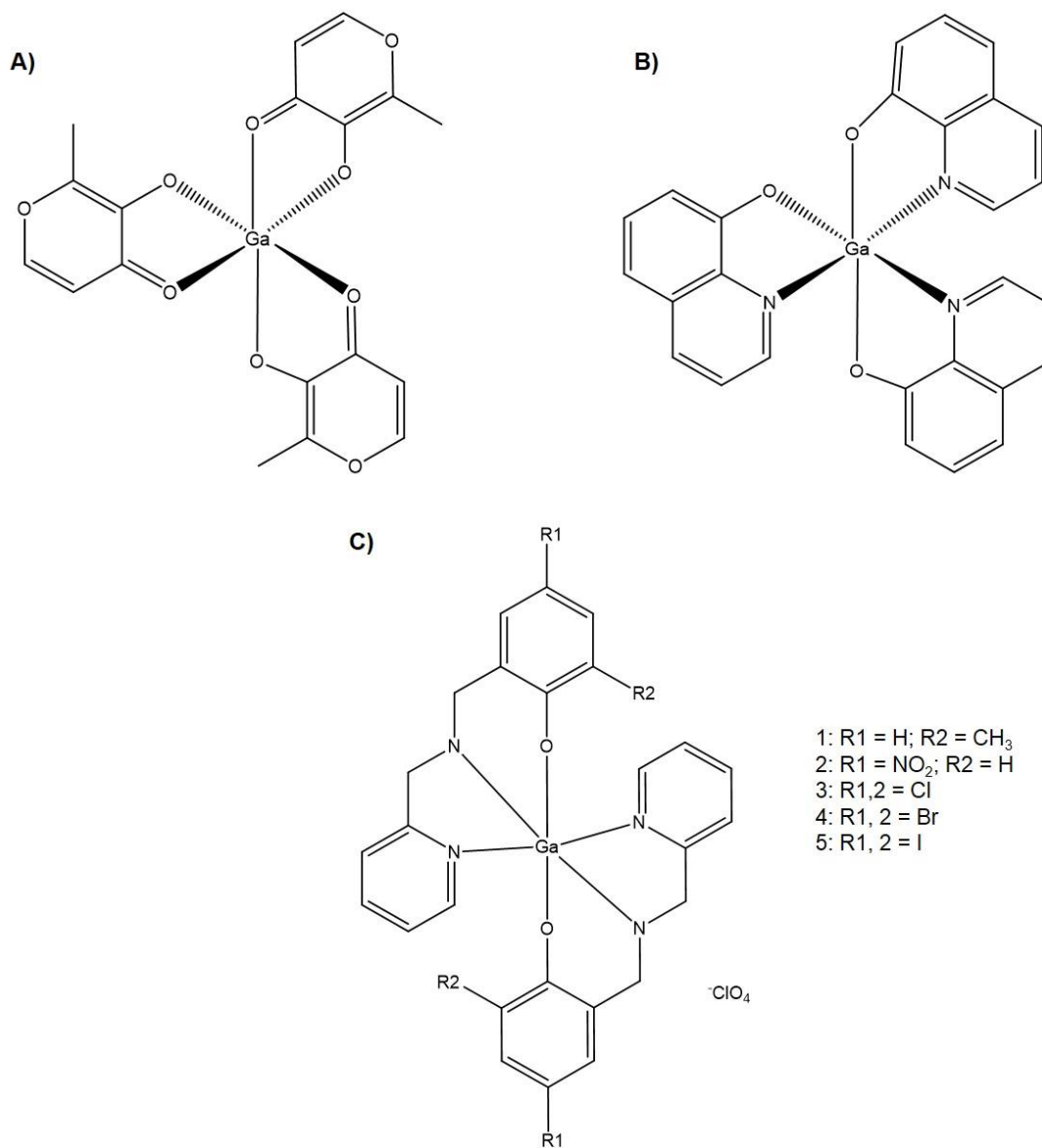


Figure 9. Structures of Gallium Complexes. A) Gallium Maltolate
 B) Tris(8-quinolonato)gallium(III) C) $[Ga^{III}(L^{R1R2})_2]ClO_4$

Gold Complexes

Although the medicinal applications of gold date back thousands of years, its rational use did not begin until Robert Koch found that $K(Au(CN)_2)$ could kill the tuberculosis bacteria in the early twentieth century. However, serious side effects have led to the use of less-toxic Au (I)-thiolate complexes, like auranofin (Figure 10A), for the treatment of tuberculosis. Additionally, Jacque Forestier used these gold complexes for the treatment of rheumatoid arthritis, and they remained the drug of choice for many years (Forestier 1935). The success of these gold compounds led to investigation into the potential anticancer activity of gold compounds. Indeed, gold (I) complexes, including auranofin analogs and phosphine-gold (I) thiosugars, exhibited potent cytotoxic activity in B16 melanoma and P388 leukemia cells, but were inactive against solid tumor cells (Milacic, et al. 2008b; Mirabelli, et al. 1986). Gold(III) complexes have also been investigated, and in spite of initial doubts due to their high redox activity and poor stability, were found to be proteasome inhibitors with potent apoptosis-inducing abilities (Messori, et al. 2003; Milacic, et al. 2006; Zhang, et al. 2010). Importantly, one study reported that treatment with a gold(III) compound (Figure 10B) was associated with generation of free radicals, suggesting that induction of oxidative stress may play a role in the cytotoxicity of these gold(III) compounds (Figure 10B) (Zhang et al. 2010). Further, the data presented in this dissertation expand on the use of gold(III) compounds as proteasome inhibitors in breast cancer (Chapter 4).

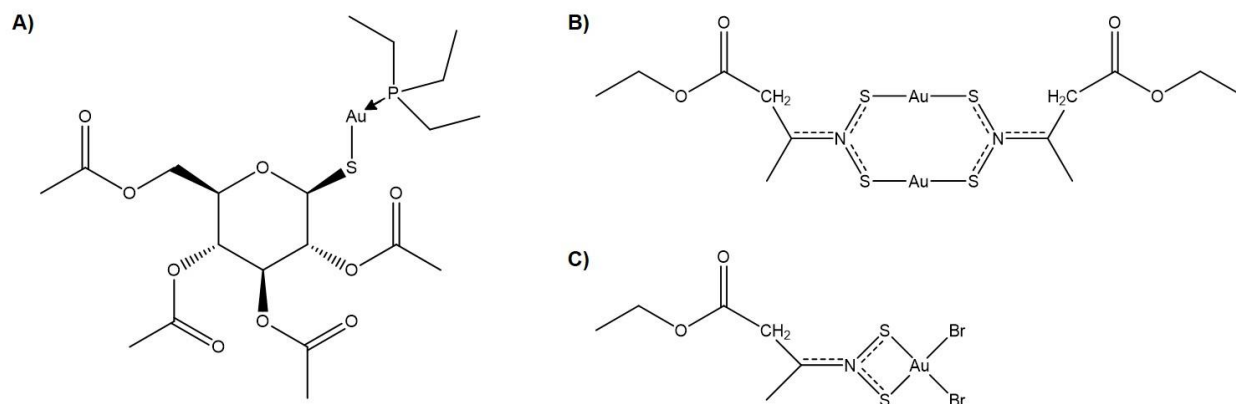


Figure 10. Structures of Gold Complexes. A) Auranofin B) AUL15; a gold(III) complex C) AUL12; a gold(I) complex

Proteasome Inhibition via Metal Chelation

The success of metal-containing drugs, coupled with the functional importance of metals like copper and zinc to normal cellular function, has resulted in studies exploring chelation of these essential metals with chelators like dithiocarbamates and hydroxyquinolones, several of which have been used previously in the treatment of various diseases, including AIDS, alcoholism and bacterial and fungal infections (Malaguarnera, et al. 2003; Reymond 1950; Schreck, et al. 1992).

Dithiocarbamates

One class of medicinally important metal-chelating compounds is the dithiocarbamates, which includes many drugs that are currently approved for the treatment of various pathologies, including bacterial and fungal infections, as well as AIDS and alcoholism (Johansson 1992; Malaguarnera et al. 2003; Meyer 1989; Schreck et al. 1992; Vallari and Pietruszko 1982). The most common of this class is disulfiram (tetraethylthiuram disulfide, DSF; Antabuse; Figure 11A), an irreversible inhibitor of aldehyde dehydrogenase, that is able to bind with copper(II) (Cen, et al. 2004) and is one of only two drugs currently approved for the treatment of alcoholism (Johansson 1992; Meyer 1989; Vallari and Pietruszko 1982).

While the ability of DSF to inhibit ALDH is well-known, other potential targets include activation of the ROS-p38 pathway (Chiba, et al. 2014), inhibition of O⁶-methylguanine-DNA methyltransferase (MGMT) (Paranjpe, et al. 2013), blockade of transcription factor binding to the cyclic AMP (cAMP)-responsive element (Brar, et al. 2004), suppression of NF-κB signaling (Westhoff, et al. 2013), superoxide dismutase, inhibition of which results in apoptosis (Marikovsky, et al. 2002), as well as proteasome (Chen, et al. 2006; Li, et al. 2008) and zinc finger- and RING-finger-containing ubiquitin E3 ligase (Brahemi, et al. 2010; Kona, et al. 2011) inhibition. Importantly, while DSF is not capable of binding biological metal ions like iron(II) or

III) or manganese(III) (Cen et al. 2004), it has been reported that DSF is able to interact with zinc(II) (Brar et al. 2004). Interestingly, studies have shown that copper-binding is necessary for the proteasome-inhibitory ability of DSF (Chen et al. 2006; Li et al. 2008), while its ability to bind zinc is responsible for its activity against E3 ligases (Brahemi et al. 2010; Kona et al. 2011). The results of preclinical studies have led to clinical trials investigating the use of DSF for the treatment of human cancers, validating metal-chelation as a viable strategy.

Hydroxyquinolines

Another class of compounds investigated for their anticancer potential is the hydroxyquinolines, of which clioquinol (5-chloro-7-iodo-8-hydroxyquinoline, CQ; Figure 11B) is a classic example. Clioquinol is a lipophilic compound that is able to form stable complexes with copper(II) (Di Vaira, et al. 2004) and reports have shown that CQ reduces and prevents the formation of amyloid plaques in Alzheimer's disease transgenic mice (Cherny, et al. 2001). This discovery led to two clinical trials validating the efficacy of CQ in Alzheimer's disease with no visible toxicity (Regland, et al. 2001; Ritchie, et al. 2003) and, ultimately, the use of CQ for the treatment of Alzheimer's and Huntington's diseases (Nguyen, et al. 2005; Ritchie, et al. 2004). In addition, prior to its use in Alzheimer's disease, CQ was used successfully to treat and prevent *shigella* and *entamoeba histolytica* infections (Gholz and Arons 1964).

Clioquinol has been shown to induce cell death via various mechanisms in several cell lines. Histone deacetylase inhibition was observed in leukemia and myeloma cells (Cao, et al. 2013), cytoplasmic clearance of XIAP occurred in prostate cancer cells (Cater and Haupt 2011) and release of tumor necrosis factor α (TNF- α) from macrophages was demonstrated in cervical cancer cells (Du, et al. 2008). Perhaps the most widely reported mechanism, however, is inhibition of the proteasome, which has been shown in breast, B-cell lymphoma lines, bladder, cervical,

leukemia, myeloma, ovarian, prostate and pancreatic cancer cell lines (Chen, et al. 2007a; Daniel, et al. 2005; Ding, et al. 2005; Mao, et al. 2009). While some reports have suggested that CQ is potent alone (Mao et al. 2009), even more have clearly shown that the toxicity of CQ is dependent on its ability to complex with copper (Barrea, et al. 2009; Chen et al. 2007a; Daniel et al. 2005; Ding et al. 2005; Zhai, et al. 2010). After validating that CQ complexed with copper in a 1:1 ratio, cells treated with a CQ-Cu complex underwent significantly more apoptosis than cells treated with CQ alone (Chen et al. 2007a; Daniel et al. 2005; Ding et al. 2005), and importantly, in mouse xenograft models, CQ alone suppressed tumor growth through inhibition of the proteasome (Chen et al. 2007a; Ding et al. 2005). These results not only confirmed the need for copper-binding to CQ, but also the ability of CQ to chelate intracellular copper within tumors, leading to apoptosis.

Therefore, compounds like DSF and CQ are potent proteasome inhibitors that require the transport of copper into cancer cells, a necessity which may contribute to their selectivity and minimal toxicity toward normal cells. Thus, these compounds may be exploited as potential novel strategies for the treatment of human malignancies. Furthermore, data presented in this dissertation build on the previous success of these copper chelators through the investigation into another previously used hydroxyquinoline compound (Chapter 4).

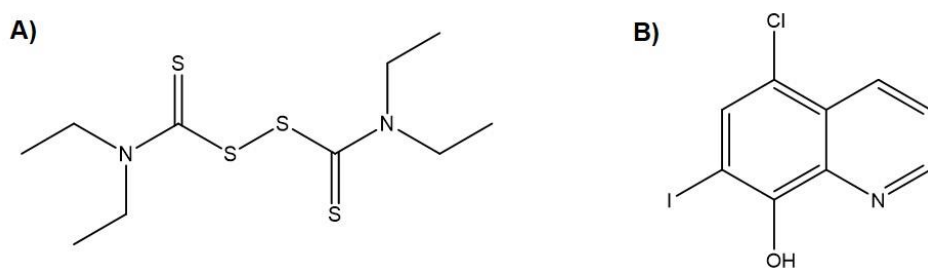


Figure 11. Structures of Metal Chelators Used as Proteasome Inhibitors.
A) Disulfiram (tetraethylthiuram disulfide; DSF) B) Clioquinol (CQ)

CHAPTER 2

MATERIALS AND METHODS

Reagents and Antibodies

Fetal bovine serum was purchased from Aleken Biologicals (Nash, TX). DMEM/F12 and RPMI-1640 media, trypsin, penicillin/streptomycin and 3-(4,5-Dimethyl-2-thiazolyl)-2,5-diphenyl-2H-tetrazolium bromide (MTT) were purchased from Life Technologies (Carlsbad, CA). Fugene-HD transfection reagent was from Promega (Madison, WI) and full-length C-terminal myc-DDK-tagged ALAD and PCMV6-Entry plasmids were from OriGene Technologies (Rockville, MD). Mouse monoclonal anti-ALAD, anti- $\alpha 2$, anti-ubiquitin, anti-myc, anti-p27, anti-Bax, anti-IkBa and anti-GAPDH, polyclonal rabbit anti-ALAD, anti- $\alpha 2$, anti-caspase-3 and anti-ubiquitin and goat anti-actin primary antibodies, as well as normal mouse and rabbit IgG and anti-goat secondary antibody were purchased from Santa Cruz Biotechnology (Santa Cruz, CA). Rabbit monoclonal anti-cleaved caspase-3 and polyclonal rabbit anti-Acetyl-Lysine antibodies were from Cell Signaling Technology (Boston, MA), mouse monoclonal anti-H3 and anti-tubulin antibodies were from Abcam (Cambridge, MA), and polyclonal rabbit anti-S10a and anti-PARP antibodies were from BioMol (Farmingdale, NY). Mouse and rabbit secondary antibodies were purchased from Bio-Rad Laboratories (Hercules, CA). Purified ATP, ubiquitin from bovine erythrocytes and ALAD from bovine liver, as well as TRITC-conjugated anti-mouse secondary antibody, DAPI, trypan blue solution and DMSO (sterile and non-sterile) were from Sigma Aldrich (St. Louis, MO). Enhanced chemiluminescence reagent and autoradiography film were purchased from Denville Scientific (Metuchen, NJ). VectaShield anti-fade solution was purchased from Vector Laboratories (Burlingame, CA). Purified human 20S proteasome was obtained from Boston Biochem (Cambridge, MA). Fluorogenic peptide substrates Suc-LLVY-AMC, Z-ARR-AMC, and

Z-LLE-AMC (for proteasomal chymotrypsin-like, trypsin-like and PGPH-like activities, respectively) and Ac-DEVD-AMC (for caspase-3 like activity) were purchased from Calbiochem (San Diego, CA). Annexin V-FITC Apoptosis Detection Kit I was purchased from BD Biosciences (San Jose, CA).

Compounds

Clioquinol, nitroxoline and trolox were purchased from Sigma-Aldrich (St. Louis, MI). Suberanolhydroxamic acid (SAHA) and bortezomib were from LC Laboratories (Woburn, MA) and MG-132 was from BIOMOL International LP (Plymouth Meeting, PA). $[\text{Co}^{\text{II}}(\text{L}^1)_2]$, $[\text{Co}^{\text{II}}(\text{L}^2)]$, and $[\text{Co}^{\text{III}}(\text{L}^1)_2]\text{ClO}_4$ (Figure 19) (Tomco, et al. 2011), $[\text{Al}^{\text{III}}(\text{L}_{\text{iodo}})_2]\text{ClO}_4$, $[\text{Cd}^{\text{II}}(\text{L}_{\text{iodo}})\text{Cl}]\cdot\text{H}_2\text{O}$, $[\text{Hg}^{\text{II}}(\text{L}_{\text{iodo}})_2]\cdot 4\text{DMSO}$, $[\text{Pb}^{\text{II}}(\text{L}_{\text{iodo}})\text{NO}_3]$, and $[\text{Sn}^{\text{IV}}(\text{L}_{\text{iodo}})\text{Cl}_3]$ (Figure 21) (Tomco, et al. 2014), as well as GaDiIBPEN and ZnDiIBPEN (Figure 22) were synthesized by Dajena Tomco in the Verani Lab, Department of Chemistry, Wayne State University (Detroit, MI). AuD6 and AuD8 ($[\text{Au}^{\text{III}}\text{Br}_2(\text{dtc-Sar-AA-O}(t\text{-Bu}))]$; AA = Gly or Aib (α -aminoisobutyric acid)) (Figure 20) (Nardon, et al. 2014) were synthesized in the Fregona Lab, Department of Chemical Sciences, University of Padova (Padova, Italy). For specific details, see corresponding publications. All compounds were dissolved in DMSO at stock concentrations of 100mM.

Cell Culture and Whole-Cell Extract Preparation

Human K562 leukemia, prostate cancer DU145, LNCaP and PC-3, MDA-MB-231 breast cancer and transformed prostate epithelial CRL2221 cell lines were purchased from American Type Culture Collection (Manassas, VA). Leukemia and prostate cells (cancer and transformed epithelial) were grown in RPMI-1640 and breast cancer cells in DMEM/F12, supplemented with 10% FBS, 100 units/ml penicillin and 100 $\mu\text{g}/\text{ml}$ streptomycin (Life Technologies; Carlsbad, CA). Cells were maintained in a humidified atmosphere containing 5% CO_2 at 37°C. Whole cell extracts

were prepared as follows: cells were harvested, washed twice with phosphate-buffered saline and lysed in a whole cell lysis buffer (50 mM Tris-HCl, pH 8.0, 150 mM NaCl, 0.5% NP40). Mixtures were vortexed for 20 minutes at 4°C, followed by centrifugation at 12,000 rpm for 12 minutes. Supernatants were collected as whole cell extracts and protein concentrations were determined using the Bio-Rad Protein Assay (Bio-Rad; Hercules, CA).

Transfection

Full-length C-terminal myc-DDK-tagged human ALAD in a PCMV6-Entry vector (OriGene Technologies; Rockville, MD) was transformed into DH5 α competent E. coli, followed by expansion and DNA purification using the QIAGEN (Venlo, Netherlands) EndoFree Plasmid Maxi Prep kit. After measurement of DNA purity and concentration, genes were transiently transfected into parental prostate cancer cells using Fugene-HD transfection reagent (Promega; Madison, WI) in Opti-MEM serum-free medium (Life Technologies; Carlsbad, CA). Empty PCMV6-Entry vector was used as a control.

Western Blot Analysis

Cell lysates (40 μ g) were separated by sodium dodecylsulfate–polyacrylamide gel electrophoresis (SDS–PAGE; 10-12%) and transferred to nitrocellulose membranes, followed by incubation with indicated primary and secondary antibodies and visualization using enhanced chemiluminescence reagent (Denville Scientific, Metuchen, NJ).

Subcellular Fractionation

Cells were grown and harvested as described previously. Following collection of the cell pellet, 500 μ L 1X hypotonic buffer (20mM Tris-HCl pH 7.4, 10mM NaCl, 3mM MgCl₂) was added and the samples were mixed by pipetting. After a 15 minute incubation on ice, 25 μ L 10% NP-40 was added, followed by vortexing for 15 seconds. The homogenate was then centrifuged

for 10 minutes at 3000 rpm at 4°C. The supernatant was then transferred and saved as the cytosolic fraction. The pellet was resuspended in 50 µL complete cell extraction buffer (100mM Tris-HCl pH 7.4, 2mM Na₃VO₄, 100mM NaCl, 1% Triton X-100, 1mM EDTA, 10% glycerol, 1mM EGTA, 0.1% SDS, 1mM NAF, 0.5% deoxycholate, 20mM Na₄P₂O₇, 1mM PMSF) and incubated on ice for 30 minutes with vortexing at 10 minute intervals, followed by centrifugation at 14,000 g for 30 minutes at 4°C. The supernatant was then transferred and saved as the nuclear fraction. Fractions were subjected to the protein concentration assay and Western blotting as previously described.

Immunoprecipitation

Cells were treated as indicated in respective figure legends and lysed as described above. Immunoprecipitation was carried out using the Pierce Classic IP Kit (Thermo Fisher; Rockford, IL). Briefly, cell lysates (500-1000 µg) were incubated with 10µg primary antibody (anti-myc, anti-α2 or anti-S10a) or IgG (as control) with rocking overnight at 4°C. Protein A/G beads were then added and the mixtures were incubated in a spin column with a 10 µm pore size with rocking for 4-18 hours at 4°C. Unbound proteins were separated by centrifugation at 3000 rpm for 1 minute and saved as the supernatant fraction. Beads were then washed three times with 1X TBS, followed by elution of bound proteins with low pH elution buffer and centrifugation at 3000 rpm for 1 minute. 4X SDS sample buffer was added to supernatant (20 µl) and eluate (pulldown) samples, which were subjected to analysis by Western blot.

Immunofluorescence

PC-3 cells were plated at a density of approximately 25,000 cells per well on 6 well chamber slides (Fisher Scientific; Pittsburgh, PA). Cells were transfected with either empty vector or full length ALAD after 24 hours as described above. After 48 hours, media was removed from

the slide with a pipette and cells were washed with PBS. The plastic chamber was then removed and the slide was allowed to dry followed by three washes in ice cold 1:1 methanol:acetone to fix and rupture cell membranes. The slide was again allowed to dry before rehydration in a PBS wash, followed by blocking in 5% BSA for 45 minutes at room temperature. The slides were then washed once with PBS and incubated with mouse anti-ALAD primary antibody in BSA overnight at 4°C. The slide was then washed with PBS three times followed by incubation in TRITC-conjugated anti-mouse secondary antibody (Sigma Aldrich; St. Louis, MO) for 2 hours at room temperature. Following three PBS washes, DAPI (Sigma Aldrich; St. Louis, MO) was added to the slide for 5 minutes and the slide was then washed a final three times in PBS before the cover slip was applied with VectaShield anti-fade solution (Vector Laboratories; Burlingame, CA). Photomicrographs were taken with a Leica DM4000 fluorescence microscope (Leica Microsystems, Inc.; Buffalo Grove, IL) at 63X magnification and signals were documented with 5.0 Openlab Improvision software (Perkin Elmer; Waltham, MA).

Cell-free Ubiquitination Assay

PC-3 cell extracts (10 µg) were incubated with purified ALAD (5 µg), purified ubiquitin (1 µg) and purified 20S proteasome (60 ng) in 50 mM reaction buffer (500 mM Tris pH 7.4, 50 mM MgCl₂, 20 mM DTT) containing purified ATP (6 mM) for 2 hours at 37°C. Either ubiquitin, 20S proteasome and/or ALAD were omitted for controls. The reaction was stopped by addition of 4X SDS sample buffer and boiling at 100°C for 5 minutes. Samples were then analyzed by Western blot.

Purified 20S and Cell Extract Proteasome Activity Assay

Purified human 20S proteasome (35 ng; Boston Biochem; Cambridge, MA), or cell extract (10 µg), was incubated with 10 µM of fluorogenic CT-like substrate, Suc-LLVY-AMC (AnaSpec;

Fremont, CA) in 100 µl assay buffer (20 mM Tris-HCl; pH 7.5), in the presence of test compounds at different concentrations or the solvent control, DMSO, for 2-4 hours at 37°C. After incubation, production of hydrolyzed AMC groups was measured using a Wallac Victor3 multilabel plate reader (PerkinElmer; Waltham, MA) with an excitation filter of 355 nm and an emission filter of 460 nm, as previously described (Chen et al. 2007b).

Cellular Proteasome Activity Assay

Cells were treated with various concentrations of the test compounds for 24 hours followed by harvesting and cell lysis as described above. Protein lysate (10 µg) was then incubated with 10 µM fluorogenic CT-like substrate, Suc-LLVY-AMC (AnaSpec; Fremont, CA), trypsin-like substrate Z-ARR-AMC, or PGPH-like substrate Z-LLE-AMC in 100 µl assay buffer (20 mM Tris-HCl; pH 7.5) for 2-4 hours at 37°C, followed by measurement of free AMC groups using a Wallac Victor3 multilabel plate reader (PerkinElmer; Waltham, MA) with an excitation filter of 355 nm and an emission filter of 460 nm, as previously described (Tomco et al. 2011).

Morphological Changes

Changes in cellular morphology were observed following each treatment using a Zeiss Axiovert 25 microscope (Thornwood, FL USA). Rounded and detached cells were considered dead.

Caspase-3 Activity Assay

Cells were treated with various concentrations of the test compounds for 24 hours followed by harvesting and cell lysis as described above. Protein lysate (25 µg) was then incubated with 40µM caspase-3 like substrate Ac-DEVD-AMC (Calbiochem; San Diego, CA) in 100 µl assay buffer (20 mM Tris-HCl, pH 7.5) for 18-24 hours at 37°C, followed by measurement of free AMC

groups using a Wallac Victor3 multilabel plate reader (PerkinElmer; Waltham, MA) with an excitation filter of 355 nm and an emission filter of 460 nm, as previously described

Cell Viability Assay

The MTT (3-(4,5-Dimethylthiazol-2-yl)-2,5-diphenyltetrazolium bromide) assay was used to measure effects of the compounds on prostate and breast cancer cell viability. PC-3 cells were grown to 70–80% confluency in 96-well plates, followed by addition of each compound at the indicated concentrations for 24 hours. MTT in PBS (1 mg/ml) was then added and incubated at 37 °C for 3 hours to allow for complete cleavage of the formazan salt by viable cells. MTT was then removed and 100 µl DMSO was added, followed by colorimetric analysis using a Victor3 multilabel plate reader (PerkinElmer; Wellesley, MA) at an absorbance of 560 nm. Absorbance values were plotted as the mean of triplicate experiments.

Trypan Blue Exclusion Assay

Suspension cells were treated in 6-well plates with various concentrations of the test compounds for 24 hours followed by addition of 0.1 mL 0.4% trypan blue in PBS to 1 mL of the cell suspension for each treatment. The trypan blue was allowed to incubate for 1-2 minutes before loading onto a hemocytometer. The number of blue staining cells versus total cells was counted under low magnification using a Zeiss Axiovert 25 microscope (Thornwood, FL USA). Blue stained cells were considered non-viable and values were recorded in quadruplicate.

Annexin-V/FITC Apoptosis Assay

Apoptotic indices were measured using the Annexin-V/fluorescein isothiocyanate (FITC) Apoptosis Detection Kit I from BD Pharmingen. MDA-MB-231 cells were grown to about 75% confluence, treated with gold-based complexes (20 µM) or DMSO as a control for 16 or 24 hours and harvested as described above. Cell pellets were washed twice with ice cold PBS and then

resuspended in $1\times$ binding buffer at a concentration of 1×10^6 cells/mL. Annexin-V/FITC and/or propidium iodide (PI; 5 μ L each), and 5 μ L Annexin-V/FITC or 5 μ L PI as controls, were added to 100 μ L cell suspension. Mixtures were gently vortexed and incubated in the dark for 15 minutes at RT followed by addition of 400 μ L $1\times$ binding buffer to each tube. Analysis by flow cytometry was performed at the Microscopy, Imaging and Cytometry Resources (MICR) Core at the Karmanos Cancer Institute, Wayne State University. Data are presented as density plots of Annexin-V (x-axis) versus PI (y-axis) staining. Unstained cells, cells stained with either PI or Annexin-V/FITC only, and untreated cells stained with both PI and Annexin-V were used to determine compensation and quadrants. The excitation wavelength was 488 nm and the detection wavelengths were 530 ± 15 and 620 ± 21 nm for Annexin-V and PI, respectively. Cells staining negative for both markers were considered viable and cells staining positive for both markers were considered to be in late apoptosis. Cells staining positive for Annexin-V only were considered in early apoptosis, whereas cells staining positive for PI only were considered dead by a necrotic pathway. Percentages of viable, apoptotic, and necrotic cells are reported in the corner of each quadrant.

Human Breast Tumor Xenografts

Seven-week-old female athymic nude mice were purchased from Harlan Laboratories (Indianapolis, USA) and housed in accordance with protocols approved by the Institutional Laboratory Animal Care and Use Committee of Wayne State University. Human breast cancer MDA-MB-231 cells suspended in 0.1 mL of serum-free DMEM/F12 cell growth medium were injected subcutaneously (s.c.) into the right flank of each mouse. When tumors reached a volume of around 115 mm³, the mice were randomly allocated into treatment groups (seven mice/group for gold compounds; four mice/group for 5NHQ) and treated five days a week by s.c. injection of

either vehicle [1:1:1 v/v PBS, DMSO, Cremophore/ethanol (1:4)] or medium containing 1.0 mg/kg AuD6 or AuD8, or 10mg/kg 5NHQ or CQ. Tumor length (L) and width (W) were measured every other day using a caliper, and tumor volumes were evaluated according to the standard formula ($\pi \cdot L \cdot W^2$)/6. Mouse weights were monitored weekly. Mice were sacrificed after 27 or 29 days (four/group for gold compounds, all mice for 5NHQ), or when tumors reached $\sim 1,800 \text{ mm}^3$, and for the gold treatments, the remaining three mice/group were sacrificed after 13 days to observe any early effects of treatments. Tumors were collected and weighed. Gold-treated tumor tissues were used to measure proteasome inhibition and caspase-3 activation by enzymatic activity assays and by Western blot analysis.

Immunohistochemistry

IHC was performed using a previously reported protocol (Yang, et al. 2006). Briefly, tumor samples were paraffin-embedded by the Pathology Core at Karmanos Cancer Institute (Detroit, MI, USA). Samples were then cut and stained for p27 or TUNEL by the BioBank at William Beaumont Hospital (Royal Oak, MI, USA). Anti-p27 (VP-P951) was from Vector Laboratories (Burlingame, CA, USA) and was used at a 1:30 dilution followed by detection by DAKO. Samples were counterstained with DAB/Hematoxylin. TUNEL staining was performed using anti-digoxigenin and peroxidase substrate, followed by counterstaining with methyl green. In both cases, brown colored cells were considered positive.

Statistical Analysis

Analysis of *in vivo* tumor growth curves following treatment with gold compounds was performed using the one-sided ANOVA test in Excel®; $p < 0.05$ was considered significant.

CHAPTER 3

THE HEME SYNTHESIS ENZYME δ -AMINOLEVULINIC ACID DEHYDRATASE (ALAD) AS AN ENDOGENOUS INHIBITOR OF THE PROTEASOME: INVOLVEMENT OF ALAD-20S PROTEASOME COMPLEXES IN UBIQUITINATION AND ACETYLATION OF PROTEASOMAL α 2 SUBUNITS

The ubiquitin-proteasome pathway has gained attention as a potential chemotherapeutic target, owing to its importance in the maintenance of protein homeostasis and the observation that cancer cells are more dependent on this pathway than normal cells. Additionally, inhibition of histone deacetylases (HDACs) by their inhibitors like Vorinostat (SAHA) has also proven a useful strategy in cancer therapy and the concomitant use of proteasome and HDAC inhibitors has been shown to be superior to either treatment alone. It has also been reported that delta-aminolevulinic acid dehydratase (ALAD) is a proteasome-associated protein, and may function as an endogenous proteasome inhibitor. While the role of ALAD in the heme biosynthetic pathway is well characterized, little is known about its interaction with, and the mechanism by which it inhibits, the proteasome. In this chapter, the ALAD-proteasome complex was further characterized in cultured prostate cancer cells and the effects of SAHA treatment on the regulation of ALAD were investigated. ALAD interacts with the 20S proteasomal core, but not the 19S regulatory cap, associated with ubiquitination of proteasomal α 2 subunits. SAHA treatment increases ALAD protein levels and promotes acetylation of ubiquitinated α 2 protein. Thus, the mechanism by which ALAD binds to the 20S proteasome, as well as its involvement in a previously unreported post-translational modification of proteasomal α subunits is described.

RESULTS

ALAD binds the 20S proteasome in place of the 19S proteasomal cap and associates with a modified form of $\alpha 2$ subunit in cultured prostate cancer cells and in human erythrocytes

Endogenous levels of ALAD were first determined by Western blot. Prostate cancer cell lines DU145, LNCaP and PC-3 exhibit varying levels of ALAD (Figure 12A), while in general, ALAD is expressed similarly in human erythrocytes from several individuals (Figure 13A). Next, to ascertain how ALAD interacts with the proteasome in cells, PC-3 cell lysates were immunoprecipitated with anti-ALAD. Immunoblotting with anti-ALAD antibody confirms the successful immunoprecipitation of ALAD with anti-ALAD, but not control IgG (Figure 12B). The proteasomal $\alpha 2$ subunit (26 kD band), along with two bands with apparent molecular masses of 34 and 38-40 kD, respectively, were recognized by anti- $\alpha 2$ antibody in the anti-ALAD pulldown, but not in the control IgG pulldown (Figure 12B). Importantly, this interaction was also observed in samples of human erythrocytes (Figure 13B). These 34 and 38 kD bands may be ubiquitinated forms of proteasomal $\alpha 2$ subunits (see below). Therefore, endogenous ALAD binds the 20S proteasome and is associated with some modified forms of proteasomal $\alpha 2$ subunit.

Because endogenous ALAD protein levels are relatively low (compared with human erythrocytes; Figure 12A), these prostate cancer cells were then transfected with either myc-tagged full length ALAD or empty vector (as a control) for 48 hours and subjected to analysis by Western blot. The transfection efficiency varies among these cell lines, with more successful transfection in LNCaP and PC-3 cells than DU145 cells (Figure 12A). Due to the high transfection efficiency in PC-3 cells, ALAD-transfected PC-3 cells were used for the remainder of experiments.

The interaction of ALAD with the modified forms of proteasomal $\alpha 2$ was then confirmed (Figure 12C) in myc-tagged ALAD-transfected PC-3 cells. Similar to the results in parental PC-3 cells (Figure 12B), an anti-myc antibody pulled down two similarly modified forms of proteasomal

$\alpha 2$ subunit (MW 34 & 38-40 kD), but not the 19S subunit Rpn7/S10a (Figure 12C), confirming that ALAD binds to a modified form of $\alpha 2$, in place of the 19S subunit. Consistently, an anti-Rpn7/S10a antibody pulled down the unmodified proteasomal $\alpha 2$, but not the modified form(s) of $\alpha 2$ or ALAD (Figure 12D). Importantly, the ALAD-associated, modified form of $\alpha 2$ appears to be ubiquitinated, as an anti-ubiquitin antibody recognizes two bands at the same molecular weights (34 & 38-40 kD) in the anti-myc pull down fraction (Figure 12C). Because both 34 and 38-40 kDa bands are recognized by anti- $\alpha 2$ and anti-ubiquitin antibodies, it is unlikely that the 34 kD band is a degraded form of the 38-40 kD band. Thus, these results indicate that ALAD binds to the 20S proteasomal core in the position of the 19S regulatory cap, associated with ubiquitination of the $\alpha 2$ subunits.

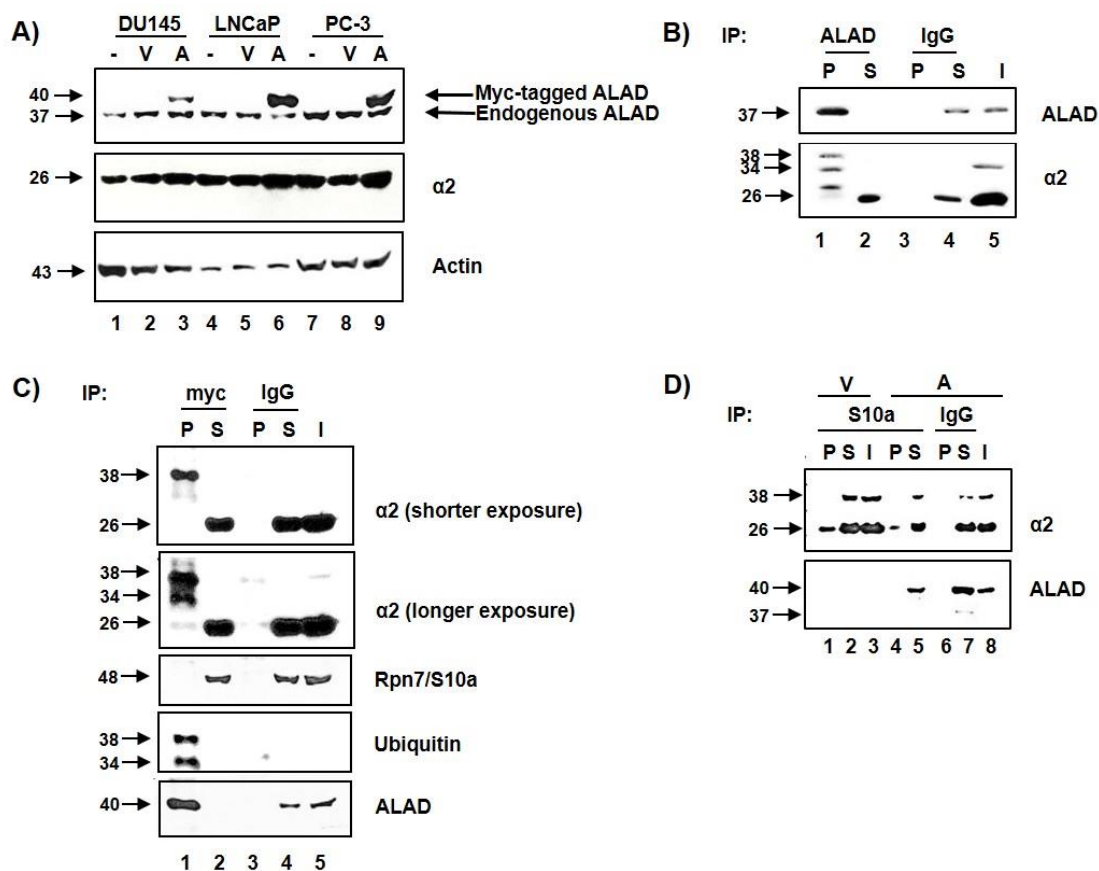


Figure 12. ALAD binds the 20S proteasome in place of the 19S regulatory cap and is associated with ubiquitinated forms of $\alpha 2$ in cultured prostate cancer cells. A) Protein levels of endogenous and tagged ALAD protein in prostate cancer cells. Several prostate cancer cell lines were transfected with empty vector or myc-tagged full length ALAD for 48 h followed by Western blot analysis. B) Endogenous ALAD interacts with a modified form of $\alpha 2$. Parental PC-3 cell lysates were immunoprecipitated with anti-ALAD followed by Western blot analysis. C) A ubiquitinated form of proteasomal $\alpha 2$, but not the 19S cap (Rpn7/S10a), is pulled down with myc-tagged ALAD in transfected PC-3 cells. Lysates from myc-tagged full length ALAD-transfected PC-3 cells were immunoprecipitated with anti-myc followed by Western blot analysis with the indicated antibodies. D) ALAD is not pulled down with the 19S proteasome. Lysates from empty vector or myc-tagged full length ALAD-transfected PC-3 cells were immunoprecipitated with anti-Rpn10 (a 19S subunit), followed by Western blot analysis. Matched IgG immunoprecipitation was performed as a control. - = No transfection; V = Vector-transfected; A = ALAD-transfected; P = Pulldown; S = Supernatant; I = Input.

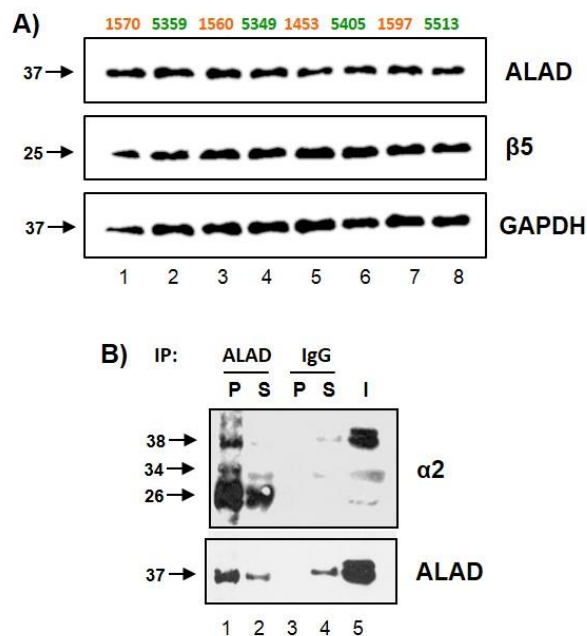


Figure 13. ALAD binds the 20S proteasome and is associated with ubiquitinated forms of $\alpha 2$ in human erythrocytes. A) Protein levels of endogenous ALAD protein in erythrocytes of prostate cancer patients and matched controls. Representative Western blot of 9/122 samples. Orange = Cases; Green = Controls. B) Endogenous ALAD in human erythrocytes interacts with a modified form of $\alpha 2$. Two samples expressing high levels of ALAD were subjected to analysis by immunoprecipitation-Western blot. Protein was immunoprecipitated with anti-ALAD followed by Western blotting with anti- $\alpha 2$. Matched IgG immunoprecipitation was performed as a control. P = Pulldown; S = Supernatant; I = Input.

ALAD inhibits proteasomal CT-like activity and is a proteasomal target protein

To verify the proteasome inhibitory ability of ALAD, PC-3 and LNCaP cells were transfected with empty vector or myc-tagged ALAD for 48 hours, followed by measurement of CT-like activity (Figure 14A). Overexpression of full length ALAD resulted in approximately 30% and 55% inhibition in PC-3 and LNCaP cells, respectively. Thus, ALAD does exhibit some proteasome inhibitory ability.

To investigate the regulation of ALAD, PC-3 cells were transfected with empty vector or myc-tagged ALAD, followed by treatment with the proteasome inhibitor MG-132. Analysis by Western blot reveals that treatment with MG-132 results in an accumulation of both endogenous and tagged ALAD proteins (Figure 14B), indicating that ALAD is a substrate protein of the proteasome.

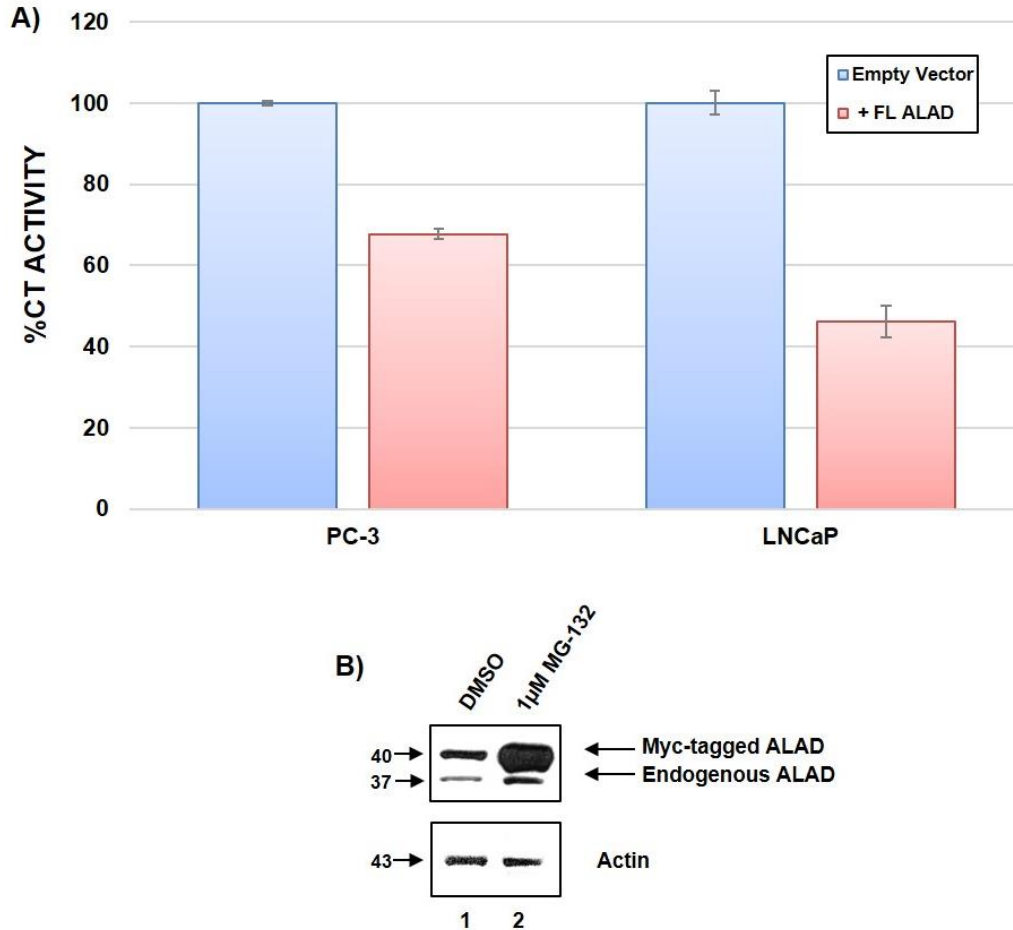


Figure 14. ALAD is both an inhibitor and a target of the proteasome. A) ALAD inhibits proteasomal CT-like activity. PC-3 or LNCaP cells were transfected with empty vector or myc-tagged full length ALAD for 48 h followed by measurement of proteasomal CT-like activity. B) ALAD is a proteasomal target protein. PC-3 cells were transfected with empty vector or myc-tagged full length ALAD for 48 h followed by treatment with 1µM MG-132 for 24 h and analysis by Western blot.

SAHA treatment enhances the ALAD-proteasome interaction, associated with acetylation of ubiquitinated $\alpha 2$ subunits

In an attempt to elucidate a role for HDAC inhibition in the regulation of ALAD and the proteasome, PC-3 cells were transfected with empty vector or myc-tagged full length ALAD for 48 h followed by treatment with 5 or 10 μM SAHA for 24 hours. Western blot analysis revealed that SAHA treatment dramatically increases expression levels of both endogenous and transfected ALAD proteins in a dose-dependent manner (Figure 15A). As a control, treatment of these cells with SAHA also increased levels of acetylated histone H3 protein (Figure 15A).

Importantly, SAHA treatment also enhances the interaction between ALAD and the 20S proteasome in ALAD-transfected PC-3 cells, compared with the solvent control (Figure 15B). Again, anti-myc pulled down a ubiquitinated protein(s) at a molecular weight identical to that of the modified $\alpha 2$ band (~ 38 kDa; Figure 15B; Lanes 5, 7), further suggesting that ALAD-associated $\alpha 2$ is ubiquitinated. Furthermore, the level of this $\alpha 2$ species was significantly increased following SAHA treatment (Figure 15B; Lanes 5 vs. 7). A specific anti-Ac-lysine antibody also recognized a similar band at ~ 38 kDa, suggesting that this modified $\alpha 2$ is also acetylated after SAHA treatment (Figure 15B; Lanes 5, 7). Again, the 19S subunit S10a was not found in the anti-myc pulldowns (Figure 15B), confirming that there is no 19S proteasome in the ALAD-20S proteasome complexes. These results suggest that in addition to increasing ALAD protein expression (presumably by inhibiting ALAD degradation), SAHA treatment also causes acetylation of ubiquitinated $\alpha 2$ subunits and enhances the ALAD-proteasome interaction.

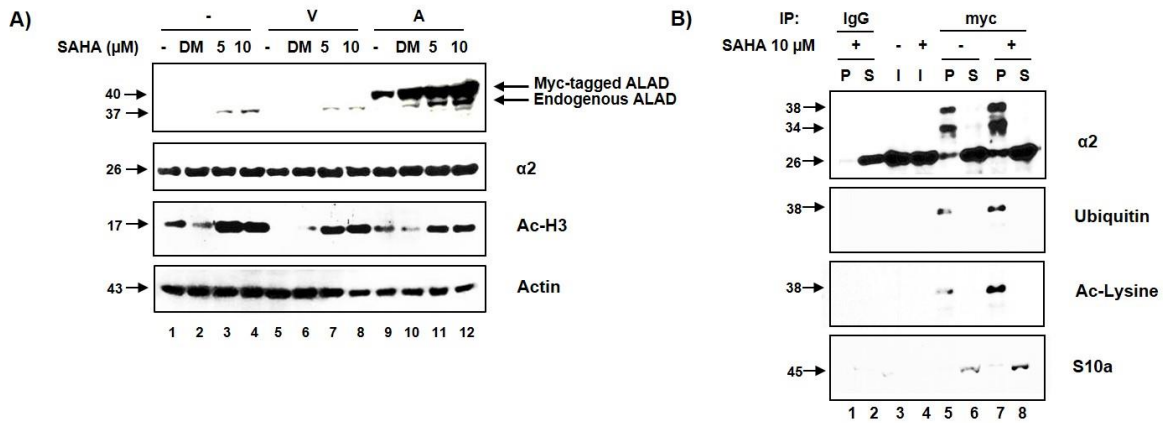


Figure 15. SAHA treatment enhances the ALAD-proteasome interaction, associated with acetylation of ubiquitinated $\alpha 2$ subunits. A) SAHA treatment enhances ALAD protein levels in a dose-dependent manner. Empty vector or myc-tagged full length ALAD-transfected PC-3 cells were treated with 5 or 10 μM SAHA for 24 h followed by Western blot analysis. V = Vector-transfected; A = ALAD-transfected; - = No treatment; DM = DMSO treatment. B) SAHA enhances the ALAD-proteasome interaction and promotes acetylation of ubiquitinated $\alpha 2$. Myc-tagged full length ALAD-transfected cells were treated with 10 μM SAHA for 24 h followed by immunoprecipitation with anti-myc and analysis by Western blot. Matched IgG immunoprecipitation was performed as a control. + = SAHA-treatment; - = DMSO treatment; P = Pulldown; S = Supernatant; I = Input.

SAHA treatment promotes nuclear localization of ALAD-proteasome complexes

It has been shown that proteasomes exist in both the nucleus and cytosol (Brooks, et al. 2000; Tanaka, et al. 1989). To ascertain whether ALAD interacts with cytosolic or nuclear proteasome, or both, ALAD-transfected PC-3 cells were fractionated into cytosolic and nuclear fractions, followed by Western blot analysis (Figure 16A). In these PC-3 cells, ALAD appears to exist only within the cytosol (Figure 15A; Lanes 3 vs. 7). Immunofluorescence was also performed and confirmed cytosolic localization of ALAD in untreated ALAD-transfected PC-3 cells (Figure 16B). However, when transfected PC-3 cells were treated with 10 μ M SAHA, followed by cellular fractionation, Western blot analysis revealed that SAHA treatment causes nuclear localization of ALAD (Figure 16A; Lanes 7 vs. 8); actin and H3 proteins were used as cytosolic and nuclear controls, respectively.

Immunoprecipitation with anti-myc following transfection and SAHA-treatment demonstrated that SAHA treatment also causes nuclear localization of ALAD-associated ubiquitinated α 2 (Figure 16C; Lane 7). Anti-myc antibody pulled down ubiquitinated α 2 in the nuclear, but not the cytosolic fraction of ALAD-overexpressing PC-3 cells after SAHA treatment, compared with DMSO-treated cells (Figure 16C). Additionally, nuclear ubiquitinated α 2 is also acetylated in the SAHA-treated (compared with DMSO-treated) ALAD-overexpressing cells (Figure 16C; Lane 7). Together, these results suggest that acetylation may function to localize ALAD-associated ubiquitinated α 2-containing proteasome complexes to the nucleus.

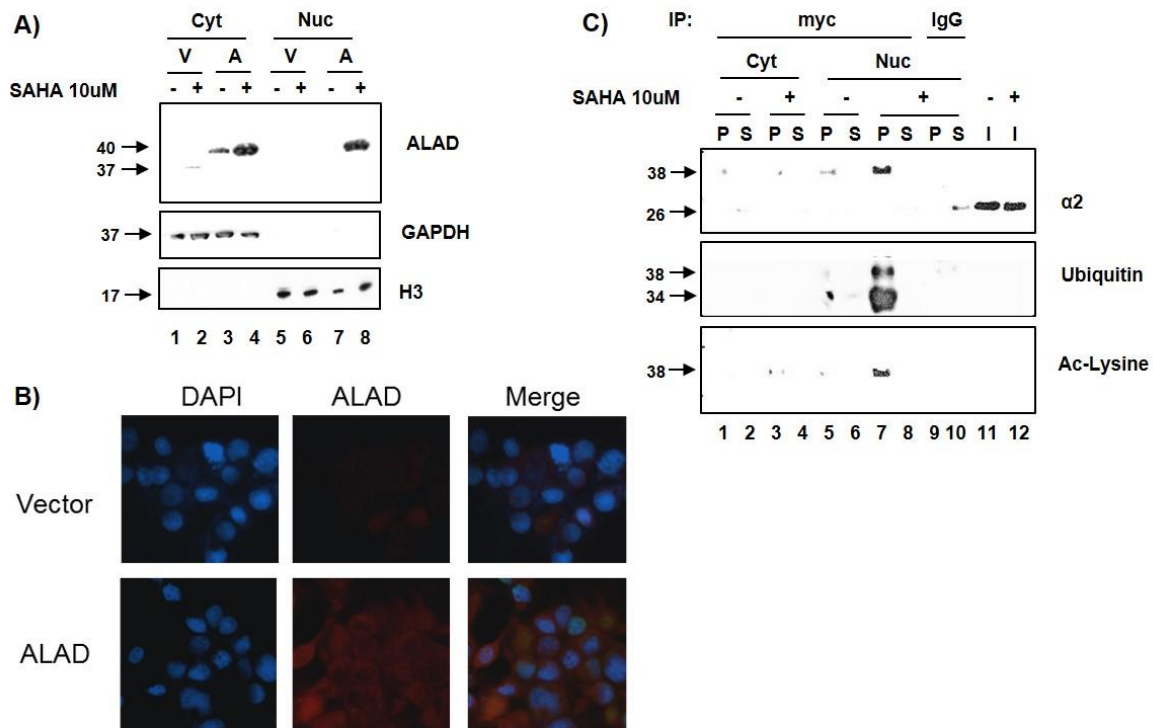


Figure 16. SAHA-treatment promotes nuclear localization of ALAD and modified $\alpha 2$. A) ALAD is a cytosolic protein that is localized to the nucleus after treatment with SAHA. Vector or myc-tagged full length ALAD-transfected PC-3 cells were treated with 10 μ M SAHA for 24 h followed by subcellular fractionation and analysis by Western blot. B) ALAD is a cytosolic protein. ALAD-transfected PC-3 cells were visualized by immunofluorescence microscopy. The lack of purple color in the nuclei indicates that ALAD exists only in the cytosol under normal conditions. C) SAHA-treatment promotes nuclear localization of acetylated/ubiquitinated $\alpha 2$. PC-3 cells transfected with myc-tagged full length ALAD for 48 h were treated with 10 μ M SAHA for 24 h, followed by subcellular fractionation, immunoprecipitation with anti-myc, and Western blot analysis. Matched IgG immunoprecipitation was performed as a control. Cyt = Cytosolic fraction; Nuc = Nuclear fraction; V = Vector-transfected; A = ALAD-transfected; + = SAHA-treatment; - = DMSO treatment; P = Pulldown; S = Supernatant; I = Input.

Purified ALAD promotes ubiquitination of proteasomal $\alpha 2$ under cell free conditions

To determine whether ALAD plays a direct role in the ubiquitination of proteasomal $\alpha 2$, a cell-free ubiquitination assay was performed. Purified ALAD, ubiquitin, and 20S proteasome were incubated with a PC-3 cell extract (to provide necessary enzymatic activities) in a buffer containing ATP for 2 hr at 37°C, followed by Western blot analysis with anti-ubiquitin. In the presence of cell lysate, ubiquitin and 20S proteasome as well as purified ALAD, a ubiquitinated protein with MW 38 kDa (Figure 17), similar to ubiquitinated proteasomal $\alpha 2$ (Figures 12, 13, 15, 16), was detected. However, it was not observed when any one of the components was missing (Figure 17), suggesting that purified ALAD is able to promote ubiquitination of proteasomal $\alpha 2$ subunits in a cell-free system.

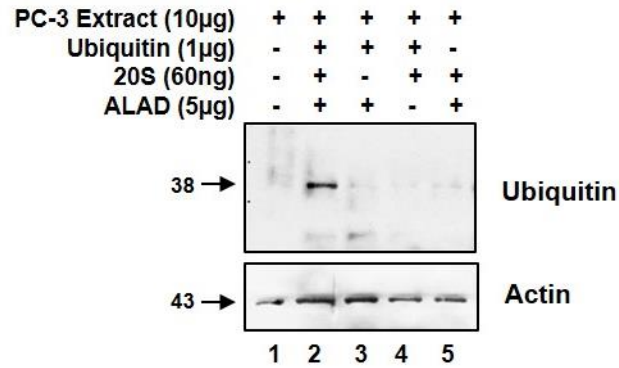


Figure 17. Purified ALAD promotes ubiquitination of proteasomal α 2 under cell free conditions. PC-3 cell lysates (10 μ g; no transfection) were incubated with 6 mM ATP and various combinations of purified ALAD (5 μ g), ubiquitin (1 μ g) and human 20S proteasome (60 ng) for 2h followed by analysis by Western blot with anti-ubiquitin or anti-actin (as control).

DISCUSSION

Many proteins are known to interact with the proteasome to carry out various functions. Some examples include Rad23 which is a carrier molecule for proteins destined for the proteasome (Elsasser, et al. 2002), HSP70 which aids in the unfolding of protein substrates prior to their degradation by the proteasome (Bercovich, et al. 1997) and ALAD, which has been reported to inhibit the proteasome (Guo et al. 1994) upon its direct binding to the proteasome (Bardag-Gorce and French 2011). Additionally, the proteasome has been reported to exist in several forms, including the constitutive 26S proteasome, which is the most common form, consisting of the 20S core and two 19S regulatory caps. Alternatively, the 20S core can be unbound, the predominant species in mature ALAD-expressing erythrocytes (Neelam, et al. 2011), or it can contain immune-specific catalytic subunits and interact with two 11S regulatory subunits to form the immunoproteasome. The data presented in this chapter have confirmed that the proteasome exists in an ALAD-bound state, in which ALAD binds in place of the 19S regulatory cap(s) (Figures 12B-D). It is possible that when ALAD is bound, substrate proteins are unable to enter the catalytic core, thus inhibiting its activity (Figure 18). Consistently, transfection of prostate cancer cells with full length ALAD did result in decreased proteasomal activity (Figure 14A). However, further studies are necessary to confirm this molecular mechanism.

These data show that ALAD promotes ubiquitination of 20S proteasomal $\alpha 2$ subunits (Figures 12B, C; 13B; 18). Post-translational modifications are important for the proper assembly and function (Iwafune, et al. 2002; Kimura, et al. 2000; Satoh, et al. 2001; Zhang, et al. 2003) of the 26S proteasome, and studies have shown that these post-translational modifications include phosphorylation, myristylation, glycosylation and acetylation (Kikuchi, et al. 2010). Monoubiquitination, unlike polyubiquitination, does not serve as a signal for degradation, rather

it can be a signal for fates like receptor internalization, vesicle sorting, DNA repair, gene silencing and subcellular localization (Gregory, et al. 2003; Johnson 2002). Additionally, monoubiquitination of the 19S subunit Rpn10/S5a has been reported to inhibit its binding to ubiquitinated protein substrates by blocking its ubiquitin-interacting motif (Isasa, et al. 2010). However, ubiquitination of 20S subunits has not been reported. Thus, a previously unreported post-translational modification to a proteasomal 20S subunit, which may serve to alter its function, is described here. The monoubiquitination of proteasomal $\alpha 2$ (Figures 12B, C; 13B) may directly inhibit its function, or it may serve as a docking point for ALAD, which when bound, inhibits proteasome activity. The exact function for this ubiquitination, as well as potential ubiquitination of other 20S core proteins must also be explored.

Due to previous success with the combination of the HDAC inhibitor SAHA and proteasome inhibitors like bortezomib, the effects of SAHA on ALAD and its interaction with the 20S proteasome were investigated. Interestingly, SAHA treatment enhances ALAD protein levels as well as the ALAD-proteasome interaction (Figure 15A, B). In addition to its enhancement of ALAD protein levels, SAHA also causes acetylation (Figure 15C) and nuclear localization (Figure 16C) of the ubiquitinated proteasomal $\alpha 2$ species. While protein acetylation has only recently been heavily explored, many functions have been suggested for the cytosolic acetylation of proteins. Several studies have revealed at least one-hundred proteins that are acetylated for purposes like cytoskeletal regulation and transport along the cytoskeleton, translation, membrane transport, and subcellular localization (Sadoul, et al. 2011). Interestingly, protein acetylation has also been described in other cellular organelles including the mitochondria, ER and Golgi apparatus (Sadoul et al. 2011). When acetylation serves as a marker for localization, it enhances the nuclear localization of some proteins and the cytosolic localization of others (Sadoul et al. 2011). While

proteasomes are expressed ubiquitously throughout the cell (Brooks et al. 2000; Tanaka et al. 1989), ALAD is a cytosolic protein (Lim and Sassa 1993), as expected, since its major role is in heme biosynthesis. Cytosolic localization of ALAD (Figure 16A, B) has also been confirmed, and the data also revealed that treatment with the HDAC inhibitor SAHA results in translocation of proteasome-bound ALAD into the nucleus (Figure 16A). Therefore, it is possible that acetylation of ALAD-bound $\alpha 2$ subunits functions to cause nuclear import of proteasomes, which might have an important function, for example, inducing tumor cell death or growth inhibition (Figure 18), which must be further investigated.

Taken together, the data in this chapter suggest the following mechanism (Figure 18): i) ALAD binds to the proteasomal α ring in place of the 19S regulatory cap, promoting ubiquitination of $\alpha 2$ (and possibly other α subunits), and ii) upon HDAC inhibition, ALAD levels are enhanced, ALAD-bound-, ubiquitinated $\alpha 2$ is acetylated and the ALAD-proteasome (with acetylated/ubiquitinated- $\alpha 2$) complex translocates into the nucleus. Further understanding of ALAD-proteasome complexes may have a clinical impact in improving proteasome inhibitor or HDAC inhibitor-based anti-cancer therapies.

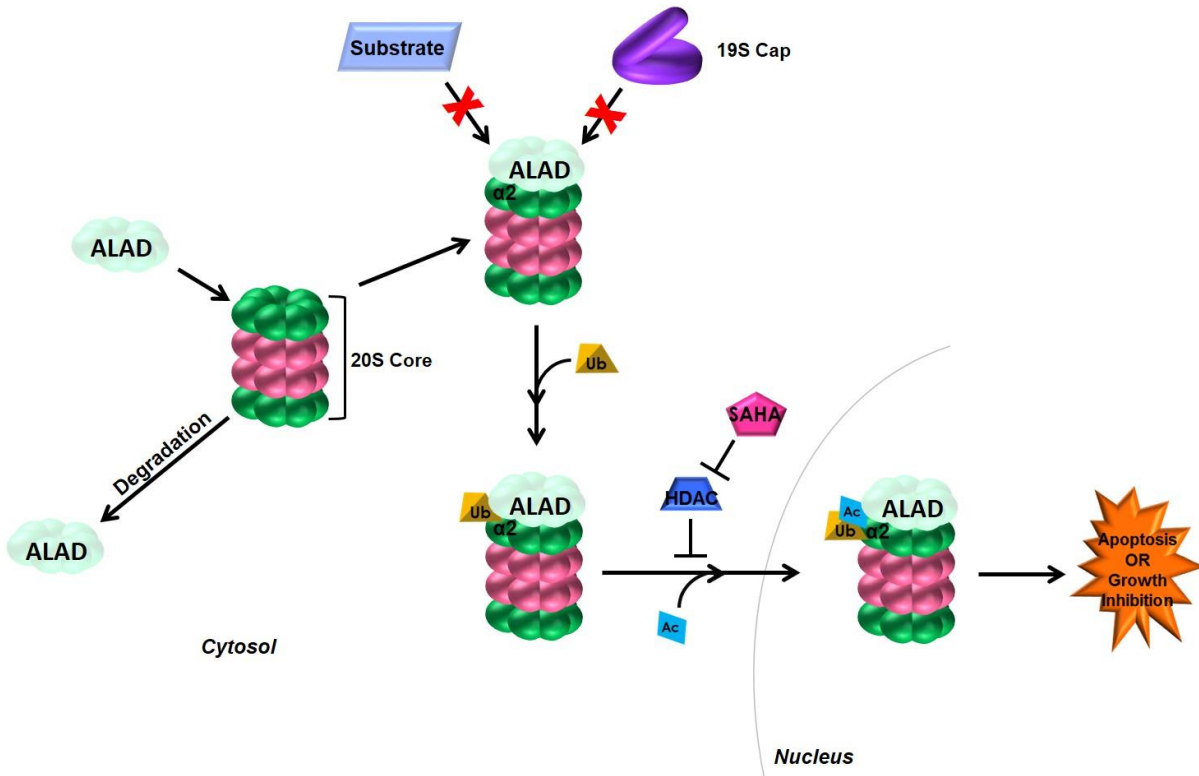


Figure 18. Proposed Mechanism of ALAD-Proteasome Binding. ALAD binds to the 20S proteasomal core in place of the 19S proteasome and promotes ubiquitination of $\alpha 2$ subunits (and potentially other α subunits). ALAD binding to the 20S core hinders binding of the 19S regulatory cap(s), thus inhibiting entry of substrate proteins into the catalytic core. Upon HDAC inhibition, ALAD levels are enhanced, ubiquitinated $\alpha 2$ is acetylated and the ALAD-proteasome (with acetylated/ubiquitinated- $\alpha 2$) complex translocates into the nucleus, likely resulting in induction of apoptosis or cell growth inhibition in tumor cells.

CHAPTER 4

METAL COMPLEXES TARGETING THE 20S PROTEASOMAL CORE

Metals have been intensively studied for decades following the success of cisplatin as a treatment for cancer. This search for new metal-based drugs, spurred by the limitations, including toxicity and resistance, of cisplatin, began with second-generation platinum-based compounds like carboplatin and oxaliplatin (Alama, et al. 2009; de Gramont, et al. 2000; Harrap 1985). Thus, the investigation into new metal-based drugs began with the design of structurally similar complexes containing platinum, with the hypothesis that similar structure leads to similar function (Calamai, et al. 1998). However, while structure and the identity of the metal center are important, the activities of these metal compounds are also influenced by oxidation state and coordination geometry of the complex, as well as redox activity, electric charge and kinetic lability.

Along this line, various metal centers with different ligand structures have been investigated for their ability to suppress tumor growth both *in vitro* and *in vivo*. Cadmium-, copper-, gallium-, gold-, ruthenium- and zinc-containing complexes (Bastow, et al. 2011; Calamai et al. 1998; Chen et al. 2007b; Cvek, et al. 2008; Frezza, et al. 2009; Hartinger, et al. 2008; Jakupec, et al. 2005; Milacic, et al. 2008a; Milacic et al. 2006; Sava, et al. 1995; Sava, et al. 1992; Zhang et al. 2010; Zhang, et al. 2013), as well as copper-chelating compounds, which take advantage of high intracellular copper levels (Chen et al. 2007a; Chen et al. 2006; Daniel, et al. 2004; Lee, et al. 2013), have all been shown to be active against many human cancers. While cisplatin is known to target DNA and form adducts, many of these metal-based complexes are potent inhibitors of the proteasome. The successful results from previous studies led to further investigation into a series of metal complexes incorporating different metals and new ligand structures, which are described in this chapter.

First, the proteasome- and tumor-inhibiting capabilities of a series of cobalt-containing complexes, $[\text{Co}^{\text{II}}(\text{L}^1)_2]$ (**1**), $[\text{Co}^{\text{II}}(\text{L}^2)]$ (**2**), and $[\text{Co}^{\text{III}}(\text{L}^1)_2]\text{ClO}_4$ (**3**) (Figure 19), were explored. These complexes contain the deprotonated forms of the previously reported $[\text{NN}'\text{O}]$ tridentate ligand **HL**¹ and its newly synthesized $[\text{N}_2\text{N}'_2\text{O}_2]$ hexadentate counterpart **H₂L**² (2,4-diiodo-6-((pyridine-2-ylmethylamino)methyl)phenol and 6,6'-((ethane-1,2-diylbis((pyridin-2-ylmethyl)azanediyl))bis(methylene))bis(2,4-diiodophenol)). Species **3**, the most inert, but redox active species was determined to be the most potent due to its tethered ligand structure combined with the redox activity of its Co(III) metal center, which promotes intracellular ligand dissociation (Tomco et al. 2011).

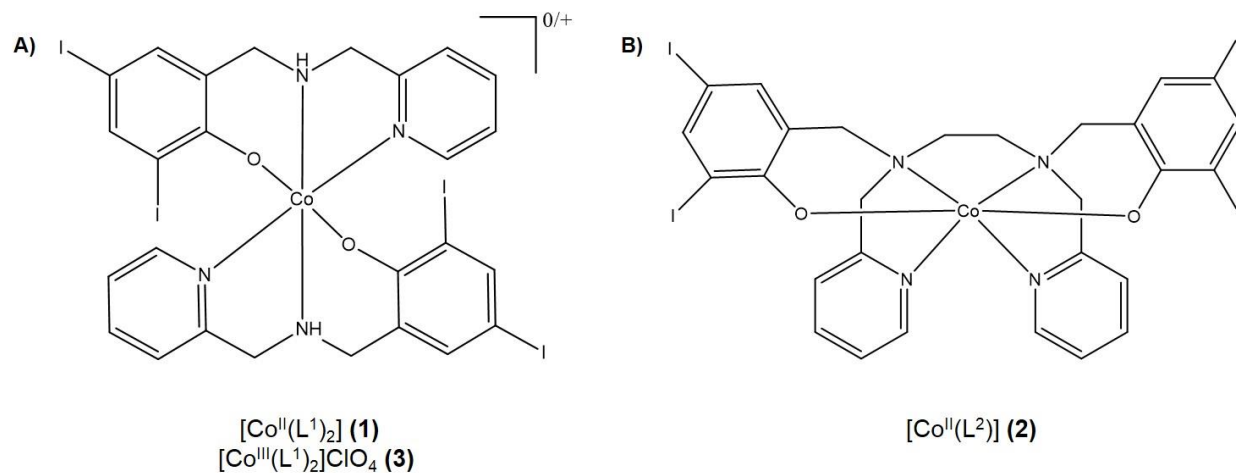


Figure 19. Structures of Cobalt Compounds. A) $[Co^{II}(L^1)_2]$ (1) and $[Co^{III}(L^1)_2]ClO_4$ (3) B) $[Co^{II}(L^2)]$ (2)

A set of novel gold(III)-based complexes, AuD6 and AuD8 ($[[\text{Au}^{\text{III}}\text{Br}_2(\text{dtc-Sar-AA-O}(t\text{-Bu}))]]$ with AA = Gly or Aib (α -aminoisobutyric acid), respectively) whose ligands are di-peptide derivatives differing only in the substituents at the α -carbon atom at the C-terminus (Figure 20), was then investigated. While both compounds proved to be potent proteasome inhibitors and tumor growth suppressors *in vitro* and *in vivo*, AuD8 was slightly more potent (Nardon et al. 2014). AuD8 was also more selective against CT-like activity, which may explain its increased tumor growth inhibitory ability compared to AuD6.

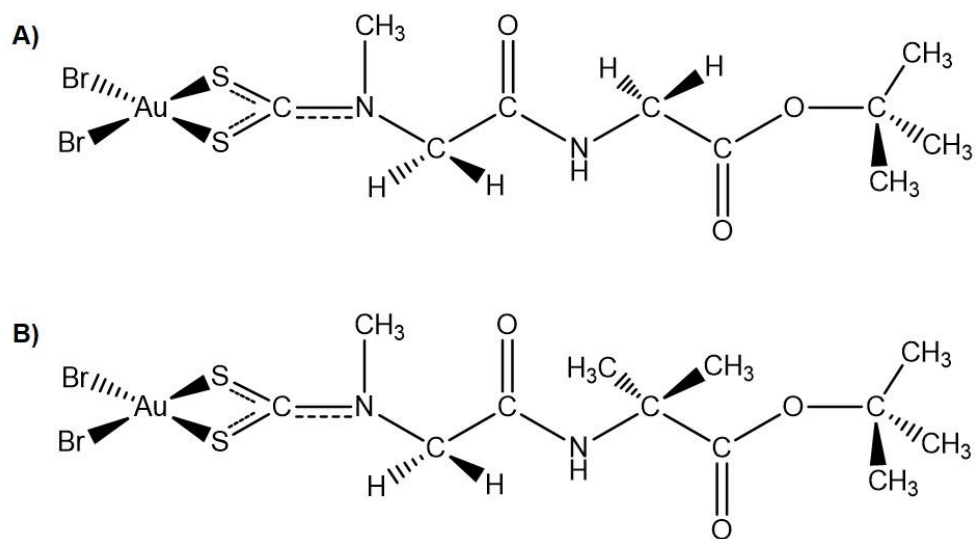


Figure 20. Structures of New Gold(III) Complexes. A) AuD6 B) AuD8

Next, proteasome inhibition as a secondary mechanism of toxicity for heavy metal species was examined. The toxicity of a series of aluminum-, cadmium-, mercury-, lead- and tin-species, $[\text{Al}^{\text{III}}(\text{L}_{\text{iodo}})_2]\text{ClO}_4$ (#1), $[\text{Cd}^{\text{II}}(\text{L}_{\text{iodo}})\text{Cl}]\cdot\text{H}_2\text{O}$ (#2), $[\text{Hg}^{\text{II}}(\text{L}_{\text{iodo}})_2]\cdot 4\text{DMSO}$ (#3), $[\text{Pb}^{\text{II}}(\text{L}_{\text{iodo}})\text{NO}_3]$ (#4), and $[\text{Sn}^{\text{IV}}(\text{L}_{\text{iodo}})\text{Cl}_3]$ (#5) (Figure 21), was confirmed in transformed human prostate cells, with the aluminum species (#1) being the most potent. However, this species, as well as the tin-containing compound (#5), showed little to no proteasome inhibitory activity, suggesting that their toxicity is likely due to mechanisms other than proteasome inhibition. The correlation between proteasome and cell growth inhibition of cadmium (#2) and lead (#4) species was somewhat stronger, indicating that the toxicity of these species may be due to proteasome inhibition. The significant proteasome inhibition coupled with potent cell growth inhibition resulting from treatment with the mercury complex (#3), suggests that proteasome inhibition is a secondary mechanism for mercury toxicity (Tomco et al. 2014).

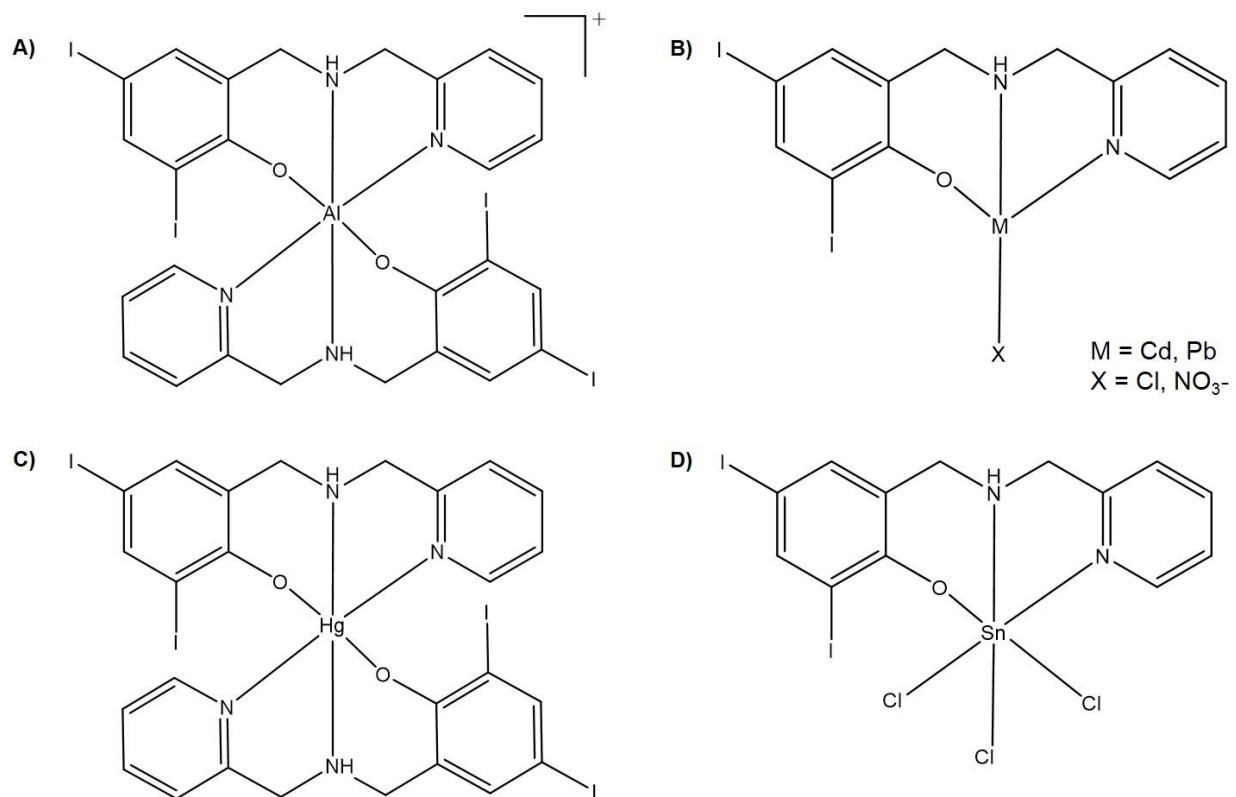


Figure 21. Structures of Heavy Metal Complexes. A) $[Al^{III}(L_{iodo})_2]ClO_4$ (#1) B) $[Cd^{II}(L_{iodo})Cl] \cdot H_2O$ (#2), $[Pb^{II}(L_{iodo})NO_3]$ (#4) C) $[Hg^{II}(L_{iodo})_2] \cdot 4DMSO$ (#3) D) $[Sn^{IV}(L_{iodo})Cl_3]$ (#5)

The proteasome-inhibitory, apoptosis-inducing activity of a second-generation tethered gallium complex, Ga^{III}DiIBPEN, was then compared to that of the same ligand containing zinc, Zn^{II}DiIBPEN (Figure 22). Unexpectedly, the 1:2 metal:ligand gallium complex was more potent than the first generation 1:1 metal:ligand gallium complex (Chen et al. 2007b), with the zinc-containing species being completely inactive. Like the cobalt species, the increased potency of the gallium(III) species is likely due to its redox activity compared to zinc(II), again promoting ligand dissociation to create the preferred 1:1 species (Tomco et al. 2011). This tethered complex may be more stable in solution, giving it more time to reach its target. Additionally, the bioavailability and promiscuity of zinc may result in the zinc(II) species being intercepted by other proteins within the cell prior to it reaching the proteasome.

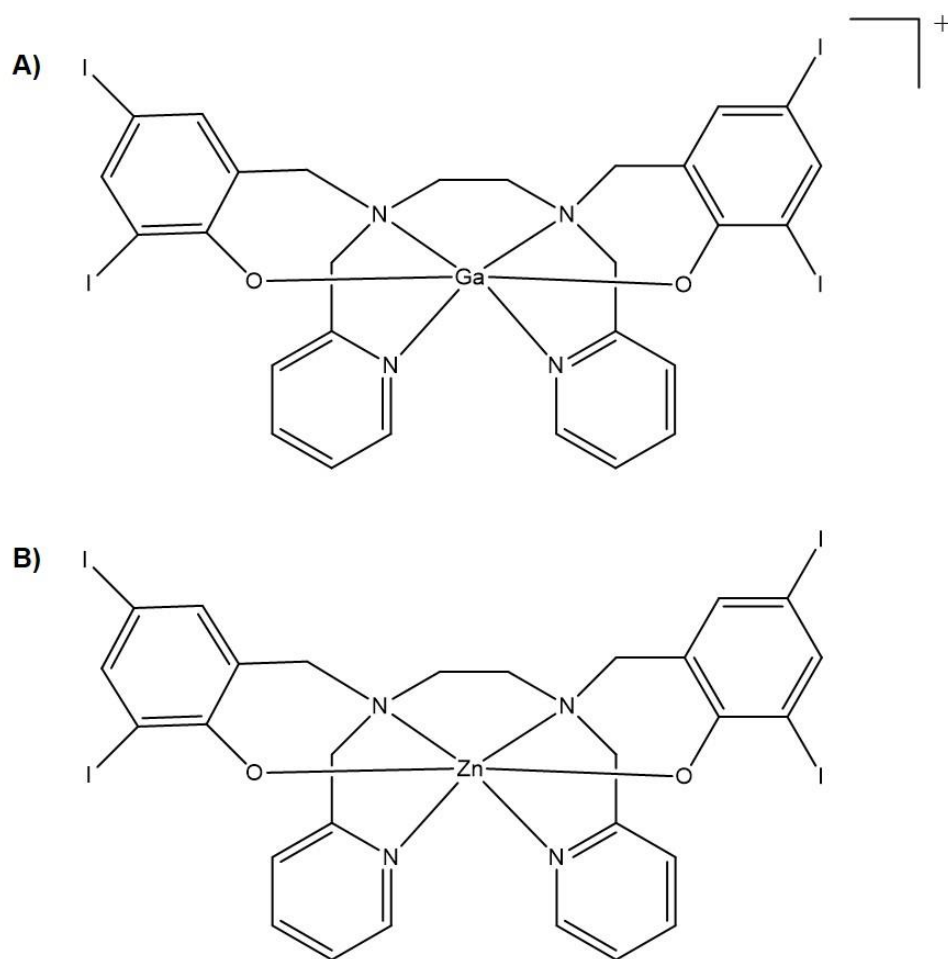


Figure 22. Structures of Tethered Ga(III) and Zn(II) Complexes.
A) $\text{Ga}^{\text{III}}\text{DiIBPEN}$ B) $\text{Zn}^{\text{II}}\text{DiIBPEN}$

Finally, the antibiotic nitroxoline (Figure 23A), a strong copper chelator (Pelletier, et al. 1994) that has been used for years for the treatment of urinary tract infections, was shown to be a more potent proteasome inhibitor and tumor growth suppressor both *in vitro* and *in vivo* than the structurally similar compound clioquinol (Figures 11B; 23B). Importantly, 5NHQ has previously been shown to induce tumor cell death by inhibition of angiogenesis in bladder cancer (Shim, et al. 2010), as well as through the generation of reactive oxygen species in lymphoma, leukemia and pancreatic cancer cells (Jiang, et al. 2011). Thus, this chapter presents a new mode of action for the antibiotic nitroxoline, further validating that using previously approved drugs is a viable strategy for the treatment of human cancers.

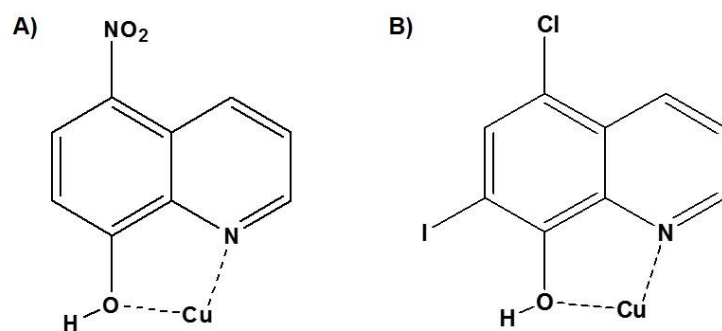


Figure 23. Structures of Nitroxoline and Clioquinol. A) Nitroxoline (5NHQ) B) Clioquinol (CQ). Dashed lines represent species bound to copper.

4.1 Effects of Tethered Ligands and of Metal Oxidation State on the Interactions of Cobalt Complexes with the 26S Proteasome

Adapted from published material in J Inorg Biochem. 2011 December; 105(12):1759–1766.

RESULTS

Complex 3, the Co(III) species, inhibits cellular proliferation

To determine the effects of complexes **1** and **3** (Figure 19) on cell proliferation, human prostate cancer PC-3 cells were treated with various concentrations of **1**, **3**, or DMSO as a solvent control, for 18 hours followed by measurement by MTT assay (Figure 24). Cells treated with **3** exhibited dramatically decreased cell proliferation in a dose-dependent manner, with a 40% decrease in cell proliferation at 20 $\mu\text{mol/L}$ and reaching nearly 100% inhibition at 30 $\mu\text{mol/L}$. In contrast, treatment with **1** resulted in little inhibition of cellular proliferation (~30%) even at the highest concentration tested.

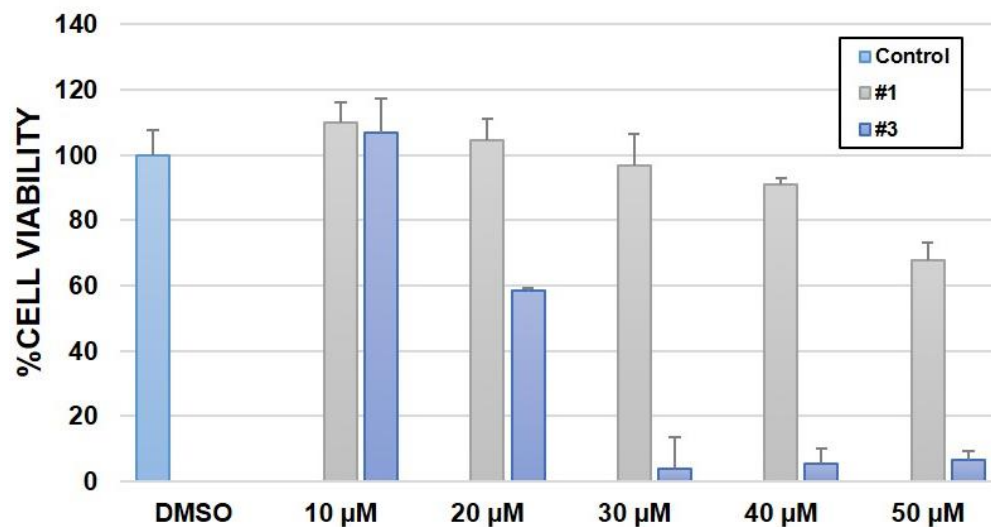


Figure 24. Complex 3, the Co(III) species, inhibits PC-3 cell proliferation. PC-3 cells were treated with 10-50 μ M compound 1 or 3 for 18 h followed by analysis by MTT assay.

Complex 3 inhibits purified 20S proteasome

To test the proteasome inhibitory ability of these species, **1**, **2** and **3** were compared under cell-free conditions. Human purified 20S proteasome was incubated with ligand alone, $\text{Co}^{\text{II}}(\text{ClO}_4)_2$ salt, or **1**, **2** and **3** at different concentrations, followed by measurement of CT-like activity. CT-like activity was drastically inhibited by **3** (Figure 25B), modestly inhibited by $\text{Co}^{\text{II}}(\text{ClO}_4)_2$ salt, but not by **1** or **2** (Figure 25A). These results indicate that Co(III) is potent against purified proteasome, while Co(II) is inactive regardless of its ligand.

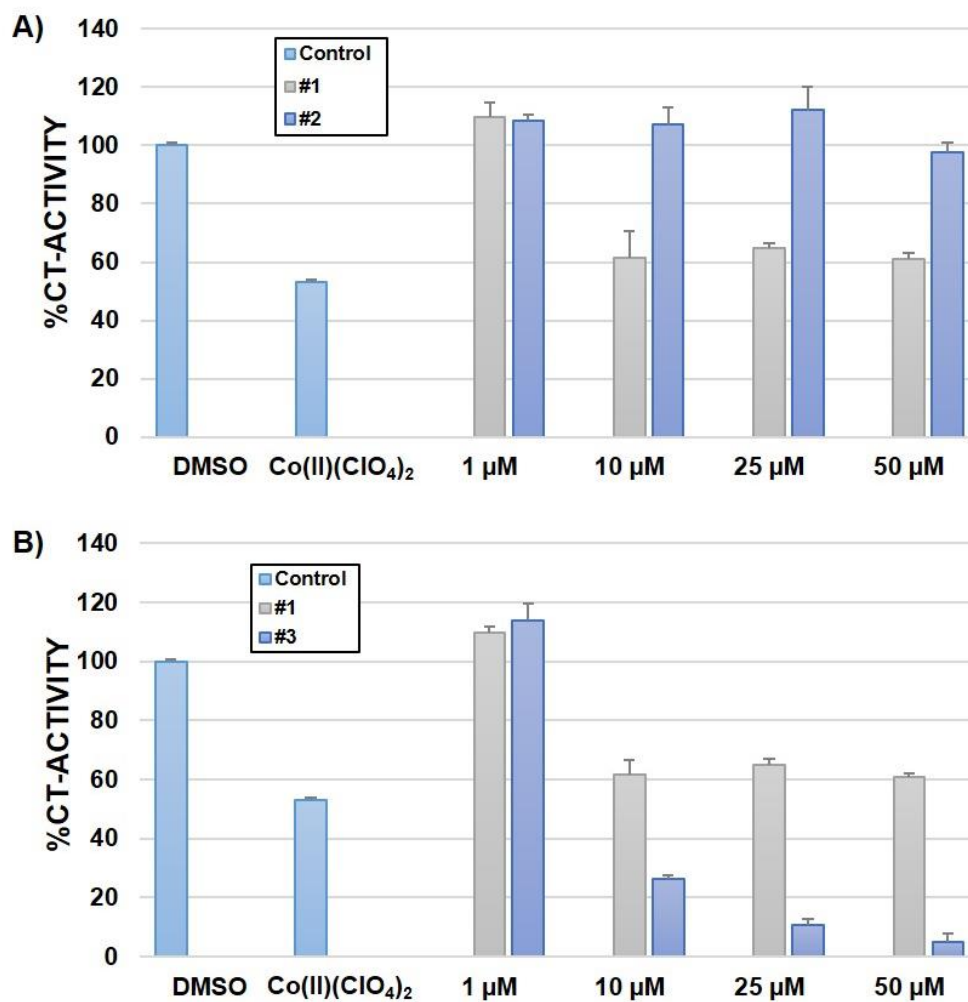


Figure 25. Complex 3 inhibits purified 20S proteasome activity. Purified proteasome was incubated with 1-50 μM compound 1, 2 or 3 for 2-4 h, followed by measurement of CT-like activity. A) Compound 1 versus 2 B) Compound 1 versus 3.

Complex 3 inhibits cellular proteasome activity and induces apoptosis in prostate cancer cells

To confirm the ability of **3** to inhibit proteasomal activity in intact tumor cells, PC-3 cells were first treated with different concentrations (up to 50 μ M) of **1** and **3** for 18 hours, followed by measurement of proteasome inhibition. PC-3 cells treated with **3** showed a dose-dependent inhibition of proteasomal activity by ~35% at 30 μ M and ~95% at 50 μ M (Figure 26). Consistently, increased accumulation of ubiquitinated proteins was also observed in a dose-dependent manner (Figure 27B). Conversely, cells treated with **1** showed negligible proteasome inhibition.

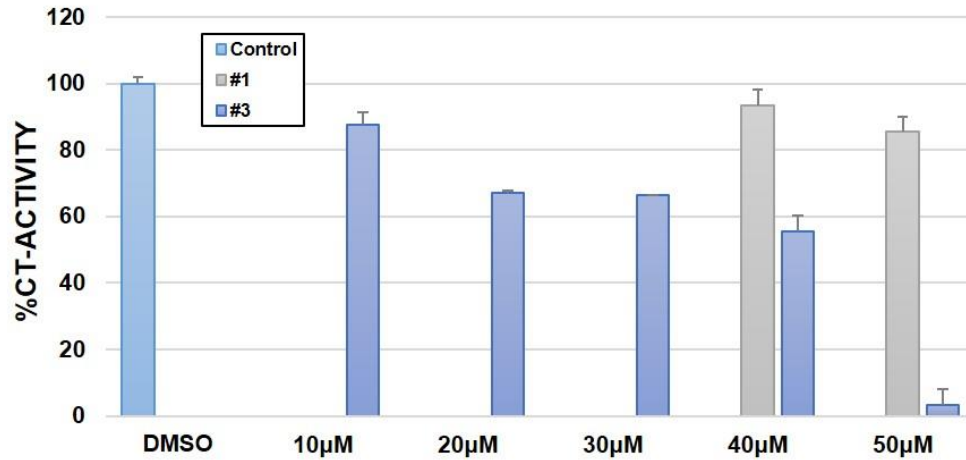


Figure 26. Complex 3 inhibits cellular proteasome activity. PC-3 cells were treated with up to 50 µM of **1** and **3** for 18h followed by measurement of proteasome activity.

To investigate whether proteasome inhibition is associated with apoptotic cell death, apoptosis-specific caspase-3 induction and PARP cleavage were measured spectrophotometrically and by Western blot analysis (Figure 27). Dramatic induction of caspase-3 was observed in cells treated with **3** at 40 μ M (Figure 27A) and, as expected, abrogation of full length PARP also occurred in cells treated with 30-50 μ M **3** (Figure 27B). Cells treated with **1** at the highest concentration tested had little visible effect. Thus, induction of apoptosis by **3** in PC-3 cells is associated with inhibition of proteasomal chymotrypsin-like activity.

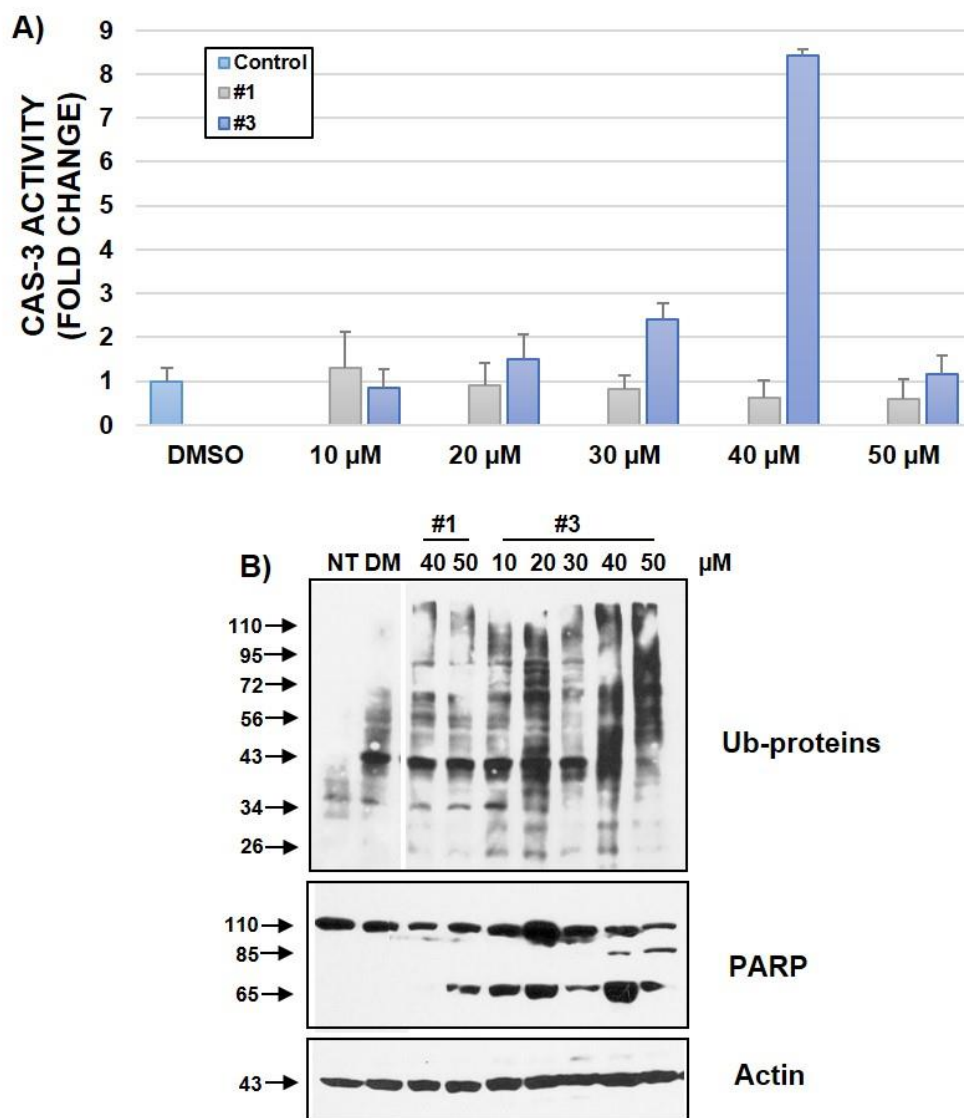


Figure 27. Complex 3 induces apoptosis in PC-3 cells. PC-3 cells were treated with 10-50 μ M of 1 and 3 for 18h followed by A) measurement of caspase-3 activity and B) Western blot analysis.

DISCUSSION

The data in this chapter describe an interaction between cobalt complexes and the 26S proteasome. Specifically, the activities of 1:2 and 1:1 metal-to-ligand six-coordinate cobalt species toward cell proliferation, purified 20S proteasome, and intact PC-3 prostate cancer cells were compared. The 1:2 species **1** and **3** are formed respectively between cobalt(II) or cobalt(III) ions and two deprotonated $[NN'O]$ ligands (L^1), whereas the 1:1 species **2** is comprised of a cobalt(II) ion and the new $[N_2N'O_2]$ ligand H_2L^2 in its deprotonated form. Proteasome inhibition is severely hampered for the 1:1 species **2**, confirming the need for ligand dissociation as a requirement for proteasome inhibition. Surprisingly, the kinetically inert **3** showed remarkable proteasome inhibition, far superior to that observed for the labile **1**, which is likely due to the fact that cobalt(III) is a redox-active species capable of being reduced to cobalt(II) within the reducing cellular environment by available reductants. This reduction has been demonstrated individually by several groups and utilized for release of alkylating agents such as nitrogen mustards (Hall, et al. 2007; Schieber, et al. 2011). In this process a labile cobalt(II) species is generated, favoring ligand dissociation and interaction with the proteasome. Additionally, it is unlikely that species **1**, which already contains a labile cobalt(II) species will remain intact within cells, prohibiting it from reaching the target, which in this case is the proteasome. Thus, the possibility of using redox-active metals that can be reduced intracellularly opens a stimulating window of opportunity to explore proteasome inhibition, both by metal activation as demonstrated here and in other studies (Souza, et al. 2009), as well as by using metal ions as carriers for drug delivery (Hall et al. 2007).

4.2 Gold(III)-Dithiocarbamate Peptidomimetics in the Forefront of the Targeted Anticancer Therapy: Preclinical Studies against Human Breast Neoplasia

Adapted from published material in PLoS One. 2014; 9(1): e84248.

RESULTS

Inhibition of MDA-MB-231 cell proliferation by AuD6 and AuD8 in comparison with cisplatin

The *in vitro* cytotoxicity of AuD6 and AuD8 (Figure 20) against MDA-MB-231 cells was assessed via MTT assay after 24 hour treatment. While both complexes inhibited tumor cell growth in a concentration-dependent manner, AuD8 was much more potent than AuD6, with an IC_{50} value \pm SD of 6.5 ± 0.6 (Figure 28A) compared to 17 ± 1 μ M (Figure 28B), respectively. Notably, MDA-MB-231 cells were resistant to cisplatin under the same experimental conditions. In fact, after 24 hour treatment with 100 μ M, the IC_{50} was not reached (Hong, et al. 2008). In concordance with previous studies reporting slower kinetics of cisplatin, about 30% inhibition was observed following 24 hour treatment with 100 μ M cisplatin (Ronconi, et al. 2006).

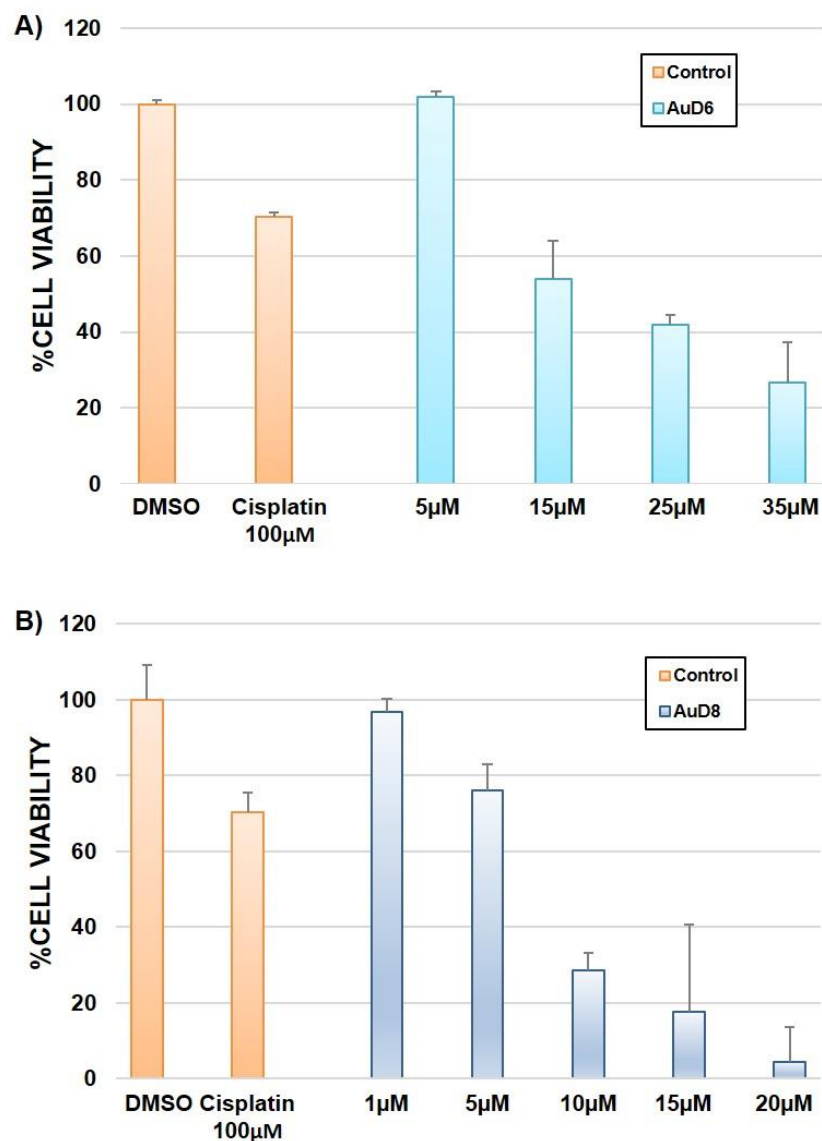


Figure 28. AuD6 and AuD8 are potent inhibitors of cellular proliferation. MDA-MB-231 cells were treated with increasing concentrations of A) AuD6 or B) AuD8, or 100 μM cisplatin for 24 h followed by measurement of cell viability by MTT assay.

The ROS scavenger Trolox enhances the antiproliferative ability of AuD6

To determine if generation of reactive oxygen species is a potential mechanism of these gold-based compounds, MDA-MB-231 cells were co-treated with AuD6 or AuD8 and Trolox (Figure 29), the hydrophobic form of vitamin E, which is able to scavenge free radicals (Arellano, et al. 2011). First, cells were pretreated with 100 μ M Trolox for 1 hour, followed by 24 hour treatment with each of the gold compounds. No changes in IC₅₀ values for either compound were recorded (Figure 29), suggesting that inhibition of cell growth is independent of ROS generation. Cells were then co-treated with each of compounds and Trolox (100 μ M) for 24 hours. As expected, higher antiproliferative activity was observed in the presence of Trolox. In fact, Trolox alone inhibited tumor cell growth by approximately 25% after 24 hours (Figure 29). Interestingly, Trolox reduced the IC₅₀ of AuD6 approximately 3-fold, with very little effect on the activity of AuD8, suggesting that AuD6 may work in concert with Trolox to induce cell death, similar to results reported in other studies (Zheng, et al. 2012).

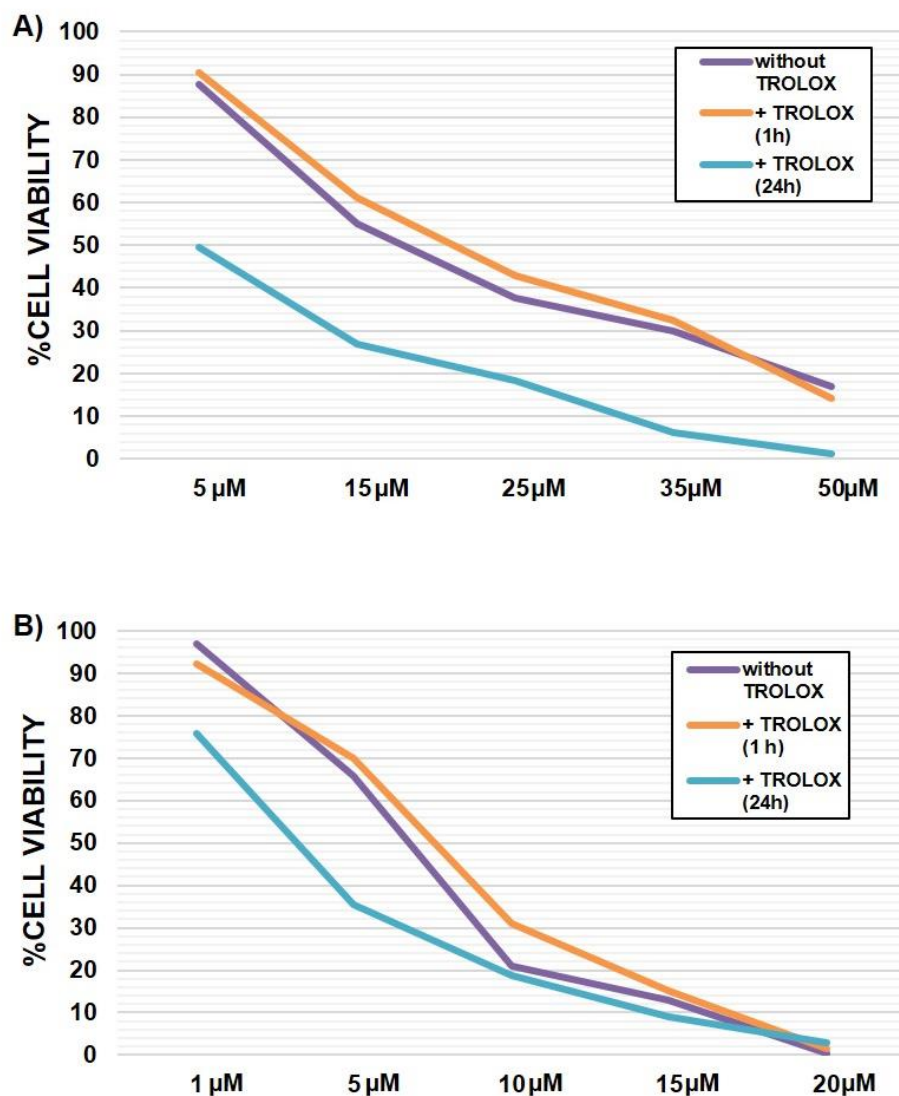


Figure 29. Trolox enhances the anti-proliferative ability of AuD6. MDA-MB-231 cells were either pretreated with 100 μM Trolox for 1 h followed by 24 h treatment with increasing concentrations of A) AuD6 or B) AuD8; or cells were co-treated for 24 h with 100 μM Trolox and increasing concentrations of A) AuD6 or B) AuD8.

AuD6 and AuD8 inhibit the proteasome under cell-free conditions

To test the hypothesis that these gold compounds possess proteasome inhibitory activity, purified human 20S proteasome or MDA-MB-231 cell extract was incubated with increasing concentrations of each compound or DMSO, as control, and proteasomal CT-like, trypsin-like and PGPH-like activities were measured fluorogenically. Both complexes inhibited all three enzymatic activities in a concentration-dependent manner, although AuD8 showed some selectivity toward CT-like activity in both purified 20S and intact cellular proteasome (Table 2). For comparison, bortezomib was used as a positive control ($IC_{50} = 2.2 \pm 0.6$ nM for CT-like activity).

Table 2. AuD6 and 8 inhibit proteasome activity under cell-free conditions. IC₅₀ values of each compound against each proteasomal activity ($\mu\text{M}\pm\text{SD}$).

	Proteasomal Activity	AuD6	AuD8
Purified 20S	<i>Chymotrypsin-like</i>	0.42±0.03	0.29±0.07
	<i>Trypsin-like</i>	0.51±0.07	0.61±0.02
	<i>PGPH-like</i>	0.49±0.09	0.54±0.08
Cell extract	<i>Chymotrypsin-like</i>	3.3±0.4	2.9±0.6
	<i>Trypsin-like</i>	3.0±0.9	5.7±0.1
	<i>PGPH-like</i>	2.3±0.8	4.5±0.9

AuD6 and AuD8 inhibit cellular proteasome activity and induce apoptosis in MDA-MB-231 cells

To elucidate to what extent these compounds inhibit cellular proteasome, MDA-MB-231 breast cancer cells were treated with increasing concentrations of each complex for 24 hours, followed by measurement of proteasomal activities. Again, AuD8 preferentially inhibited CT-like activity (Figure 30B), and notably, both compounds were also able to inhibit PGPH-like activity (Figure 30).

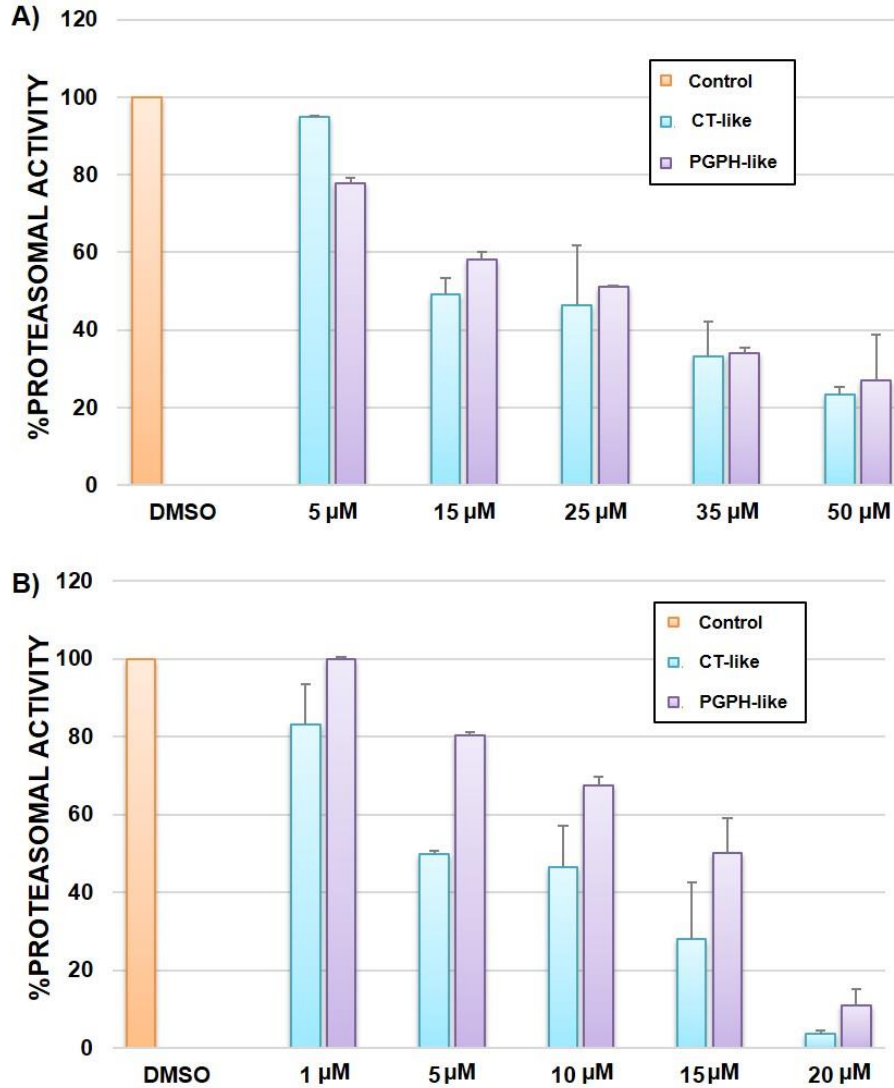


Figure 30. AuD6 and 8 inhibit intact cellular proteasome in MDA-MB-231 cells. MDA-MB-231 cells were treated with increasing concentrations of A) AuD6 or B) AuD8 for 24 h followed by measurement of proteasomal CT-like and PGPH-like activities.

To further investigate the effects of these compounds in cells, MDA-MB-231 cells were treated with increasing concentrations (5, 10, 15 and 20 μM) of AuD6 or AuD8 for 24 hours (Figure 31A, B), followed by Western blot analysis. Marked accumulation of ubiquitinated proteins and proteasome target proteins p27 and I κ B α , as well as caspase-3 activation and PARP cleavage were observed after treatment with AuD8. AuD8 treatment also resulted in enhanced levels of p36/Bax and consequent decrease or complete disappearance of p21/Bax and p18/Bax fragments. Additionally, morphological changes associated with apoptosis (rounding, detachment) were also observed in cells treated with AuD8 at concentrations as low as 10 μM (Figure 31C).

The AuD6 complex was less potent than AuD8, as expected, based on their IC₅₀ values (Figure 28). Indeed, only minimal effects on apoptotic markers (*i.e.*, PARP cleavage and caspase-3 activation) were observed following treatment with higher concentrations of AuD6 (Figure 31A). Similarly, morphological changes were only evident in cells treated with 20 μM AuD6 (the highest concentration tested; Figure 31C).

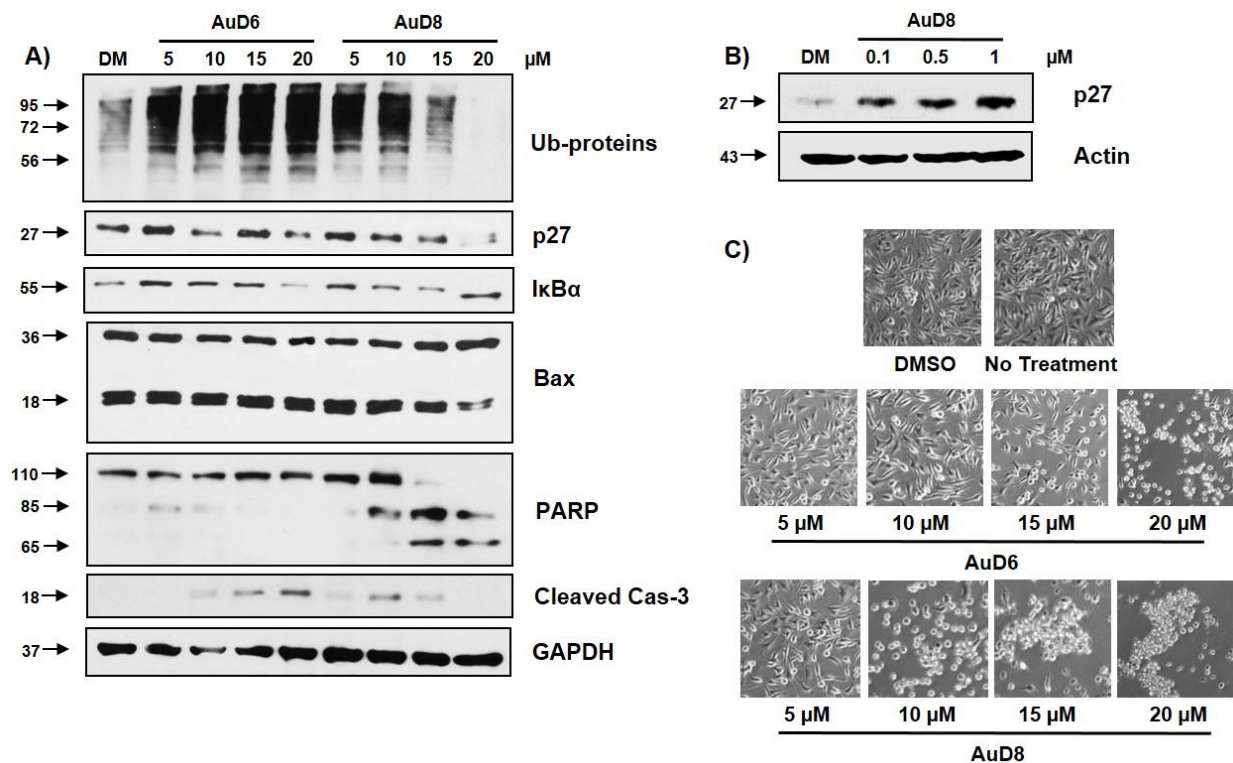


Figure 31. AuD6 and 8 inhibit intact cellular proteasome and induce apoptosis in MDA-MB-231 cells. MDA-MB-231 cells were treated with increasing concentrations of AuD6 or AuD8 for 24 h followed by Western blot analysis and observation of morphological changes. A) Western blot analysis B) Western blot analysis for p27 following 24 h treatment with low concentrations of AuD8. C) Morphological changes; rounded, detached cells are considered apoptotic. DM = DMSO treatment.

To further validate that these compounds mediate cell death *via* apoptosis, MDA-MB-231 cells were treated with 20 μ M AuD6 or AuD8 for 16 or 24 hours followed by Annexin-V/PI staining and flow cytometry. The percentage of cells undergoing non-apoptotic cell death was comparable to solvent control (Figure 32). However, after 16 hour treatment with AuD8 the majority of cell death (62.9%) occurred by apoptosis (late stage), with increased apoptosis observed after 24 hours (74.1%; Figure 32). While both compounds resulted in similar amounts of early stage apoptosis (7–9%), AuD6 was less potent in terms of late stage apoptosis, with only about 49% induction after 24 hours (Figure 32).

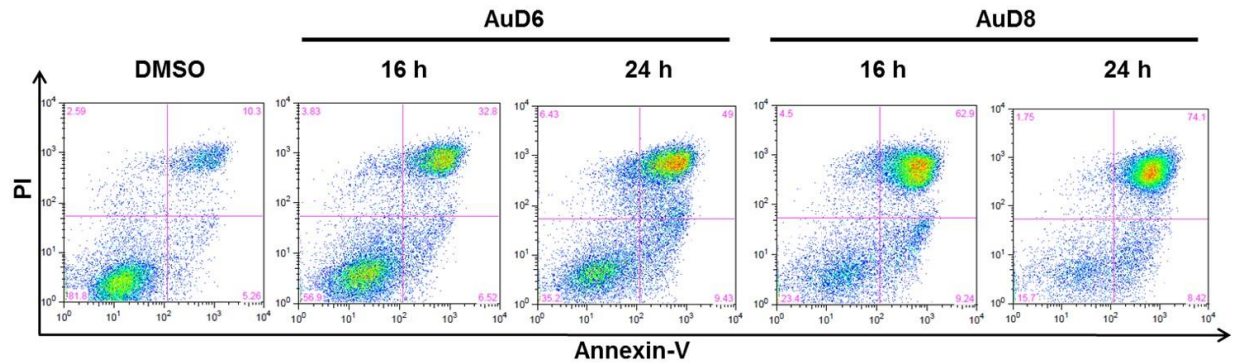


Figure 32. AuD6 and 8 induce apoptosis in MDA-MB-231 cells. MDA-MB-231 cells were treated with 20 μ M AuD6 or AuD8 for 16 or 24 h. Cells were then labeled with Annexin-V FITC and PI, followed by flow cytometry analysis. Early apoptotic cells are represented in the lower right quadrant while late apoptotic cells are the upper right. The lower left quadrant represents viable cells and the upper left, non-apoptotic cell death.

AuD8 inhibits the proteasome and suppresses tumor growth in vivo

Finally, the anticancer activity of both compounds was investigated *in vivo* in female athymic nude mice bearing MDA-MB-231 tumor xenografts. Mice (n=21) were randomly divided into three groups of seven, and treated daily with either solvent control or AuD6 or AuD8 (1.0 mg/kg/d). At day 13, three mice per group were sacrificed to determine if anti-tumor effects could be observed after only a short treatment period, and the remaining four mice per group were sacrificed at day 27 or when control tumors reached approximately 1,800 mm³. As expected, AuD8 was slightly more potent than AuD6 (Figure 33A). AuD8 treatment resulted in about 53% inhibition of tumor growth compared to control (p<0.05; Figure 33A and Insert), and when only the most responsive mice are taken into account (40%), 85% inhibition was observed after 13 days (p<0.01; Figure 33B), with some mice exhibiting tumor shrinkage.

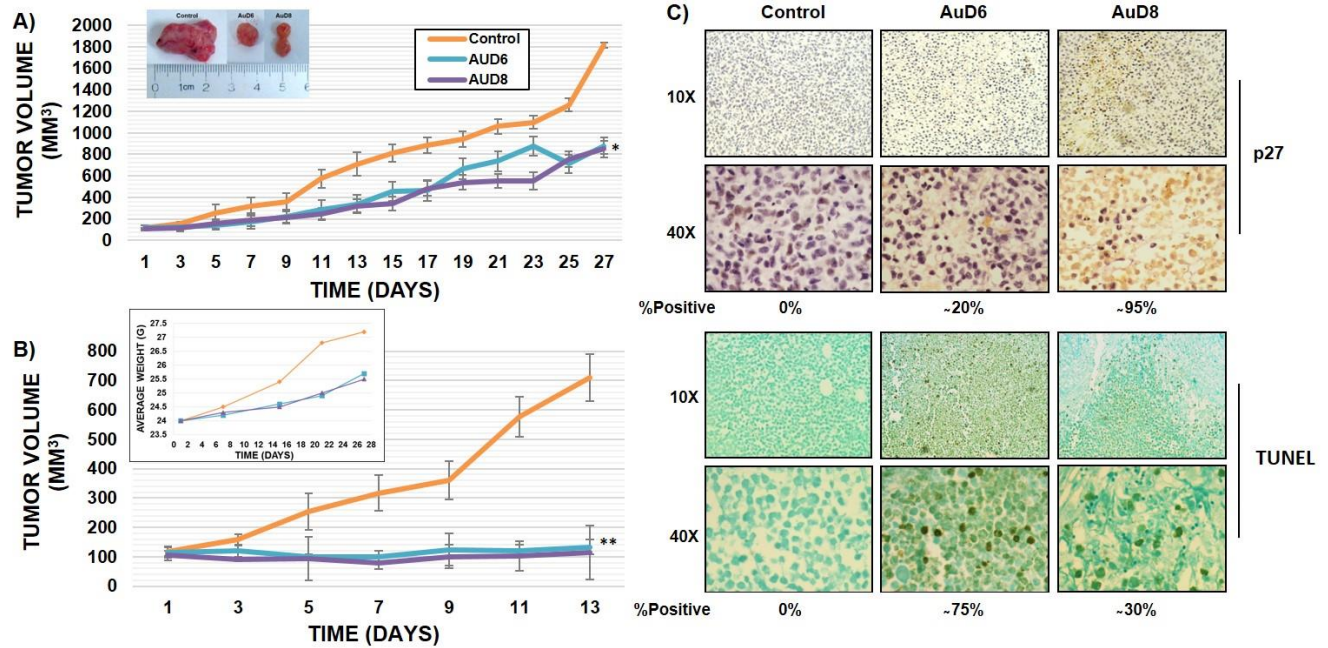


Figure 33. AuD8 inhibits the proteasome and tumor growth *in vivo*. Female nude mice bearing MDA-MB-231 tumors were treated with vehicle control, AuD6 or AuD8 (1 mg/kg/d). A) Inhibition of xenograft growth by both complexes. Tumor volumes were measured every other day. Points represent the mean \pm SD (bars) of seven mice per group. Insert: representative tumors from each treatment group; * = $p < 0.05$. B) Xenograft growth inhibition in the most responsive mice. Insert: Average weights of mice over time; ** = $p < 0.01$. C) Immunohistochemical staining of p27 and TUNEL levels. Brown colored cells are considered positive.

AuD8 treatment also resulted in a significant (~95%) increase in p27 expression levels compared to control (Figure 33C). However, only a moderate increase in p27 was observed following AuD6 treatment (~20%). These results are similar to those seen *in vitro*, with AuD8 being a more potent proteasome inhibitor than AuD6. Western blot analysis confirmed the proteasome-inhibitory activity of these gold-based compounds. AuD8 was a more potent proteasome inhibitor than AuD6 (33% compared to 14% inhibition, respectively; Figure 34D) and AuD8 treatment also resulted in greater accumulation of I κ B- α and Bax (Figure 34A, B).

Importantly, proteasome inhibition was accompanied by apoptosis induction *in vivo*. AuD6 treatment resulted in greater TUNEL positivity compared to AuD8 treatment (~75% vs. ~30%; Figure 33C). Consistently, AuD6 was a more potent activator of caspase-3 than AuD8 (Figure 34A–C). In contrast to results obtained *in vitro*, AuD6 appears to be a more potent inducer of apoptosis *in vivo*; a variability which may be due to induction of different apoptotic cascades (i.e. caspase-dependent versus independent) by each compound. Importantly, mice exhibited minimal changes in body weight over the course of the experiment (Figure 33C, Insert), indicating little to no toxicity resulting from these compounds. Notably, some variation in replicates was observed (Figure 33B), likely due to various individual mouse backgrounds. Taken together, these data suggest that these gold compounds are potent inhibitors of the proteasome, but proteasome inhibition may not be the only major mechanism responsible for apoptotic cell death mediated by these gold compounds.

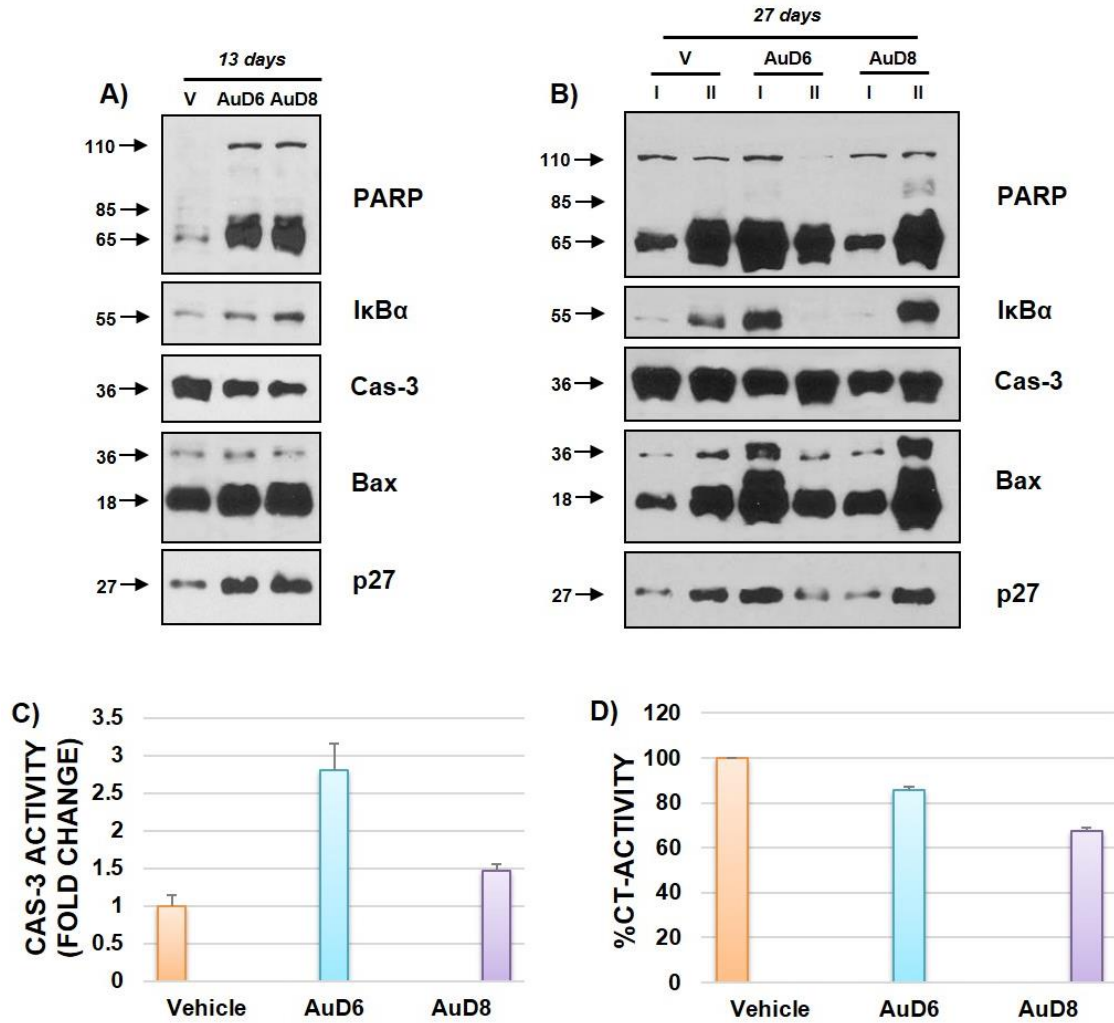


Figure 34. AuD8 inhibits the proteasome and induces apoptosis *in vivo*. Female nude mice bearing MDA-MB-231 tumors were treated with vehicle control, AuD6 or AuD8 (1 mg/kg/d). Tumors were collected and prepared for Western blot analysis after either A) 13-day treatment or B) 27-day treatment. I and II denote separate mice. Tissues (27-day treatment) were also subjected measurement of C) caspase-3 activity and D) proteasomal CT-like activity.

DISCUSSION

The data in this chapter demonstrate that the gold(III) dithiocarbamate-peptide derivatives AuD6 and AuD8 inhibit MDA-MB-231 tumor growth both *in vitro* ($IC_{50} = 6.5 \pm 0.6$ and 17 ± 1 μ M, respectively) and *in vivo* at a dose of 1.0 mg/kg per day. Xenograft tumor growth was inhibited by 53% compared to control after 27 days and 85% after 13 days (Figure 33A, B). Notably, mice appeared healthy and active throughout the treatment. These gold compounds are also potent proteasome inhibitors and, although AuD6 and AuD8 resemble cisplatin structurally (*i.e.*, square planar geometry with a d^8 electronic configuration), these compounds are electrophilic coordination compounds (Dalla Via, et al. 2012), much like bortezomib. These similar chemical properties may explain the proteasome inhibitory ability of the gold complexes compared to cisplatin, suggesting that the metal center is more important than structure in determining intracellular targets. Thus, the metal center Au(III) could bind to proteasomal active sites, but it may also be involved in a redox process that would lead to the formation of gold(I)-containing species or metallic gold by oxidation of some residue, such as the nucleophilic threonine, within the proteasome.

Additionally, previous studies indicated that toxicity of gold compounds is associated with generation of reactive oxygen species (Zhang et al. 2010), which is not surprising considering the redox-activity of gold. These derivatives however, appeared more potent in combination with Trolox, suggesting that cell death commitment is triggered by apoptotic mechanisms independent of free radical formation. Overall, these data confirm that the design of these gold compounds allows them to both stabilize the heavy metal center and avoid non-specific activity in healthy tissues that could give rise to systemic toxicity (Ronconi and Fregona 2009).

The encouraging results presented in this chapter have resulted in an international patent for the use of these novel gold compounds in cancer chemotherapy (Fregona, et al. 2010). Nevertheless, although the proteasome has been validated as one of the targets of these compounds, their potential interactions with other cellular targets, as well as any effects on gene modification are under investigation.

4.3 Inhibition of the 26S Proteasome as a Possible Mechanism for Toxicity of Heavy Metal Species

Adapted from published material in J Inorg Biochem. 2014 Jan 8. pii: S0162-0134(14)00002-6.

RESULTS

Heavy metal species suppress CRL2221 cellular proliferation

To evaluate the effects of heavy metal complexes on cellular proliferation, CRL2221 transformed human prostate epithelial cells were treated with various concentrations of **1–5** (Figure 21) or DMSO as a control for 72 hours followed by MTT analysis (Figure 35). All complexes inhibited cellular proliferation in a concentration-dependent manner, with IC_{50} values of 2 μ M, 4 μ M, 6 μ M, 3 μ M and 4 μ M, for complexes **1–5**, respectively. At lower concentrations, aluminum-containing **1** and lead-containing **4** exhibit the greatest inhibition of cell proliferation (89 and 95% and 84 and 86%, at 5 and 10 μ M, respectively), followed by complex cadmium-containing **2** (99% at 10 μ M). Treatment with **2**, **3**, and **4** (Cd, Hg, and Pb, respectively) resulted in even higher inhibition of cellular proliferation (97–99%) at 25 and 50 μ M. Complex **5** (Sn) resulted in a dose-dependent decrease in cell proliferation with 95% inhibition at 50 μ M. These results suggest that heavy metal species are toxic toward cell proliferation in non-tumor cells. Aluminum-containing **1** is quite toxic at all concentrations, while cadmium-containing **2** and lead-containing **4** show similar profiles where toxicity is marked at concentrations of 10, 25, and 50 μ M and mercury- and tin-containing species **3** and **5** exhibit pronounced toxicity only at higher concentrations.

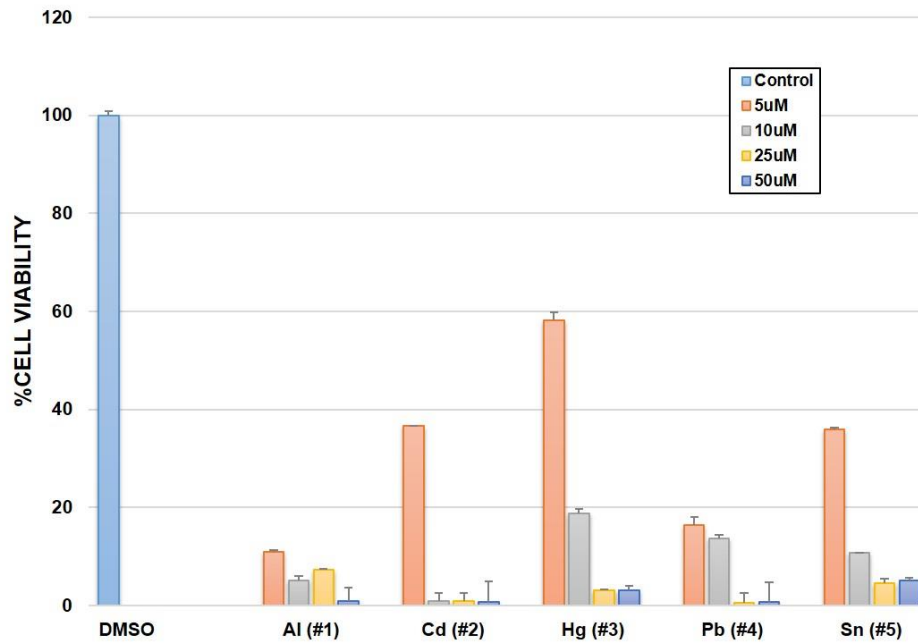


Figure 35. Heavy metal complexes suppress cell proliferation in CRL2221 cells. CRL2221 cells were treated with increasing concentrations of **1-5** for 72 h followed by analysis by MTT assay.

Inhibition of purified 20S CT-like activity by heavy metals

To determine whether these heavy metal complexes are able to inhibit proteasomal CT-like activity, species **1–5** were incubated with purified human 20S proteasome, followed by measurement of CT-like activity (Figure 36). At lower concentrations (1 and 5 μM), mercury-containing complex **3** showed the greatest activity, inhibiting 88 and 98% CT-like activity respectively, followed by cadmium-containing **2** with 70 and 84% inhibition. Dose-dependent inhibition of 84% and 83%, resulted from treatment with 25 μM complexes **1** and **4**, respectively, whereas only 30–40% inhibition occurred following treatment with **5**, regardless of concentration (Figure 36). While previous reports indicated that the HL_{iodo} ligand had negligible effects on purified CT-like activity (Hindo, et al. 2009), these results suggest that this ligand is toxic when it contains heavy metal species. It is evident that high concentrations of **1**, **4**, and **5** are necessary for inhibition of purified 20S proteasome, and while **2** is more potent, **3** is the most potent from 10 to 50 μM , suggesting a potential link between proteasome inhibition and cellular toxicity.

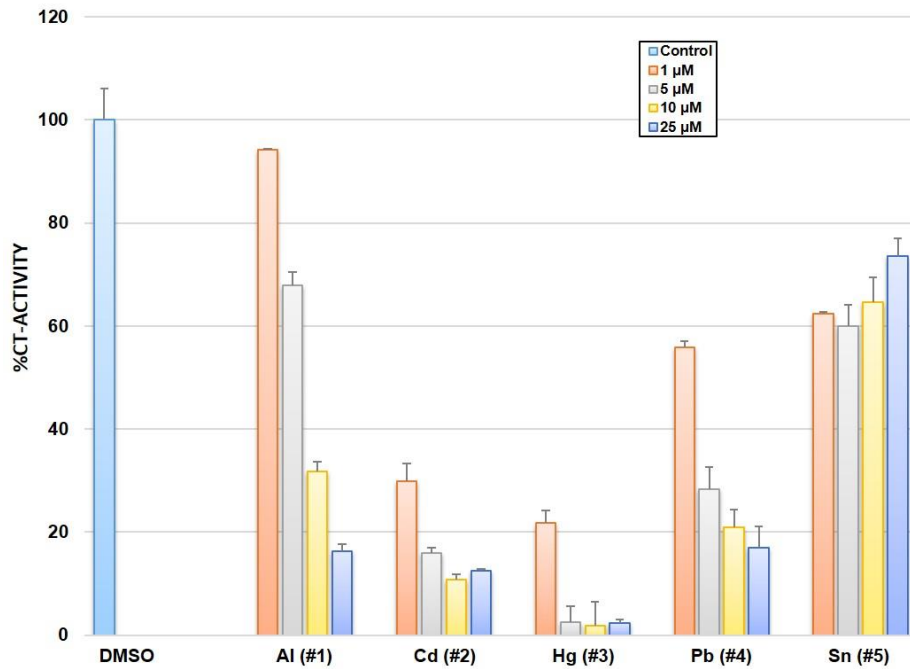


Figure 36. Heavy metal complexes inhibit purified proteasome activity. Purified human 20S proteasome was incubated with increasing concentrations of **1-5** for 2 h, followed by analysis of CT-like activity.

Heavy metal species inhibit cellular proteasome activity in intact cells

To verify the ability of **2–5** to inhibit proteasome activity, intact CRL2221 transformed human prostate epithelial cells were treated with increasing concentrations (up to 25 μM) of each complex for 48 h, followed by measurement of proteasome activity (Figure 37). Cells treated with lead-containing **4** showed dose-dependent inhibition of proteasomal CT-like activity, with 41% inhibition at 5 μM , 46% at 10 μM and 73% at 25 μM (Figure 35). Consistently, levels of proteasomal CT-like activity were decreased by 52 and 43% after treatment with 10 μM cadmium- and mercury-species **2** and **3**, respectively. In contrast, cells treated with the tin-containing **5** showed negligible proteasome inhibition at lower concentrations, and only about 50% inhibition at 25 μM (Figure 37). This suggests that higher concentrations of **2–5** are necessary for inhibition of proteasomal CT-like activity, indicating that some of these toxic species may be prevented from crossing the cell membrane or be deterred by other intracellular targets before reaching the proteasome.

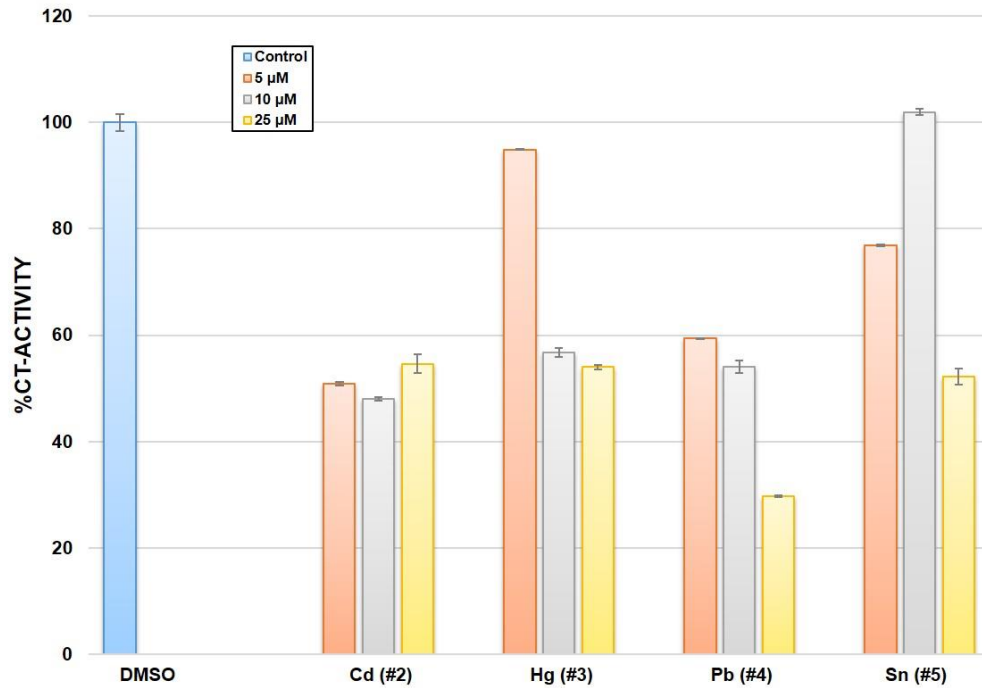


Figure 37. Heavy metal complexes inhibit cellular proteasome activity. CRL2221 cells were treated with increasing concentrations of 2-5 for 48 h, followed by measurement of CT-like activity.

Heavy metal species inhibit proteasome activity in cell extracts

Inhibition of proteasomal CT-like activity was also measured in CRL2221 cell extracts after 24 hour treatment with complexes **1–5** (Figure 38). Mercury-containing complex **3** induced the greatest CT-like inhibition in a dose-dependent manner, reaching 99% inhibition at 25 μM . On the contrary, treatment with aluminum-containing complex **1** resulted in no proteasome inhibition even at the highest concentration (25 μM). CRL2221 cell extracts treated with **4** and **5** exhibited only about 30% inhibition at 25 μM (Figure 38). These data suggest that the mercury-containing complex **3** is the most potent proteasome inhibitor in cell extracts, further supporting the hypothesis that toxicity toward epithelial prostate cells might be associated with proteasome inhibition.

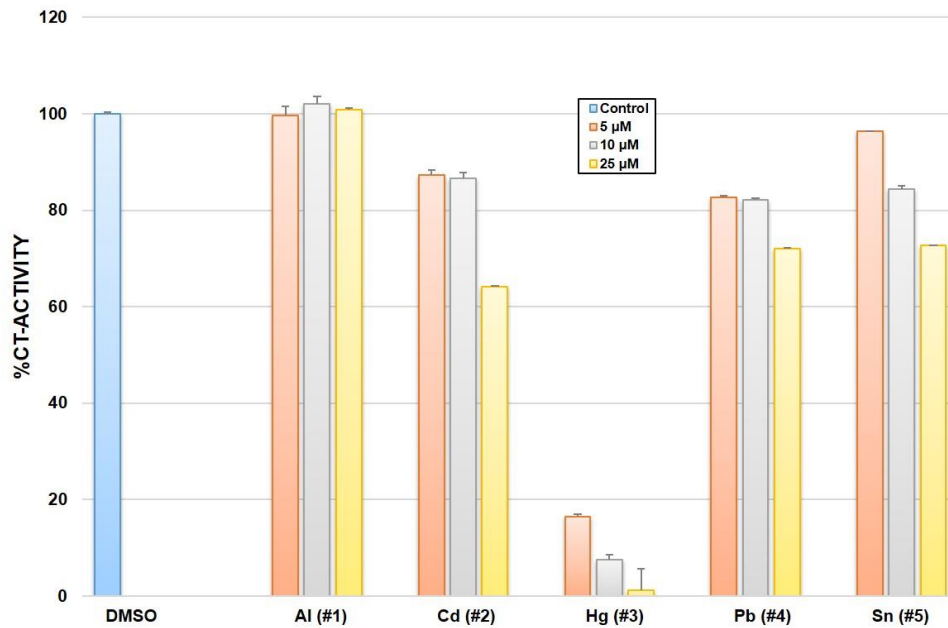


Figure 38. Heavy metal complexes inhibit proteasome activity in cell extracts. CRL2221 cell extracts (20μg) were incubated with increasing concentrations of **1-5** for 24 h, followed by measurement of CT-like activity.

DISCUSSION

Earlier investigations of copper(II) complexes with the HL_{iodo} ligand suggested that a 1:1 metal:ligand_{iodo} species is necessary for potent inhibition of proteasomal CT-like activity (Frezza et al. 2009; Hindo et al. 2009; Verani 2012) and studies of cobalt(L_{iodo}) complexes (Tomco et al. 2011) linked proteasome inhibitory activity to preferential oxidation states of the metal ion (Tomco, et al. 2012). In this chapter, the toxicity of five new species $[Al(III)(L_{\text{iodo}})_2]ClO_4$ (**1**), $[Cd(II)(L_{\text{iodo}})Cl] \cdot H_2O$ (**2**), $[Hg(II)(L_{\text{iodo}})_2] \cdot 4DMSO$ (**3**), $[Pb(II)(L_{\text{iodo}})NO_3]$ (**4**), and $[Sn(IV)(L_{\text{iodo}})Cl_3]$ (**5**) toward CRL2221 transformed prostate epithelial cells was investigated. These metals have been previously shown to be associated with a number of conditions affecting normal cellular function. For instance, organoaluminum species accumulate in bone and the central nervous system through interaction with erythrocytes and desferrioxamine, as well as impairing mitochondrial function resulting in globular astrocyte generation (Lemire and Appanna 2011) (Jeffery 1995). Cadmium demonstrates a lack of specificity towards cell organelles, interacts with DNA, and increases oxidative stress (Larregle and Ferranola 2010; Moulis 2010; Wolfgang and Jean-Marc 2013). Organomercury species can accumulate in the mitochondria and irreversibly inhibit selenoenzymes, leading to nervous system damage (Guzzi and La Porta 2008; Neustadt and Pieczenik 2007; Yang, et al. 2008). Organolead can substitute divalent metal ions, like calcium in ATPase pumps, thus disrupting homeostasis (Yasuhiro and Toshiyuki 2012). Finally, organotin species (Blunden and Wallace 2003) can incorporate into the Golgi apparatus, as well as coordinating to intracellular phospholipids (Arakawa 2000). While extensive knowledge on the primary toxicity mechanisms of these species exists, only little evidence is available associating proteasome inhibition to cadmium and lead in erythrocytes (Neslund-Dudas, et al. 2012) and with

organometallic tin species (Shi, et al. 2009), and it is likely that other secondary cellular targets are involved.

All five species demonstrated high levels of inhibition of cell growth in a concentration-dependent manner, with aluminum-containing complex (1) being the most potent and tin-containing (5), the least. The cadmium, mercury and lead species (2), (3) and (4) were the most active against the chymotrypsin-like activity of purified 20S, as well as intact proteasome in CRL2221 cells. Mercury-containing complex (3) proved to be the most potent against CT-like activity, with 2 and 4 as distant next candidates, particularly in cell extracts. Taken together, these results indicate that the toxicity of the aluminum species, albeit high, cannot be directly associated to proteasome inhibition. A similar conclusion can be drawn regarding the tin-containing complex. On the other hand, the toxicity of cadmium- and lead-containing complexes is potentially associated with proteasome inhibition, although this is not definitively proven based on proteasome inhibition in cell extracts. The mercury species, particularly at higher concentrations, was potent in regards to cell growth and CT-like inhibition in purified proteasome, cell extracts and intact cells, suggesting a strong relationship between proteasome inhibition and mercury toxicity. Therefore, in spite of known prevalent mechanisms of cellular toxicity for mercury species, in particular inhibition of selenoenzymes, proteasome inhibition is a viable secondary route of toxicity.

4.4 Differential Effects of Ga(III)- and Zn(II)-Tethered Ligands on Proteasome Activity and Apoptosis in Cultured Prostate Cancer Cells

RESULTS

Tethered Ga(III), but not Zn(II), inhibits purified proteasome activity

To evaluate whether these new tethered complexes could inhibit the proteasome, a cell-free proteasome activity assay was performed by incubating purified human 20S (Figure 39A) or 26S proteasome (Figure 39B) with different concentrations of Ga^{III}DiIBPEN (Figure 22; Figure 39A, B) or Zn^{II}DiIBPEN (Figure 39A). Interestingly, the Ga(III) complex potently inhibited CT-like activity in both purified proteasome species, whereas the Zn(II) complex had little inhibitory effect (Figure 39A, B). Taken together, these results show that Ga^{III}DiIBPEN, but not Zn^{II}DiIBPEN possesses the ability to inhibit CT-like proteasomal activity in a cell-free system.

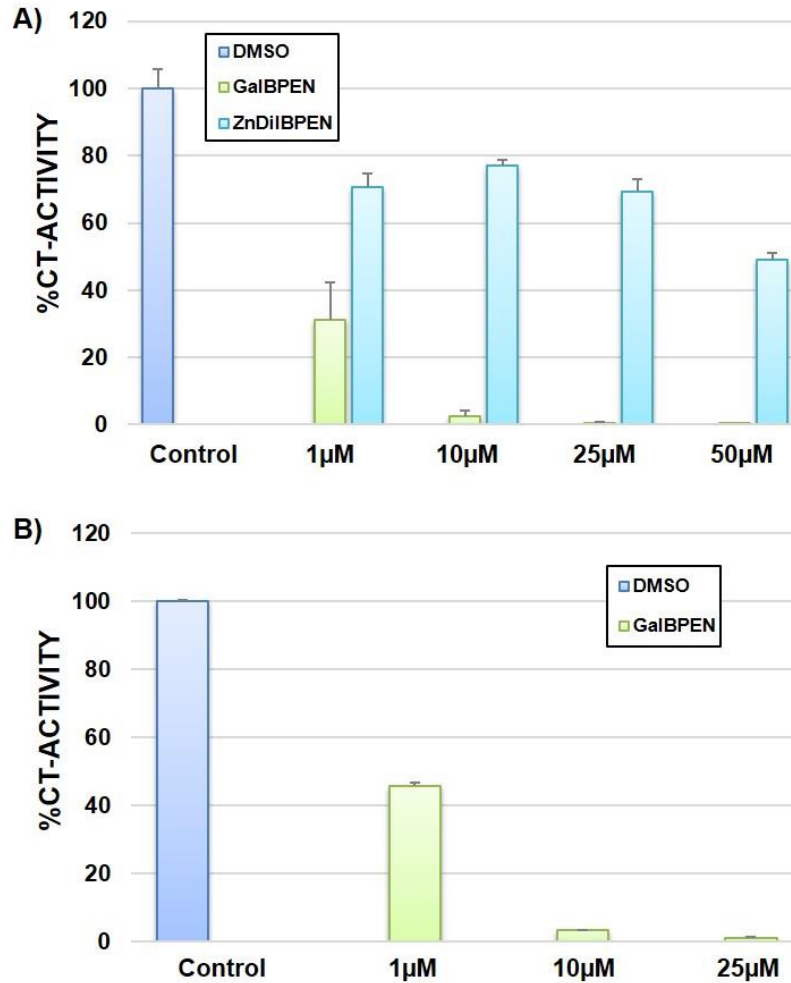


Figure 39. Tethered Ga(III) inhibits purified proteasome activity. Purified human A) 20S or B) 26S proteasome was incubated with increasing concentrations of Ga^{III}DiIBPEN or Zn^{II}DiIBPEN for 2 h followed by measurement of CT-like activity.

Tethered Ga(III), but not Zn(II), inhibits proteasome activity and cell viability in PC-3 cells

Similarly, the proteasome-inhibitory effects of these complexes were also measured in PC-3 human prostate cancer cells. PC-3 cells were treated for 24 hours with increasing concentrations of Ga^{III}DiIBPEN or Zn^{II}DiIBPEN up to 50 μM, followed by measurement of proteasomal CT-like activity. Unsurprisingly, the Ga(III) complex was much more potent (IC₅₀ ≈ 22.5 μM) than the Zn(II) complex (no inhibition at 50 μM) against cellular proteasome activity in intact prostate cancer cells (Figure 40A).

Following the determination that Ga^{III}DiIBPEN is a potent inhibitor of purified and cellular proteasomal CT-like activity, its effects on cellular viability in PC-3 human prostate cancer cells were examined. An MTT experiment revealed that Ga^{III}DiIBPEN inhibits cellular viability in a dose-dependent manner (Figure 40B). Again, the Zn(II) complex was ineffective, with only ~17% cell growth inhibition at 50 μM (Figure 40B). Thus, Ga^{III}DiIBPEN suppresses cellular proteasome activity, as well as cellular viability in PC-3 prostate cancer cells.

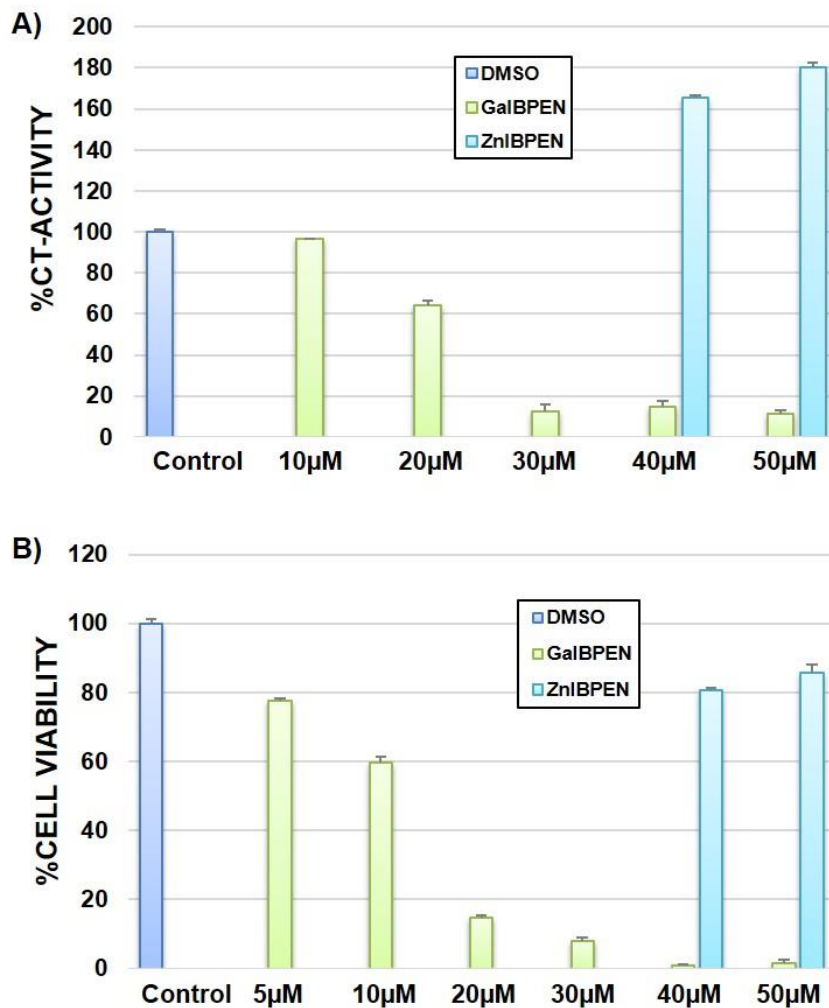


Figure 40. Tethered Ga(III) inhibits cellular proteasome activity and cell proliferation. PC-3 cells were treated with increasing concentrations of Ga^{III}DiIBPEN or Zn^{II}DiIBPEN for 24 h followed by measurement of A) CT-like activity and B) cell viability.

Tethered Ga(III) but not Zn(II) induces apoptosis in PC-3 cells

To further confirm the proteasomal inhibition induced by Ga^{III}DiIBPEN, PC-3 cells were treated with increasing concentrations of Ga^{III}DiIBPEN or Zn^{II}DiIBPEN for 24 hours, followed by Western blot analysis. A dose-dependent accumulation of ubiquitinated proteins following treatment with the Ga(III) complex was observed (Figure 41A). Additionally, apoptosis-associated PARP cleavage and cellular morphological changes were observed in these cells. A decrease in full length PARP is obvious at 30 μM Ga^{III}DiIBPEN, and a cleavage fragment is visible at 50 μM; while no PARP cleavage occurred following Zn^{II}DiIBPEN treatment (Figure 41A). Cellular morphological changes confirm cell death caused by the Ga(III), but not Zn(II), complex. As shown in Figure 41B, no changes in cellular shape occur at 40 or 50 μM Zn^{II}DiIBPEN treatment, but cells treated with Ga^{III}DiIBPEN display distinct apoptosis-related changes, including becoming round and detached, at only 20 μM treatment (Figure 41B). Therefore, Ga^{III}DiIBPEN is a potent apoptosis-inducer in PC-3 prostate cancer cells.

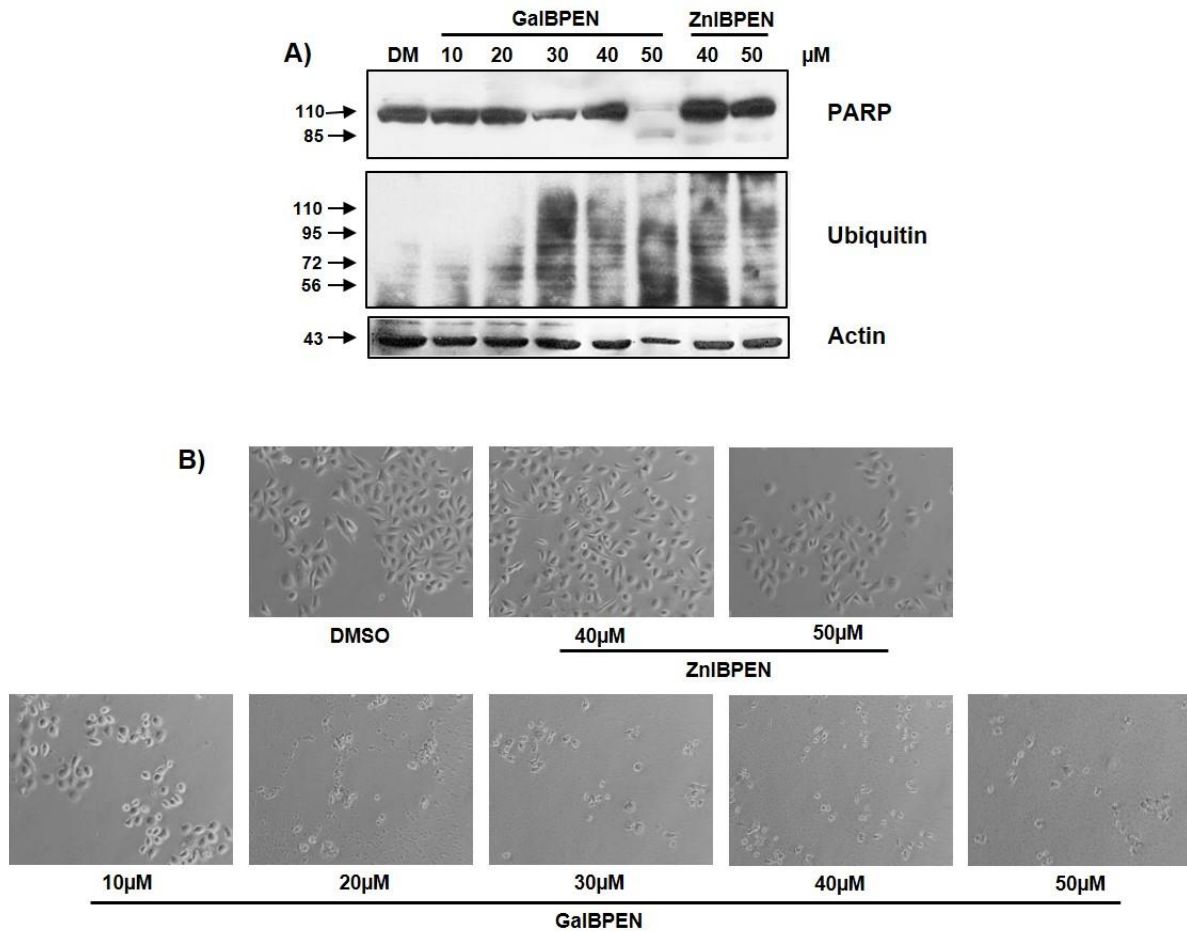


Figure 41. Tethered Ga(III) inhibits cellular proteasome activity and induces apoptosis. PC-3 cells were treated with increasing concentrations of Ga^{III}DiIBPEN or Zn^{II}DiIBPEN for 24 h followed by A) Western blot analysis and B) observation of apoptosis-associated morphological changes.

Tethered Ga(III) and Zn(II) complexes have no effect proteasome activity in normal, immortalized CRL2221 cell extracts

To evaluate the toxicity of these complexes in non-cancer cells, human normal, immortalized CRL2221 prostate cell extracts were incubated with increasing doses of Ga^{III}DiIBPEN or Zn^{II}DiIBPEN, up to 50µM, for 8 hours, followed by measurement of proteasomal CT-like activity. The fluorogenic assay revealed that neither complex is able to induce proteasome inhibition, as 50µM Ga^{III}DiIBPEN resulted in only ~20% inhibition (Figure 42). The lack of proteasome inhibition by these compounds in normal, immortalized cell extracts suggests that the effects of Ga^{III}DiIBPEN are specific to tumor cells.

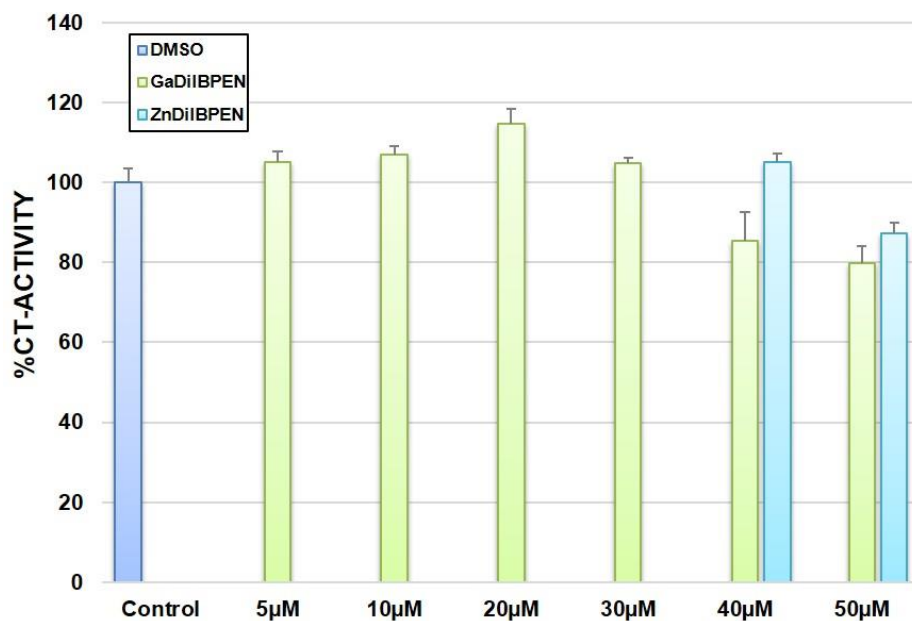


Figure 42. Tethered Ga(III) and Zn(II) complexes have no effect on proteasome activity in CRL2221 cells. CRL2221 cell extracts were treated with increasing concentrations of Ga^{III}DiIBPEN or Zn^{II}DiIBPEN for 8 h, followed by measurement of CT-like activity.

DISCUSSION

Gallium, unlike zinc, has no history of clinical use or known biological function, but can interact with proteins and play a role in some cellular processes. Gallium is primarily used for diagnostic purposes (Chitambar 2010) and gallium nitrate is used to treat hypercalcemia. Additionally, some gallium complexes have entered clinical trials toward the goal of optimizing their pharmacokinetics (Galanski et al. 2003; Jakupec and Keppler 2004; Rudnev, et al. 2006). Previous reports have also shown that gallium complexes are able to inhibit cellular proliferation in cisplatin-resistant neuroblastoma cells (Shakya et al. 2006), as well as inhibiting the proteasome and inducing cell death in prostate cancer cells (Chen et al. 2007b).

The previous success of gallium-based compounds led to the synthesis of second-generation gallium complexes, which proved more potent against tumor proteasome activity and cell growth than the original complexes (Chen et al. 2007b). The potency of these 1:2 metal:ligand complexes was somewhat unexpected, but is likely due to the 3+ oxidation state of gallium, considering the redox inactive 2+ zinc complex was ineffective. Previous studies indicated that a 1:1 metal:ligand ratio is the active species, and it is probable that the intracellular reduction of the Ga(III) species within the tumor microenvironment encourages ligand dissociation into the active 1:1 metal:ligand complex (Tomco et al. 2011). In addition to its oxidation state, the zinc(II) complex may be inactive due to its bioavailability and promiscuity within the cell, causing it to be diverted prior to reaching the proteasome. Taken together, the results presented in this chapter further suggest that gallium-based complexes have the potential to be used as cancer chemotherapeutic agents.

4.5 Nitroxoline Inhibits the Tumor Proteasome and Suppresses Tumor Growth

RESULTS

Nitroxoline-copper complex inhibits purified 20S proteasome activity more potently than clioquinol-copper

Due to the structural similarities between clioquinol (CQ) and nitroxoline (5NHQ) (Figure 23), it is likely that 5NHQ is able to complex with copper in a manner similar to CQ (Chen et al. 2007a; Di Vaira et al. 2004). To test this, 5NHQ or CQ (as a control) were mixed with CuCl_2 at 1:1 molar ratios. As expected, a dramatic color change was observed (Figure 40A), indicating the formation of a 5NHQ-copper complex. Interestingly, the observed color change was much more dramatic than that observed when CQ was mixed with CuCl_2 , suggesting that 5NHQ may be a stronger copper chelator than CQ.

Next, because copper chelators like CQ, in complex with copper, have been shown to be potent proteasome inhibitors *in vitro* (Chen et al. 2007a), the proteasome-inhibitory ability of 5NHQ was investigated in the presence and absence of copper. Indeed, when purified human 20S proteasome was incubated with CQ, 5NHQ, CuCl_2 or the CQ-Cu and 5NHQ-Cu complexes, proteasome inhibition occurred in a dose-dependent manner, most significantly in the copper-containing complexes. Both CuCl_2 and 5NHQ alone inhibited about 60% activity at the high concentration of 20 μM , whereas the 5NHQ-Cu complex had an IC_{50} of approximately 3.75 μM (Figure 42B), indicating that 5NHQ is a potent proteasome inhibitor when complexed with copper. For comparison, CQ alone only inhibited about 5% CT-like activity at 20 μM , and the CQ-Cu complex had an IC_{50} close to 20 μM . Thus, 5NHQ in complex with copper is a more potent inhibitor of purified proteasome than CQ-Cu.

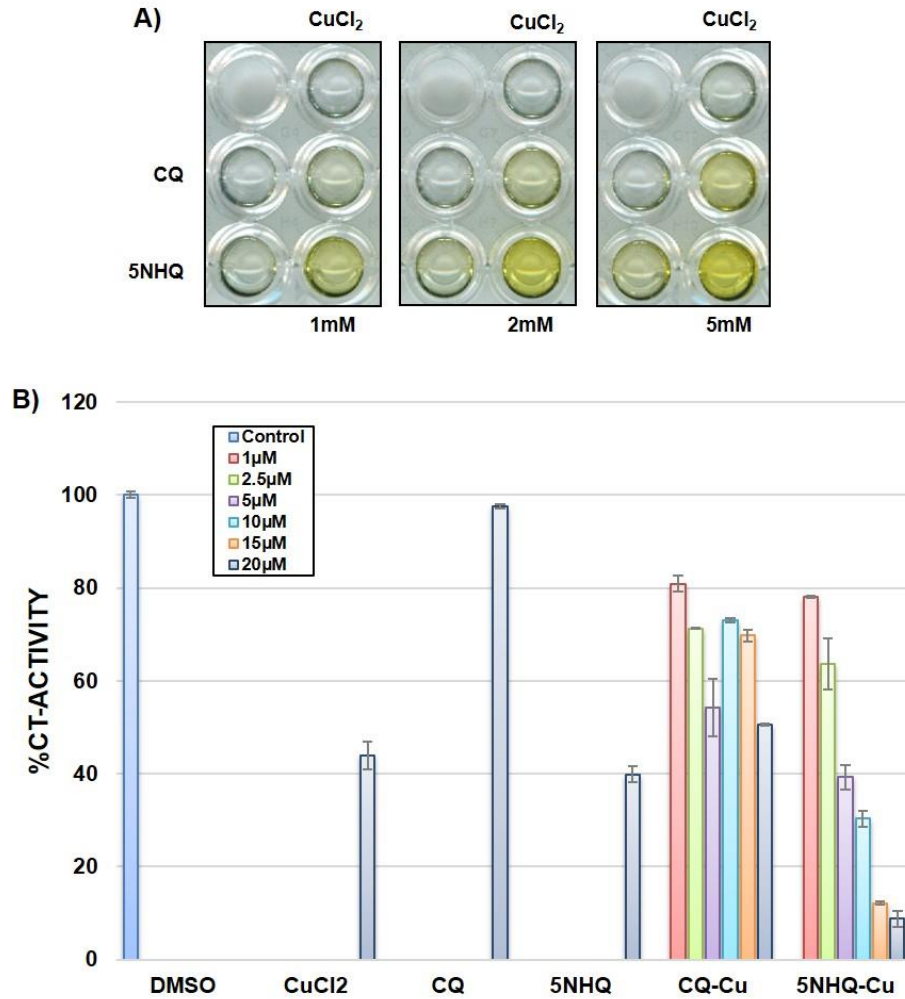


Figure 43. Nitroxoline complexes with copper and inhibits purified 20S proteasome. A) CQ or 5NHQ was mixed with CuCl_2 in a 1:1 ratio (1, 2 and 5 mM). Color change to deep yellow indicates complex formation. B) Purified proteasome was incubated with increasing concentrations of 5NHQ-Cu, CQ-Cu or controls for 2h followed by measurement of CT-like activity.

5NHQ-Cu complex inhibits proteasome activity and induces apoptosis in human leukemia cells

To determine if the 5NHQ-Cu complex was active against the 26S proteasome in cultured leukemia cells, human K562 cells were treated for 24 hours with 1-5 μM 5NHQ-Cu, or with 1-5 μM CQ-Cu and 5 μM 5NHQ, CQ or CuCl_2 as controls. Following treatment, proteasomal CT-like activity was measured using the fluorometric activity assay (Figure 44A). The results indicate that the 5NHQ-Cu complex is a potent inhibitor of intact 26S proteasome in K562 leukemia cells, with 80% inhibition at 5 μM , whereas CQ-Cu, as well as all other controls, had little to no effect on CT-like activity in intact K562 cells (Figure 44A).

Inhibition of CT-like activity has been shown to be associated with suppression of cellular growth and induction of apoptosis in malignant cells (An et al. 1998; Lopes et al. 1997), so the effects of 5NHQ-Cu on cell death were also measured. First, K562 cells were treated with increasing concentrations (2.5-10 μM) of 5NHQ-Cu or 10 μM 5NHQ alone (or DMSO, 10 μM CuCl_2 or CQ, and increasing concentrations of CQ-Cu as controls), for 24 hours, followed by analysis by Trypan Blue assay (Figure 44B). The 5NHQ-Cu complex induced cell death in approximately 80% of cells at a concentration of 10 μM , whereas 5NHQ induced only 10% cell death at 10 μM . In comparison, all other controls caused less than 10% cell death at all concentrations tested (Figure 44). Finally, PARP cleavage was also observed following treatment with 5 and 10 μM 5NHQ-Cu only (Figure 44C), with no cleavage observed following treatment with any of the controls.

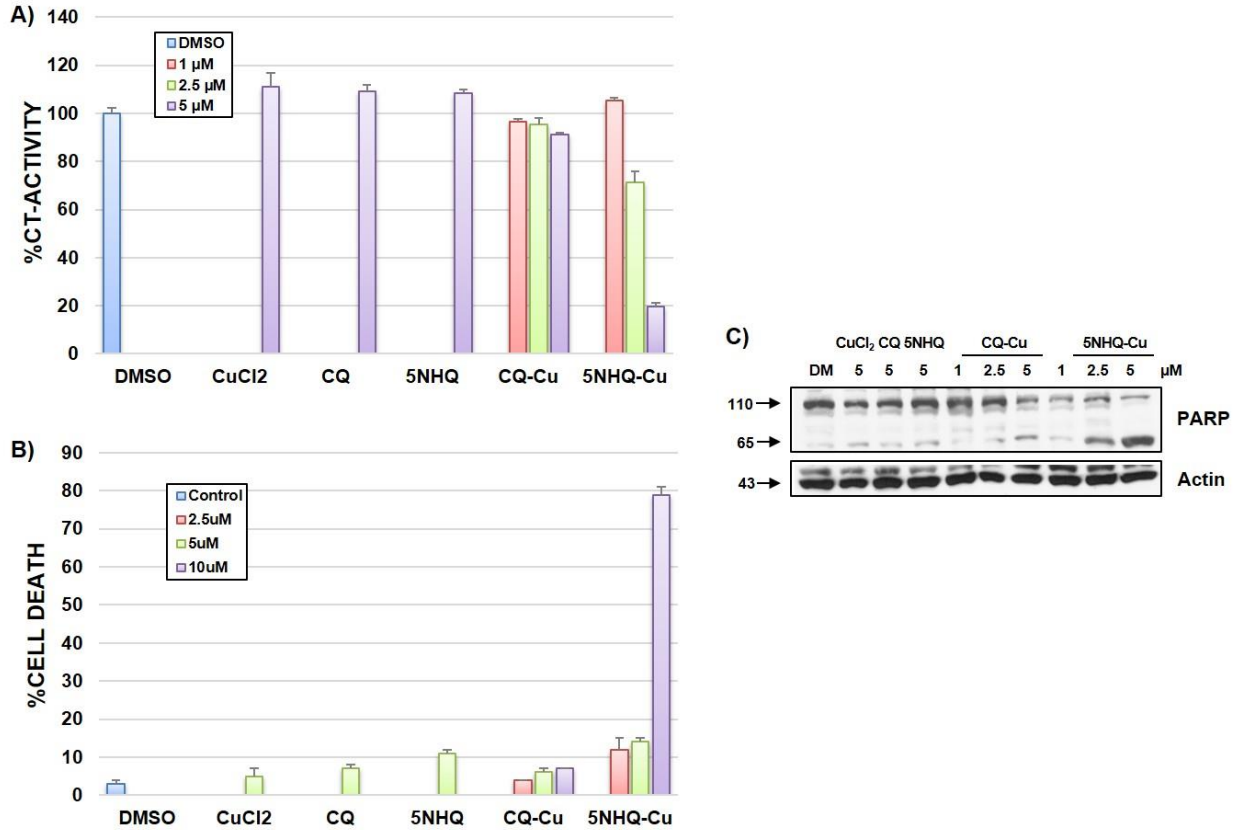


Figure 44. 5NHQ-Cu inhibits proteasome activity and induces apoptosis in human leukemia cells. K562 cells were treated with increasing concentrations of 5NHQ-Cu, CQ-Cu, or other controls, for 24 h followed by measurement of A) CT-like activity, B) cell death via Trypan blue exclusion assay and C) Western blot analysis.

5NHQ-Cu complex suppresses cell proliferation and proteasome activity and causes apoptosis in human prostate and breast cancer cells

To confirm that the effects of 5NHQ-Cu observed in K562 cells are not cell-line specific, PC-3 prostate cancer (Figure 45) and MDA-MB-231 breast cancer (Figure 46) cells were treated with 1-10 μM 5NHQ-Cu, 10-20 μM 5NHQ, or other controls (DMSO, 10-20 μM CuCl_2 or CQ, and 1-10 μM CQ-Cu) for 0-24 hours, followed by measurement of CT-like activity by both the fluorometric assay and Western blot analysis. Inhibition of 90% at only 5 μM 5NHQ-Cu and nearly 100% at 10 μM was observed in PC-3 cells (Figure 45A) and approximately 95% at 5 and 10 μM in MDA-MB-231 cells (Figure 46A). In contrast, 5NHQ alone inhibited only about 60% activity at 10 and 20 μM in both cell lines (Figures 45A and 46A, respectively). Similarly, all other control treatments resulted in approximately 60% inhibition in PC-3 cells (Figure 45A), and 10-20% (CuCl_2 and 5 and 10 μM CQ-Cu) or 60% (CQ) inhibition in MDA-MB-231 cells (Figure 46A). Consistently, Western blot analysis revealed accumulation of ubiquitinated proteins in MDA-MB-231 cells (Figure 46C), following treatment with 5NHQ-Cu, confirming its cellular proteasome inhibitory ability.

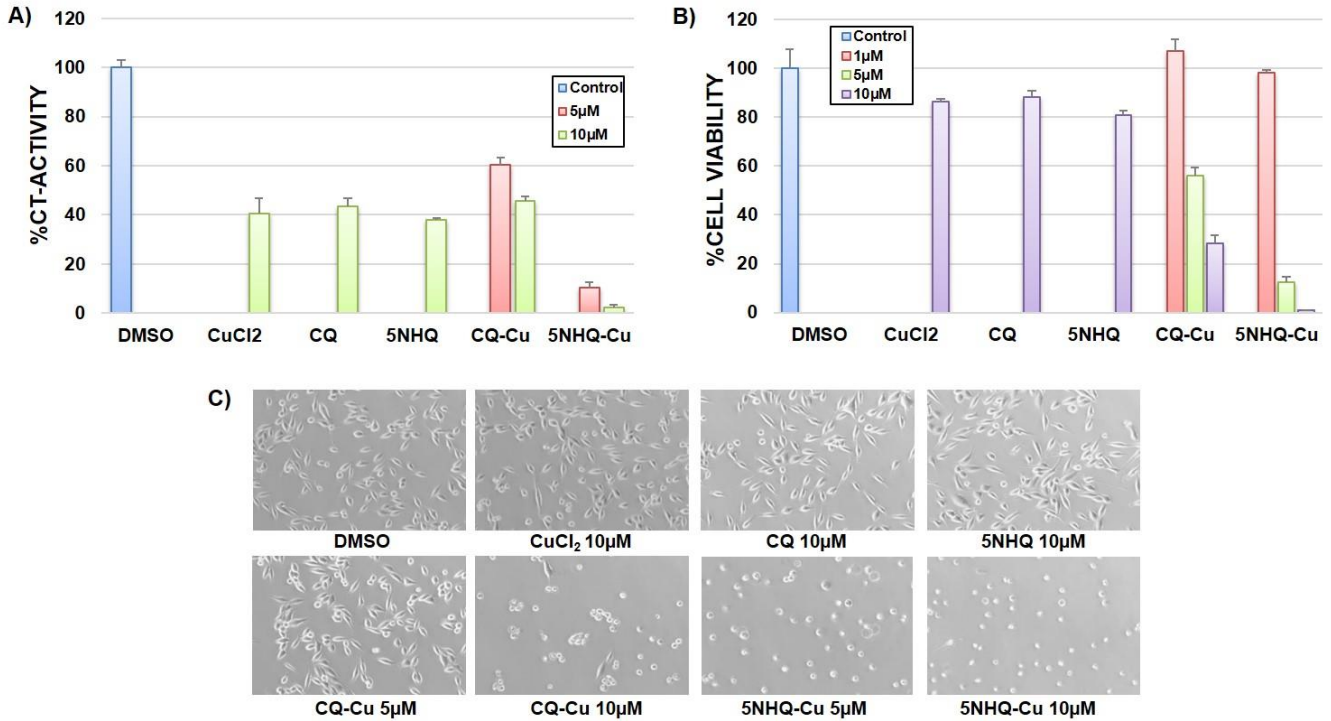


Figure 45. 5NHQ-Cu suppresses cell proliferation and proteasome activity and induces apoptosis in prostate cancer cells. PC-3 prostate cancer cells were treated with increasing concentrations of 5NHQ-Cu, CQ-Cu, or other controls, for 24 h followed by measurement of A) CT-like activity, B) cell viability via MTT, C) observation of apoptosis-associated morphological changes.

To verify the cell death-inducing abilities of 5NHQ-Cu in these cell lines, suppression of cell growth was first measured by MTT assay. PC-3 and MDA-MB-231 cells were treated with increasing concentrations of 5NHQ-Cu, 10 μ M 5NHQ alone, or other controls (DMSO, 10 μ M CuCl₂ or CQ, and increasing concentrations of CQ-Cu), for 24 hours, followed by analysis by MTT (Figures 45B and 46B). The 5NHQ-Cu complex suppressed cell proliferation by about 85% and nearly 100% at 5 μ M in PC-3 (Figure 45B) and MDA-MB-231 (Figure 46B) cells, respectively. 5NHQ alone (10 μ M) suppressed only about 20% PC-3 and 40% MDA-MB-231 cell growth. In comparison, CQ-Cu (5 μ M) inhibited approximately 40% and less than 10% cell growth in PC-3 (Figure 45B) and MDA-MB-231 (Figure 46B) cells, respectively. Finally, PARP cleavage was observed following treatment with 5NHQ-Cu in MDA-MB-231 cells (Figure 46C) and classic apoptotic morphological changes, including becoming spherical and detaching from the culture surface, were observed in both PC-3 and MDA-MB-231 cells (Figures 45C and 46D).

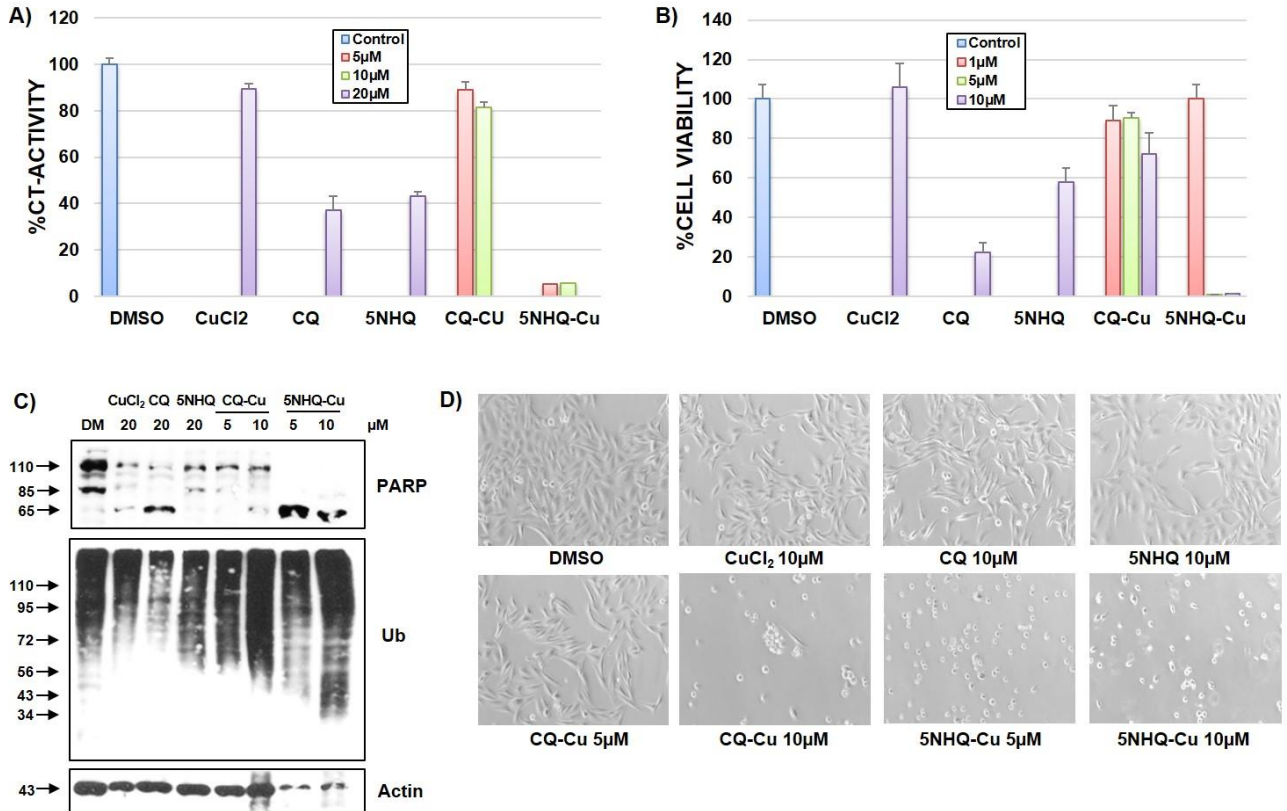


Figure 46. 5NHQ-Cu inhibits cell proliferation and proteasome activity and causes apoptosis in breast cancer cells. MDA-MB-231 breast cancer cells were treated with increasing concentrations of 5NHQ-Cu, CQ-Cu, or other controls, for 24 h followed by measurement of A) CT-like activity, B) cell viability via MTT, C) Western blot analysis and D) observation of morphological changes.

5NHQ suppresses tumor growth in vivo

The *in vitro* data presented above reveal proteasome inhibition as a new mechanism for 5NHQ-Cu induced cell death in cultured leukemia, prostate and breast cancer cells. It has been shown that treatment with copper chelators like tetrathiomolybdate, and clioquinol inhibit tumor growth in breast, lung and prostate xenograft models (Chen et al. 2007a; Pan et al. 2002; van Golen, et al. 2002). This tumor growth inhibition is likely due to the reportedly high copper levels in various tumors (Habib et al. 1980; Huang, et al. 1999; Nayak et al. 2003; Rizk and Sky-Peck 1984; Turecky et al. 1984).

To determine if 5NHQ alone could suppress tumor growth *in vivo*, MDA-MB-231 cells were implanted subcutaneously in female athymic nude mice (n=12). Upon tumor initiation, mice were randomly divided into three groups (n=4/group) and treated daily with DMSO, CQ or 5NHQ (10 mg/kg/day) for 29 days or until tumors reached approximately 1800 mm³. Inhibition of 65% in tumor growth was observed in 5NHQ-treated mice (Figure 47), compared to vehicle control. In contrast, tumor growth was only inhibited by about 35% in mice treated with CQ (Figure 47). Additionally, tumors from 5NHQ-treated mice weighed 80% less than vehicle control tumors (Figure 47, Inset). Taken together, these results are consistent with those observed *in vitro* and confirm that 5NHQ in complex with copper is a potent inhibitor of the proteasome and inducer of apoptosis.

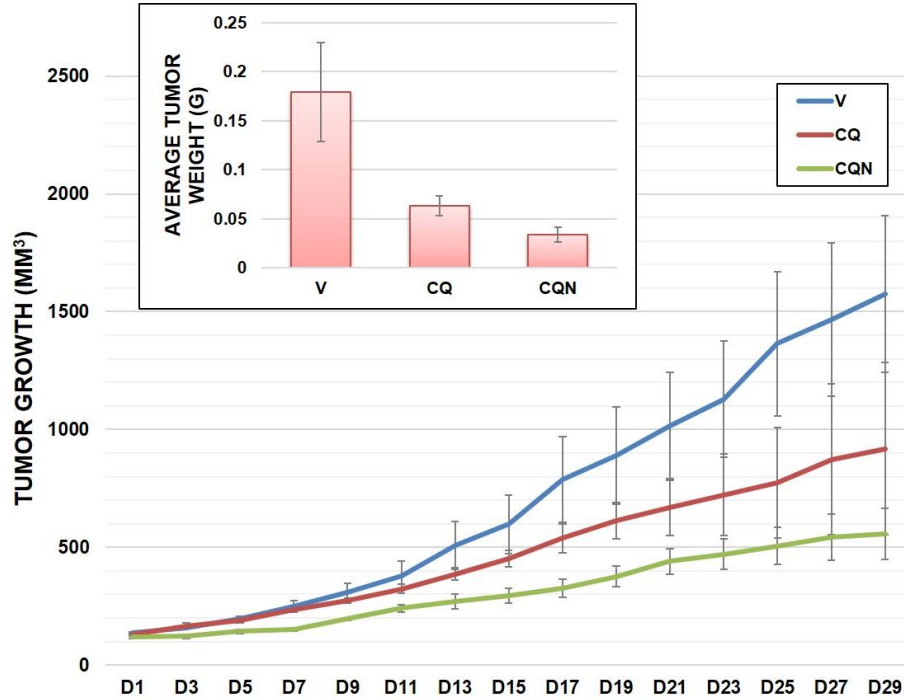


Figure 47. 5NHQ suppresses tumor growth *in vivo*. Female athymic nude mice bearing MDA-MB-231 xenografts were treated with 10 mg/kg/d 5NHQ, CQ or solvent control for 29 days or until tumors reached 1800mm³. Tumor volumes were measured every other day and tumors were weighed at the conclusion of the experiment. *Statistics were not performed due to the small sample size.

DISCUSSION

Several studies have reported high levels of copper in various tumors, including brain, breast, colon, lung and prostate (Habib et al. 1980; Huang et al. 1999; Nayak et al. 2003; Rizk and Sky-Peck 1984; Turecky et al. 1984). Additionally, the importance of copper to tumor angiogenesis (Brem 1999; Brewer 2001) makes the use of copper chelators a promising strategy. Indeed, several organic copper complexes, including clioquinol-copper, have been shown to possess potent tumor proteasome inhibitory activity (Chen et al. 2007a; Daniel et al. 2005; Daniel et al. 2004; Zhai et al. 2010).

The structural similarities between nitroxoline (5NHQ) and clioquinol (CQ) led to the hypothesis that 5NHQ, in complex with copper, like CQ possesses proteasome inhibitory activity (Chen et al. 2007a). 5NHQ is also a potent chelator of metals like copper and magnesium (Pelletier et al. 1994), which strengthens this hypothesis. The data presented in this chapter indicate that 5NHQ-Cu is, in fact, a more potent proteasome inhibitor and tumor growth suppressor than CQ-Cu. 5NHQ-Cu was tested in human leukemia, prostate and breast cancer cells and potently inhibited the cellular proteasome, associated with significant cell death. Importantly, 5NHQ alone also suppressed tumor growth in a MDA-MB-231 mouse xenograft model. Thus, 5NHQ interacts with intracellular copper to form an active proteasome inhibitory complex, which is able to induce apoptosis in tumor cells and tissues. Together these results suggest that targeting intracellular copper is an effective means of proteasome inhibition, and indicate that copper chelators like 5NHQ could be used successfully in cancer prevention or treatment.

CHAPTER 5

METAL CHELATORS DESTABILIZE THE E3 LIGASE X-LINKED INHIBITOR OF APOPTOSIS (XIAP): NOVEL POLYPYRIDYL CHELATORS DEplete CELLULAR ZINC AND DESTABILIZE THE X-LINKED INHIBITOR OF APOPTOSIS PROTEIN (XIAP) PRIOR TO INDUCTION OF APOPTOSIS IN HUMAN PROSTATE AND BREAST CANCER CELLS

Adapted from published material in J Cell Biochem. 2012 Aug;113(8):2567-75.

X-linked inhibitor of apoptosis protein, XIAP, inhibits the initiation and execution phases of the apoptotic pathway. XIAP is the most potent member of the inhibitor of apoptosis protein (IAP) family of the endogenous caspase inhibitors. Therefore, targeting XIAP may be a promising strategy for the treatment of apoptosis-resistant malignancies. In this chapter, the relationships of chemical structures of several novel ligands to their zinc-binding ability and effects on the molecular target XIAP and tumor cell death-inducing activity were studied systematically. Treatment of PC-3 prostate cancer and MDA-MB-231 breast cancer cells with these membrane-permeable zinc-chelators with different zinc affinities results in varying degrees of XIAP depletion. Following degradation of XIAP protein, apoptosis-related caspase activation and cellular morphological changes were also observed upon treatment with strong zinc-chelators N4Py and BnTPEN. Addition of zinc has a full protective effect on cells treated with these chelators, while iron addition has only partial protection that can, however, be further increased to a comparable level of protection as zinc by inhibition of ROS generation, indicating that cell death effects mediated by iron- but not zinc-complexes involve redox cycling. These findings suggest that strong zinc-chelating agents may be useful in the treatment of apoptosis-resistant human cancers.

RESULTS

Structures and Zn binding affinity of polypyridyl ligands determined under cell-free conditions

Several unique, cell-permeable nitrogen-containing polypyridyl ligands (Figure 48) have varying denticity, from three for DPA to six for TPEN. These ligands can bind to metal ions such as Fe, Zn or Cu to form stable metal complexes (Anderegg, et al. 1977) with different binding affinities. The structure-biological activity relationships of these ligands have never been systematically investigated. Therefore, the Zn-binding affinities of these ligands in solution were determined and compared: the rank of their Zn-binding affinities under cell-free conditions was TPEN > BnTPEN > N4Py > TPA > DPA (Figure 48, Insert). The relationship of the Zn-binding strengths and biological activities of these ligands was then investigated in intact human cancer cells.

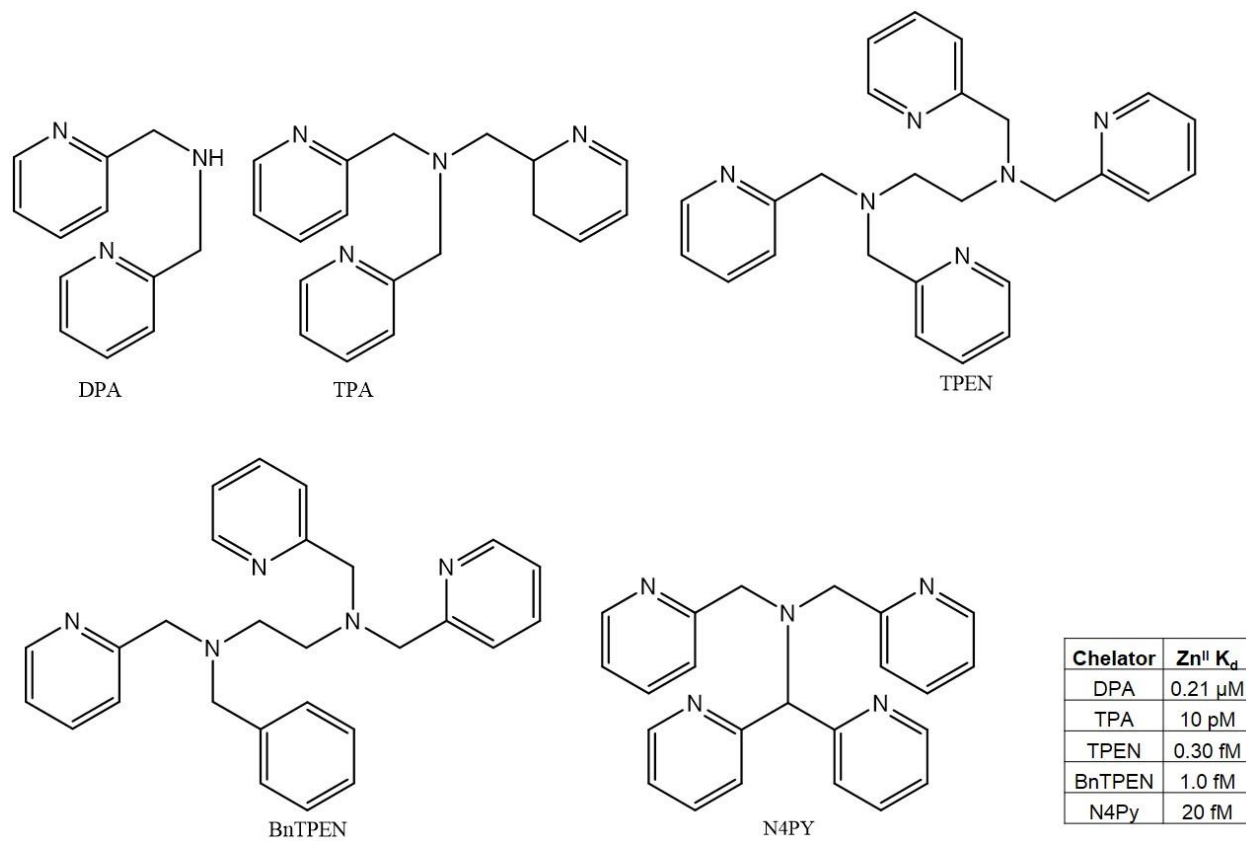


Figure 48. Structures and Zn-binding affinities (Zn^{II} K_d) of tested chelators.

Inhibition of prostate cancer cell viability and induction of apoptosis by the tested polypyridyl chelators are associated with depletion of XIAP

XIAP uses Zn(II) ion as a cofactor and, therefore, the cellular Zn-binding ability of these ligands can be exploited by measuring effects on XIAP protein levels. Thus, whether these Zn chelators could remove Zn from XIAP, causing its degradation and leading to cell death and growth inhibition, and whether the rank of biological activities of these ligands in cultured cancer cells matches that found in solution was investigated. TPEN and TPA are known to be cell permeable (Ghosh, et al. 2010; Hashemi, et al. 2007) and because N4Py and BnTPEN are structurally and functionally similar to TPEN (vide infra), they should be cell permeable as well.

To determine the effects of these chelators on cell viability, human prostate cancer PC-3 cells were treated with each of the selected agents at 1, 2.5 or 5 μM or with DMSO, as a solvent control, for 24 hours, followed by measurement via MTT assay (Figure 49A). Cells treated with TPEN, BnTPEN, N4Py and TPA at 5 μM exhibited dramatically decreased cell viability (about 100%, 100%, 90% and 90%, respectively). When cells were treated with 2.5 μM TPEN, BnTPEN, N4Py and TPA, cell viability was reduced by about 70%, 90%, 20% and 15%, respectively (Figure 49A), which roughly matched the rank of their Zn-binding strengths in solution (Figure 48). The slight differences in relative potency of these ligands may be due to differences in stability and permeability in solution compared with in cells. None of the ligands exhibited any inhibitory effect at 1 μM (Figure 49A). Additionally, treatment with DPA even at 5 μM resulted in no inhibition of cellular viability (Figure 49A). These data suggest that the ability of these ligands to inhibit cellular viability corresponds with their zinc-binding ability in solution.

Additionally, to determine the effects of chelators on cancer cell death, Western blot analysis was performed on PC-3 cell lysates after 16 hour treatment with 2.5 or 5 μM of each chelator. Apoptosis-associated PARP cleavage was observed in cells treated for 16 hours with

TPEN, BnTPEN, N4Py and TPA at 5 μM (Figure 49B). Less dramatic PARP cleavage was observed following 2.5 μM treatment (Figure 49B). Again, some slight changes in relative potency of these ligands under cellular conditions compared to in solution were observed. Importantly, depletion of XIAP, associated with induction of apoptosis, was observed in cells treated with 2.5 μM TPEN, BnTPEN, N4Py and TPA, and XIAP was completely undetectable when these ligands were used at 5 μM (Figure 49B), suggesting that XIAP depletion is associated with inhibition of cell proliferation and induction of PARP cleavage, and these effects are, at least partially dependent on Zn-binding affinity. Again, DPA treatment generated neither PARP cleavage nor XIAP degradation (Figure 49B).

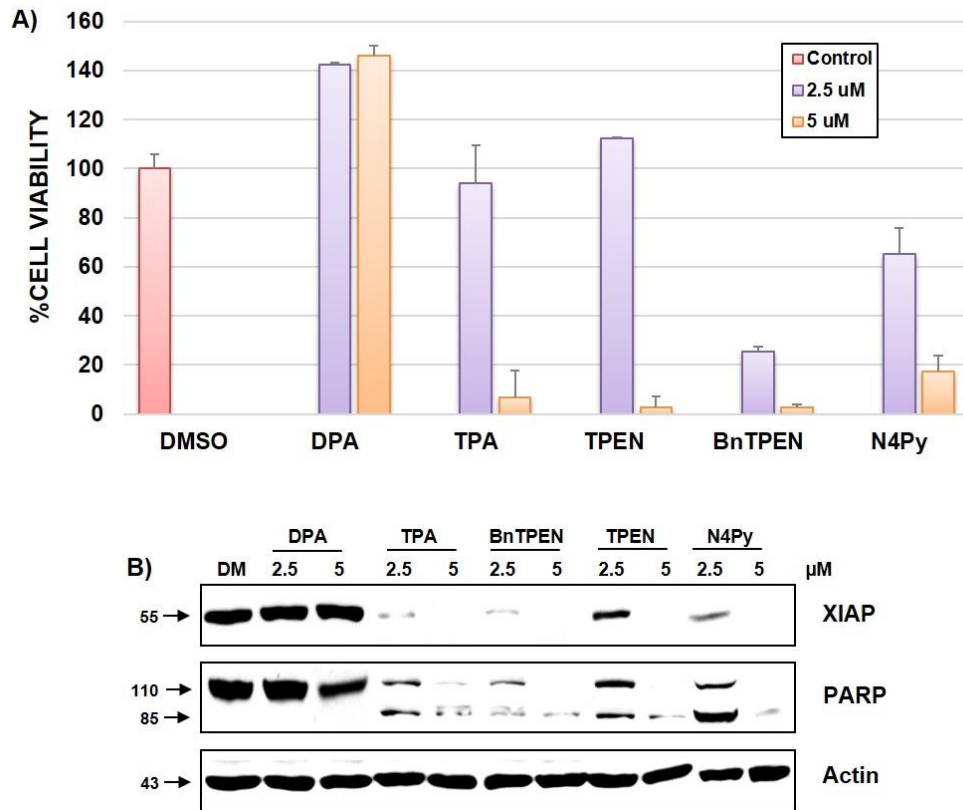


Figure 49. Polypyridyl chelators inhibit cell proliferation and induce apoptosis in prostate cancer cells associated with XIAP depletion and dependent on Zn-binding. A) MTT assay (24 h) B) Western blot analysis (16 h). The concentration of each compound used was 2.5 or 5 μ M, as indicated. DM = DMSO treatment.

Inhibition of cell viability and induction of apoptosis associated with XIAP depletion are also observed in human breast cancer cells

Similar effects were also observed in the breast cancer cell line, MDA-MB-231. MDA-MB-231 cells were treated with the chelators at 10 and 15 μM or with the solvent DMSO for 48 hours, followed by measurement of cellular viability by MTT assay. TPA, TPEN, BnTPEN and N4Py treatment resulted in inhibition of cellular viability, while DPA was again the least potent chelator, causing only about 50% inhibition at 15 μM (Figure 50A). However, the chelators (TPA, TPEN, BnTPEN and N4Py) were much less potent in these cells, reaching a maximum of only 70–85% inhibition at 15 μM (Figure 50A), than in PC-3 cells, where a maximum inhibition of nearly 100% was reached after treatment with only 5 μM (Figure 49A), which may suggest that this strategy may be more useful in treating prostate cancer than breast cancer.

Also similar to the results observed in PC-3 cells, Western blot analysis showed that 3 hour treatment with 10 μM TPA, TPEN, BnTPEN and N4Py induced depletion of full-length XIAP, with almost complete disappearance as a result of BnTPEN treatment (Figure 50B). Following XIAP depletion after 3 hour treatment, caspase-3 activation was detected after treatment with 10 μM TPA, TPEN, BnTPEN and N4Py for 24 hours, evident by cleavage of caspase-3 into its active form (17 kDa) (Figure 50B) and induction of caspase-3 enzymatic activity (Figure 50C). Because an antibody specific for the cleaved caspase-3 fragment (17 kD) was used, no full-length caspase-3 bands (36 kD) were detected. Maximum caspase activation occurred after 24 hour treatment with TPA, TPEN, BnTPEN and N4Py (approximately, 12-, 7-, 16- and 13-fold, respectively). This was also accompanied by decreased levels of full-length PARP and/or the appearance of cleaved PARP after 24 hour treatment (Figures 50B). Little to no PARP cleavage was observed after 3 hours (Figure 50B), suggesting that apoptosis occurs after XIAP depletion. In contrast, treatment with DPA induced neither XIAP depletion at 3 hours nor apoptosis at 24 hours (Figure 50B, C).

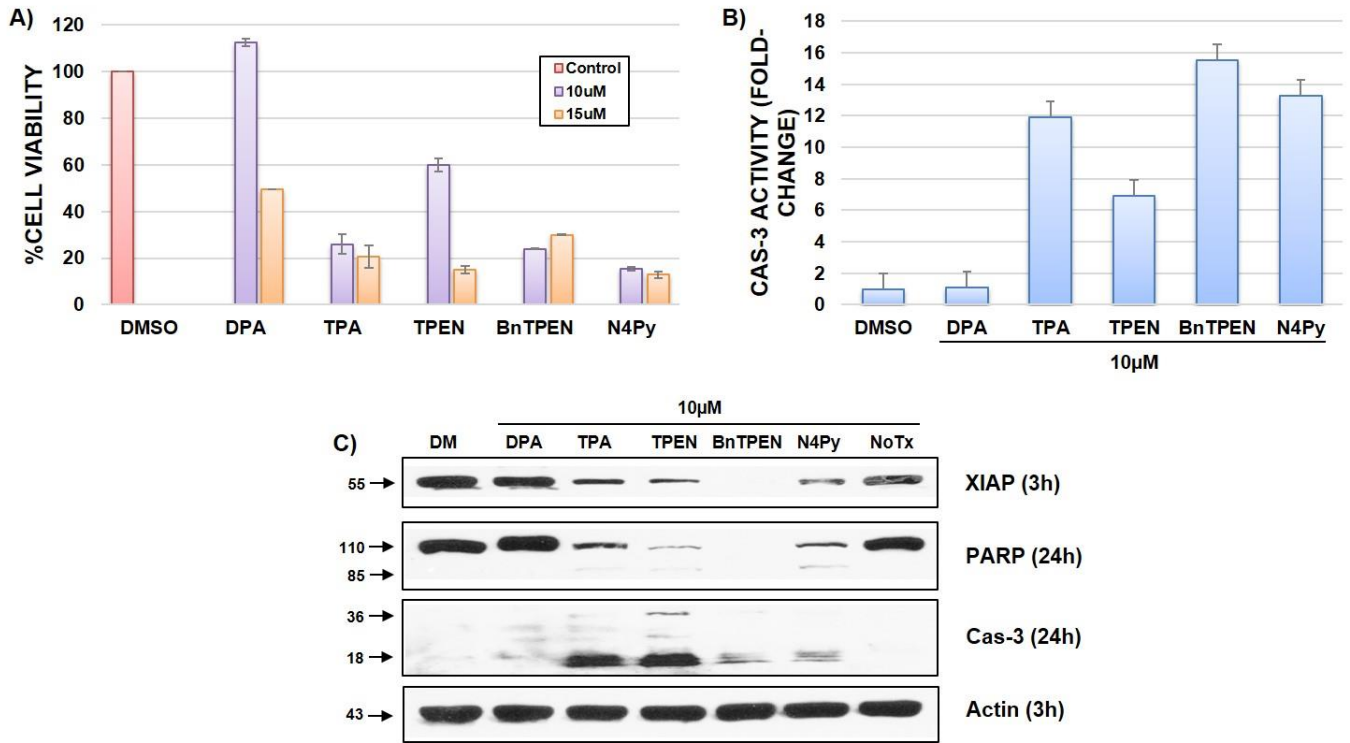


Figure 50. Polypyridyl chelators inhibit cell proliferation and induce apoptosis in breast cancer cells associated with XIAP depletion and dependent on Zn-binding. A) MTT assay (48 h) B) Western blot analysis (3 h and 24 h) C) Caspase-3 activity assay (24 h). The concentrations of each compound used were 10 (A-C) or 15 μ M (A). DM = DMSO treatment.

Addition of Zn and Fe has differential effects on BnTPEN- and N4Py-induced cell viability inhibition and apoptosis

To determine the effect of metal addition on BnTPEN- and N4Py-mediated inhibition of cell viability, PC-3 cells were treated with each chelator at 5 μM in the absence or presence of FeCl_2 or ZnCl_2 at various concentrations. Cell viability was subsequently measured by MTT assay (Figure 51A). Addition of ZnCl_2 at concentrations as low as 0.5 (data not shown) to 10 μM reversed 5 μM N4Py-mediated cell growth inhibition, but FeCl_2 , even at concentrations of 5 and 10 μM exhibited little rescue of cellular viability (Figure 51A). Also, addition of ZnCl_2 at concentrations of 2.5 (data not shown) to 10 μM , but not FeCl_2 even at concentrations as high as 10 μM , reversed inhibition of cell growth by BnTPEN (Figure 51B).

Similarly, ZnCl_2 completely, while FeCl_2 partially, reversed PARP cleavage induced by treatment with N4Py and BnTPEN, as found by Western blot analysis (Figure 51C). XIAP depletion at 3 hours by N4Py was reversed by both FeCl_2 and ZnCl_2 , while XIAP depletion by BnTPEN was reversed completely with ZnCl_2 , but only partially by FeCl_2 (Figure 51C). Similarly, the morphological changes induced by both ligands were reversible only by ZnCl_2 and not FeCl_2 (Figure 51D). Although FeCl_2 partially reversed PARP cleavage and XIAP depletion induced by both ligands, FeCl_2 addition did not prevent cells from undergoing cell death (Figure 51D), consistent with its failure to rescue cells from growth inhibition mediated by the ligands (Figure 51A), which may be explained by the ligand binding to Fe and producing oxidative stress. The ability of FeCl_2 to rescue XIAP depletion by N4Py, but only partially rescue that induced by BnTPEN is concordant with N4Py binding Fe rather than Zn. Inhibition of XIAP degradation upon FeCl_2 addition may partially contribute to decreased apoptosis (Figure 51C).

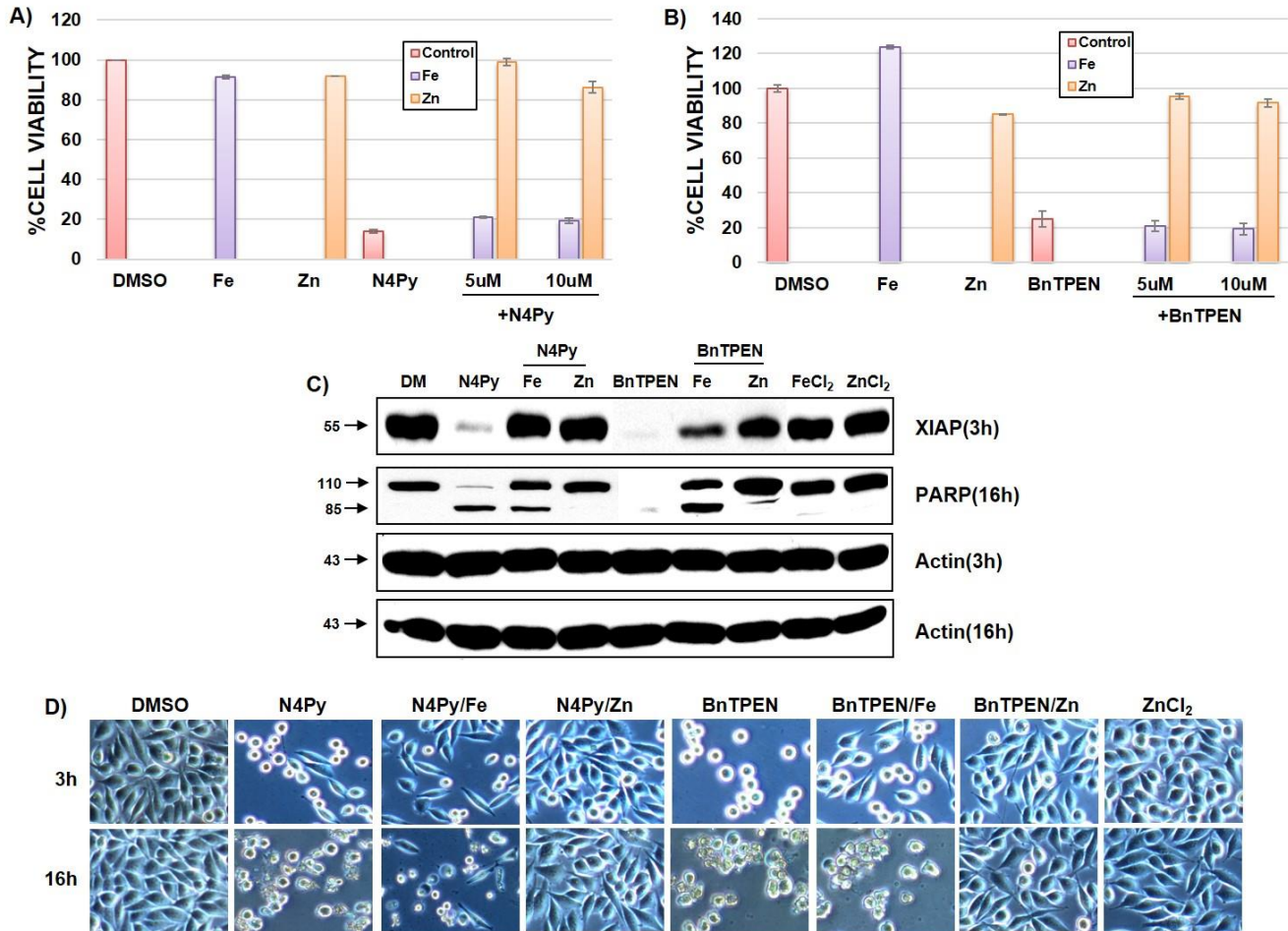


Figure 51. Addition of Zn and Fe has differential effects on BnTPEN- and N4Py-induced cell viability inhibition and apoptosis. A) MTT: Zn but not Fe reverses inhibition of cell viability by N4Py. B) MTT: Only Zn reverses effect of BnTPEN. Concentrations and time points used: Fe and Zn alone = 10 μ M, N4Py and BnTPEN alone and in combination with metals = 5 μ M, 24 h treatment. C) Western blot: Fe and Zn have different protective effects on N4Py- and BnTPEN-mediated XIAP depletion. Fe partially, while Zn completely, rescues N4Py- and BnTPEN-induced PARP cleavage. D) Zn, but not Fe, completely reverses N4Py- and BnTPEN-associated morphological changes. DM = DMSO treatment.

Pre-treatment with Zn, but not Fe, reverses the effects of both N4Py and BnTPEN

To determine if the time at which metal is added affects the reversal of chelator-mediated effects, PC-3 cells were first treated with 100 μM FeCl_2 or ZnCl_2 for 48 hours, followed by co-treatment with 10 μM N4Py or BnTPEN for an additional 3 or 20 hours. Cell viability was then assessed via MTT assay (Figure 52A). Cells pre-treated with ZnCl_2 displayed increased viability compared to cells treated with either N4Py or BnTPEN alone (Figure 52A). In contrast, the inhibition of cell growth by N4Py and BnTPEN was sustained in cells pre-treated with FeCl_2 (Figure 52A). Western blot analysis revealed that apoptosis-associated PARP cleavage mediated by N4Py and BnTPEN could also be reversed by ZnCl_2 but not FeCl_2 (Figure 52B). Importantly, pre-treatment with ZnCl_2 , but not FeCl_2 also had a protective effect against XIAP depletion and apoptosis-associated morphological changes mediated by both N4Py and BnTPEN (Figure 52B, C).

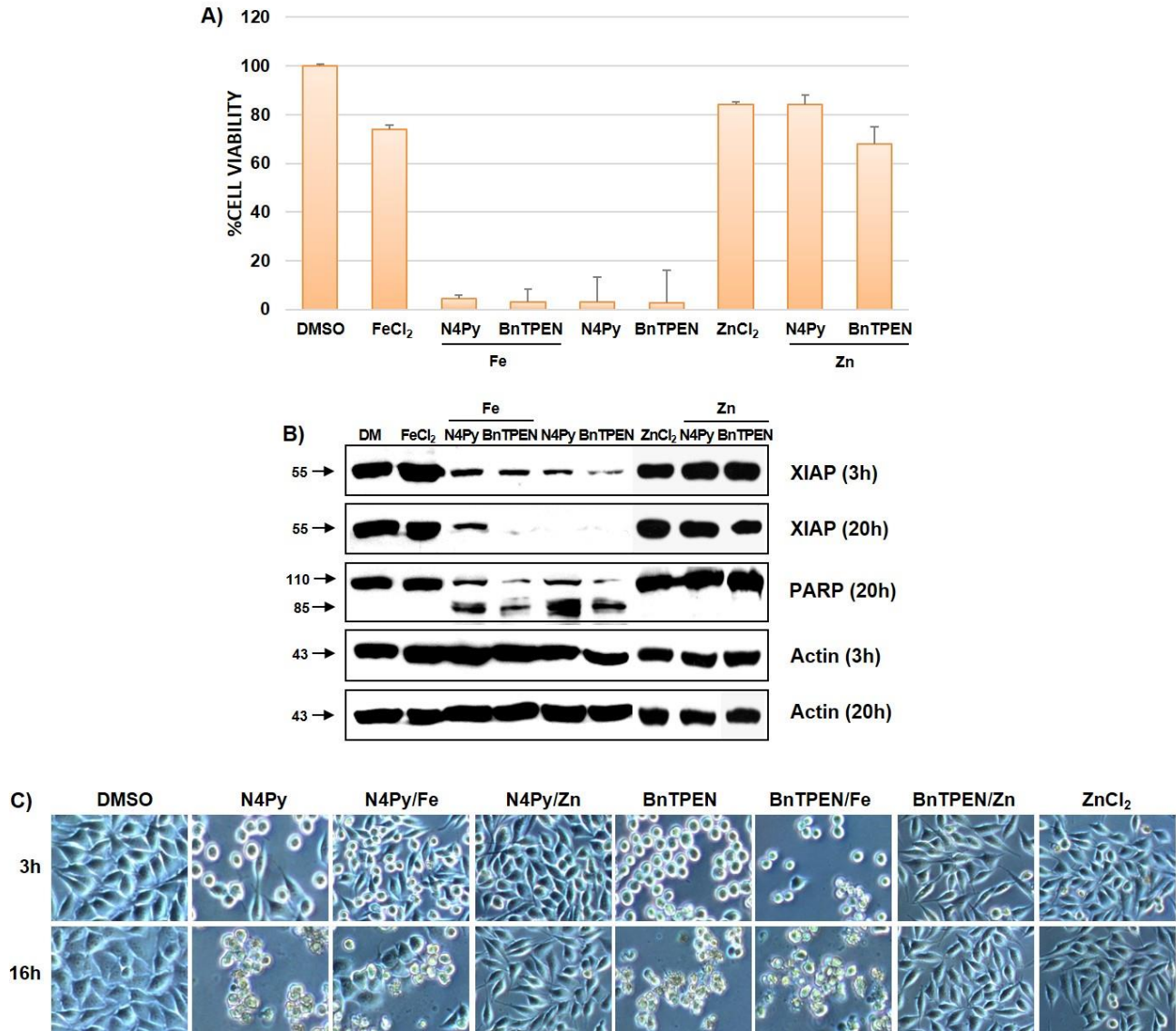


Figure 52. Effects of N4Py and BnTPEN in PC-3 cells are reversed by pre-treatment with Zn. A) MTT assay B) Western blot assay C) Morphological changes. Treatment with iron alone (data not shown) resulted in similar effects as that with zinc alone. Concentrations and time points used: Fe and Zn = 100 μ M, N4Py and BnTPEN = 10 μ M. 48 h metal pre-treatment, followed by 3 h or 20 h co-treatment with ligand. DM = DMSO treatment.

Treatment with N-acetylcysteine (NAC) reverses N4Py-mediated effects

To elucidate the possible mechanism by which FeCl₂ is only able to partially reverse N4Py-mediated effects as compared to full reversal by ZnCl₂, PC-3 cells were treated with 5 μM N4Py, 10 μM FeCl₂ or ZnCl₂, and 250 μM N-acetylcysteine (NAC). NAC is a scavenger of reactive oxygen species (Aruoma, et al. 1989), which may be generated in cells treated with FeCl₂, which can redox cycle, but not in cells treated with ZnCl₂. When cell viability was measured by MTT assay, it was observed that treatment with NAC and FeCl₂ almost completely reversed the effects of N4Py, to a level comparable to those observed in cells treated with N4Py and ZnCl₂ (Figure 53A).

To further validate the effects of NAC addition, Western blot analysis was performed on PC-3 cell lysates after treatment with N4Py, ZnCl₂ or FeCl₂ and NAC. Interestingly, XIAP depletion by N4Py was partially reversed by NAC treatment, but PARP cleavage was not further reversed (Figure 53B). The partial reversal of XIAP depletion may be due to the tighter binding of N4Py to Zn compared to Fe (77 times stronger), suggesting that Fe-N4Py may be able to strip Zn from XIAP to form a more potent cell death-inducing Zn-N4Py complex. Similarly, cell death associated morphological changes induced by N4Py were also partially reversed by addition of NAC (Figure 53C). These results suggest that some Fe/N4Py-mediated cell death effects may be due to ROS generated through Fe-redox cycling.

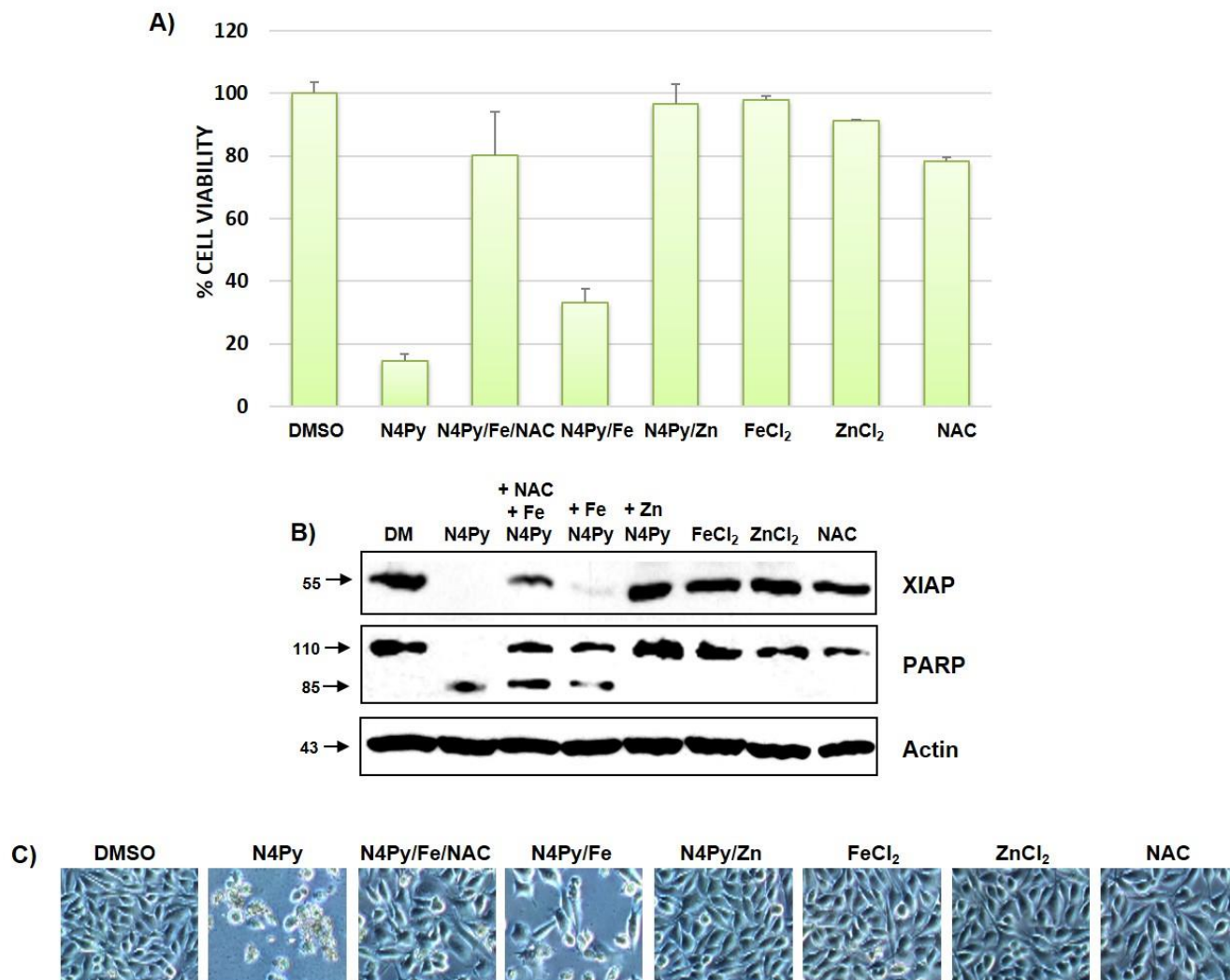


Figure 53. Effects of N4Py are reversible by treatment with NAC. A) MTT assay B) Western blot analysis C) Morphological changes. Concentrations and time points used: NAC = 250 μ M, Fe and Zn = 10 μ M, N4Py = 5 μ M, 20 h treatment. NAC = N-Acetylcysteine; DM = DMSO treatment.

DISCUSSION

Zinc is a known enzyme inhibitor with a well-documented catalytic role in metalloenzymes, and the removal of zinc from inhibitory enzymatic sites leads to increased enzyme activity (Maret, et al. 1999). However, in some RING-finger containing proteins, such as XIAP, it is well documented that zinc is important for structural stability of these enzymes, but the mechanism by which Zn-chelators induce XIAP depletion is not well-defined. One proposed mechanism suggests that depletion of full length XIAP may be a marker for cell death rather than a protective mechanism (Deveraux, et al. 1999; Johnson, et al. 2000; Levkau, et al. 2001). Therefore, this mechanism, as well as others by which these zinc-chelators induce apoptosis must be further investigated. In this chapter, a series of novel ligands with various zinc-binding abilities was used to investigate this important mechanism. It is probable that removal of zinc from the BIR-2 and -3 motifs by novel metal chelators like BnTPEN and N4Py destabilizes XIAP and causes breakdown of the enzyme, similar to the previously reported action of TPEN (Makhov, et al. 2008). Upon depletion of XIAP, caspases are consequently activated and cells undergo apoptosis (Figure 54).

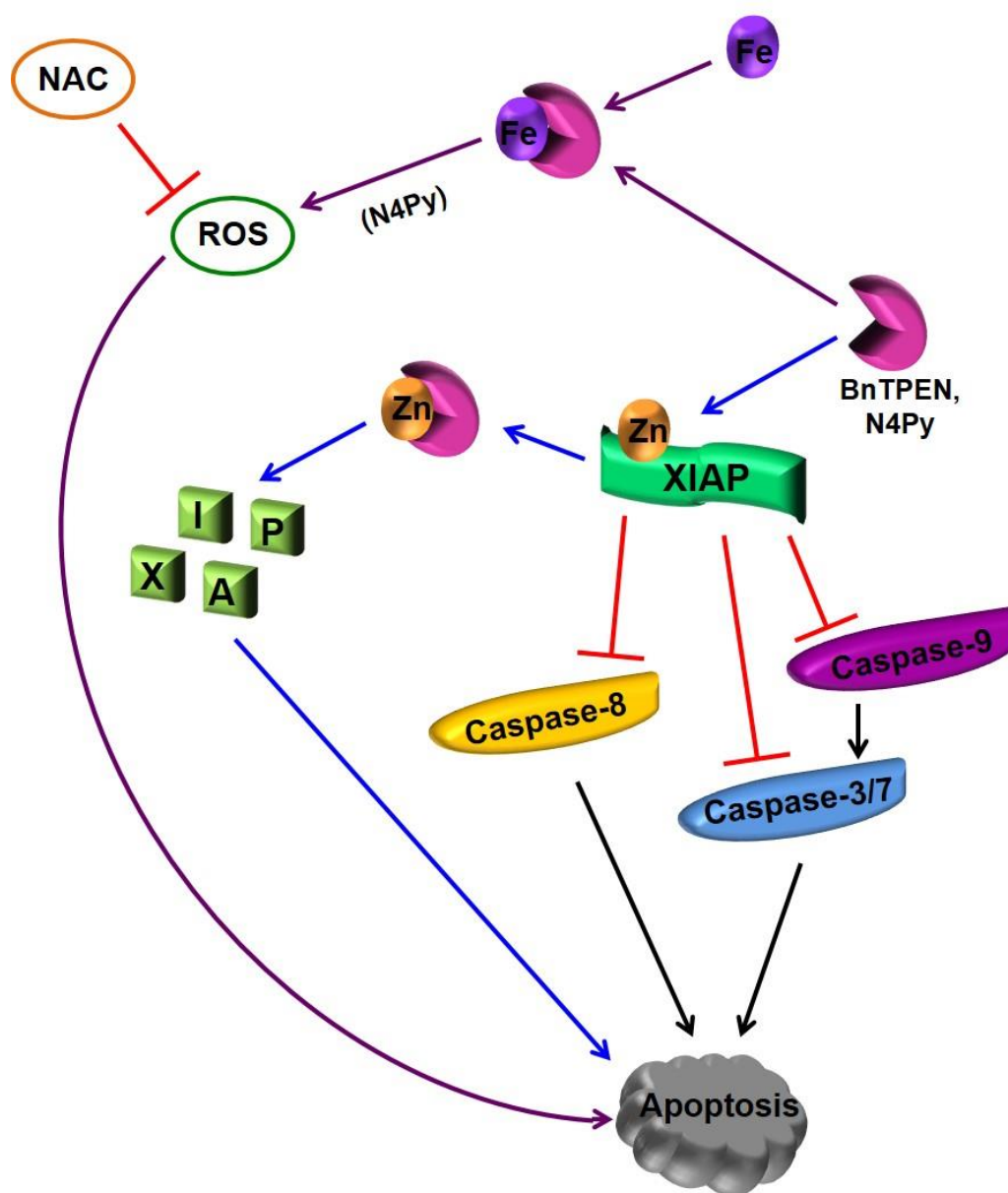


Figure 54. Proposed mechanism by which Zn-chelators BnTPEN and N4Py induce cellular death. Zn-chelators with high Zn-binding affinity remove Zn from XIAP, causing degradation of the enzyme and ultimately leading to apoptotic cell death. Furthermore, the Fe-binding ability of these compounds may also contribute to induction of cell death *via* an XIAP-independent pathway involving Fe redox cycling.

These chelators may also bind intracellular iron, albeit with a lower affinity, but the Fe-binding ability of these compounds may also contribute to induction of cell death *via* an XIAP-independent pathway involving Fe redox cycling (Figure 54). The interaction of these chelators with intracellular Fe and Fe-containing proteins must be examined. Importantly, other metals such as copper and cadmium may also bind to XIAP and induce conformational changes which are associated with destabilization of the enzyme (Mufti, et al. 2006), suggesting that further exploration into possible interactions of these metals with the tested chelators is also necessary. Additionally, while other members of the IAP family contain Zn-binding RING-finger motifs, less is known about the effect of metal chelation on these enzymes. This is a relationship that must be further elucidated. Finally, the mechanisms of action of these ligands found in cultured tumor cells should be confirmed *in vivo* in the future.

Because cancer cells have been shown to express high levels of XIAP, this may be a potential target for emerging therapeutics and while some success has been observed after treatment with small molecule XIAP inhibitors, recent studies have suggested a possibility for development of resistance to these inhibitors (Schimmer, et al. 2006). More recent reports also suggest important roles for XIAP in non-apoptotic pathways such as NF- κ B, MAPK and the ubiquitin-proteasome pathway, which may have greater than previously anticipated effects on normal cellular processes (Srinivasula and Ashwell 2008; Yang, et al. 2009). Therefore, the use of strong Zn-chelating compounds that induce depletion of XIAP may be a very promising strategy for the treatment of human malignancies.

REFERENCES

- Adams, J. 2002. Preclinical and clinical evaluation of proteasome inhibitor PS-341 for the treatment of cancer. *Curr Opin Chem Biol* 6, 493-500.
- Adams, J. 2003. The proteasome: structure, function, and role in the cell. *Cancer Treat Rev* 29 Suppl 1, 3-9.
- Adams, J. 2004a. The development of proteasome inhibitors as anticancer drugs. *Cancer Cell* 5, 417-421.
- Adams, J. 2004b. The proteasome: a suitable antineoplastic target. *Nat Rev Cancer* 4, 349-360.
- Adams, J., Palombella, V. J., Sausville, E. A., Johnson, J., Destree, A., Lazarus, D. D., Maas, J., Pien, C. S., Prakash, S. & Elliott, P. J. 1999. Proteasome inhibitors: a novel class of potent and effective antitumor agents. *Cancer Res* 59, 2615-2622.
- Adams, J. M. & Cory, S. 1998. The Bcl-2 protein family: arbiters of cell survival. *Science* 281, 1322-1326.
- Alama, A., Tasso, B., Novelli, F. & Sparatore, F. 2009. Organometallic compounds in oncology: implications of novel organotin as antitumor agents. *Drug Discov Today* 14, 500-508.
- An, B., Goldfarb, R. H., Siman, R. & Dou, Q. P. 1998. Novel dipeptidyl proteasome inhibitors overcome Bcl-2 protective function and selectively accumulate the cyclin-dependent kinase inhibitor p27 and induce apoptosis in transformed, but not normal, human fibroblasts. *Cell Death Differ* 5, 1062-1075.
- Anderegg, G., Hubmann, E., Podder, N. G. & Wenk, F. 1977. Pyridine derivatives as complexing agents. XI. Thermodynamics of metal complex formation with bis-, tris- and tetrakis[(2-pyridyl)methyl]amines. *Helv Chim Acta* 60, 123-140.

- Arakawa, Y. 2000. Invasion of biofunctions by organotins -immune system. *Res Trace Elements* 11, 259-286.
- Arellano, J. B., Li, H., Gonzalez-Perez, S., Gutierrez, J., Melo, T. B., Vacha, F. & Naqvi, K. R. 2011. Trolox, a water-soluble analogue of alpha-tocopherol, photoprotects the surface-exposed regions of the photosystem II reaction center in vitro. Is this physiologically relevant? *Biochemistry* 50, 8291-8301.
- Arion, V. B., Jakupec, M. A., Galanski, M., Unfried, P. & Keppler, B. K. 2002. Synthesis, structure, spectroscopic and in vitro antitumour studies of a novel gallium(III) complex with 2-acetylpyridine (4)N-dimethylthiosemicarbazone. *J Inorg Biochem* 91, 298-305.
- Aruoma, O. I., Halliwell, B., Hoey, B. M. & Butler, J. 1989. The antioxidant action of N-acetylcysteine: its reaction with hydrogen peroxide, hydroxyl radical, superoxide, and hypochlorous acid. *Free Radic Biol Med* 6, 593-597.
- Baker, S. P. & Grant, P. A. 2005. The proteasome: not just degrading anymore. *Cell* 123, 361-363.
- Bardag-Gorce, F. & French, S. W. 2011. Delta-aminolevulinic dehydratase is a proteasome interacting protein. *Exp Mol Pathol* 91, 485-489.
- Barrea, R. A., Chen, D., Irving, T. C. & Dou, Q. P. 2009. Synchrotron X-ray imaging reveals a correlation of tumor copper speciation with Clioquinol's anticancer activity. *J Cell Biochem* 108, 96-105.
- Bastow, M., Kriedt, C. L., Baldassare, J., Shah, M. & Klein, C. 2011. Zinc is a potential therapeutic for chemoresistant ovarian cancer. *J Exp Ther Oncol* 9, 175-181.
- Baumeister, W., Walz, J., Zuhl, F. & Seemuller, E. 1998. The proteasome: paradigm of a self-compartmentalizing protease. *Cell* 92, 367-380.

- Bercovich, B., Stancovski, I., Mayer, A., Blumenfeld, N., Laszlo, A., Schwartz, A. L. & Ciechanover, A. 1997. Ubiquitin-dependent degradation of certain protein substrates in vitro requires the molecular chaperone Hsc70. *J Biol Chem* 272, 9002-9010.
- Berenson, J. R., Ma, H. M. & Vescio, R. 2001. The role of nuclear factor-kappaB in the biology and treatment of multiple myeloma. *Semin Oncol* 28, 626-633.
- Berlin, A. & Schaller, K. H. 1974. European standardized method for the determination of delta-aminolevulinic acid dehydratase activity in blood. *Z Klin Chem Klin Biochem* 12, 389-390.
- Blunden, S. & Wallace, T. 2003. Tin in canned food: a review and understanding of occurrence and effect. *Food Chem Toxicol* 41, 1651-1662.
- Bogyo, M., McMaster, J. S., Gaczynska, M., Tortorella, D., Goldberg, A. L. & Ploegh, H. 1997. Covalent modification of the active site threonine of proteasomal beta subunits and the Escherichia coli homolog HslV by a new class of inhibitors. *Proc Natl Acad Sci U S A* 94, 6629-6634.
- Brahemi, G., Kona, F. R., Fiasella, A., Buac, D., Soukupova, J., Brancale, A., Burger, A. M. & Westwell, A. D. 2010. Exploring the structural requirements for inhibition of the ubiquitin E3 ligase breast cancer associated protein 2 (BCA2) as a treatment for breast cancer. *J Med Chem* 53, 2757-2765.
- Brar, S. S., Grigg, C., Wilson, K. S., Holder, W. D., Jr., Dreau, D., Austin, C., Foster, M., Ghio, A. J., Whorton, A. R., Stowell, G. W., et al. 2004. Disulfiram inhibits activating transcription factor/cyclic AMP-responsive element binding protein and human melanoma growth in a metal-dependent manner in vitro, in mice and in a patient with metastatic disease. *Mol Cancer Ther* 3, 1049-1060.

- Breinig, S., Kervinen, J., Stith, L., Wasson, A. S., Fairman, R., Wlodawer, A., Zdanov, A. & Jaffe, E. K. 2003. Control of tetrapyrrole biosynthesis by alternate quaternary forms of porphobilinogen synthase. *Nat Struct Biol* 10, 757-763.
- Brem, S. 1999. Angiogenesis and Cancer Control: From Concept to Therapeutic Trial. *Cancer Control* 6, 436-458.
- Brewer, G. J. 2001. Copper control as an antiangiogenic anticancer therapy: lessons from treating Wilson's disease. *Exp Biol Med (Maywood)* 226, 665-673.
- Brooks, P., Fuertes, G., Murray, R. Z., Bose, S., Knecht, E., Rechsteiner, M. C., Hendil, K. B., Tanaka, K., Dyson, J. & Rivett, J. 2000. Subcellular localization of proteasomes and their regulatory complexes in mammalian cells. *Biochem J* 346 Pt 1, 155-161.
- Calamai, P., Carotti, S., Guerri, A., Mazzei, T., Messori, L., Mini, E., Orioli, P. & Speroni, G. P. 1998. Cytotoxic effects of gold(III) complexes on established human tumor cell lines sensitive and resistant to cisplatin. *Anticancer Drug Des* 13, 67-80.
- Cao, B., Li, J., Zhu, J., Shen, M., Han, K., Zhang, Z., Yu, Y., Wang, Y., Wu, D., Chen, S., et al. 2013. The antiparasitic clioquinol induces apoptosis in leukemia and myeloma cells by inhibiting histone deacetylase activity. *J Biol Chem* 288, 34181-34189.
- Cater, M. A. & Haupt, Y. 2011. Clioquinol induces cytoplasmic clearance of the X-linked inhibitor of apoptosis protein (XIAP): therapeutic indication for prostate cancer. *Biochem J* 436, 481-491.
- Cen, D., Brayton, D., Shahandeh, B., Meyskens, F. L., Jr. & Farmer, P. J. 2004. Disulfiram facilitates intracellular Cu uptake and induces apoptosis in human melanoma cells. *J Med Chem* 47, 6914-6920.

- Chakravarty, P. K., Ghosh, A. & Chowdhury, J. R. 1986. Zinc in human malignancies. *Neoplasma* 33, 85-90.
- Chang, K. L., Hung, T. C., Hsieh, B. S., Chen, Y. H., Chen, T. F. & Cheng, H. L. 2006. Zinc at pharmacologic concentrations affects cytokine expression and induces apoptosis of human peripheral blood mononuclear cells. *Nutrition* 22, 465-474.
- Chauhan, D. & Anderson, K. C. 2003. Mechanisms of cell death and survival in multiple myeloma (MM): Therapeutic implications. *Apoptosis* 8, 337-343.
- Chauhan, D., Singh, A. V., Aujay, M., Kirk, C. J., Bandi, M., Ciccarelli, B., Raje, N., Richardson, P. & Anderson, K. C. 2010. A novel orally active proteasome inhibitor ONX 0912 triggers in vitro and in vivo cytotoxicity in multiple myeloma. *Blood* 116, 4906-4915.
- Chen, D., Cui, Q. C., Yang, H., Barrea, R. A., Sarkar, F. H., Sheng, S., Yan, B., Reddy, G. P. & Dou, Q. P. 2007a. Clioquinol, a therapeutic agent for Alzheimer's disease, has proteasome-inhibitory, androgen receptor-suppressing, apoptosis-inducing, and antitumor activities in human prostate cancer cells and xenografts. *Cancer Res* 67, 1636-1644.
- Chen, D., Cui, Q. C., Yang, H. & Dou, Q. P. 2006. Disulfiram, a clinically used anti-alcoholism drug and copper-binding agent, induces apoptotic cell death in breast cancer cultures and xenografts via inhibition of the proteasome activity. *Cancer Res* 66, 10425-10433.
- Chen, D., Frezza, M., Shakya, R., Cui, Q. C., Milacic, V., Verani, C. N. & Dou, Q. P. 2007b. Inhibition of the proteasome activity by gallium(III) complexes contributes to their anti prostate tumor effects. *Cancer Res* 67, 9258-9265.
- Chen, Z. J. & Sun, L. J. 2009. Nonproteolytic functions of ubiquitin in cell signaling. *Mol Cell* 33, 275-286.

- Cherny, R. A., Atwood, C. S., Xilinas, M. E., Gray, D. N., Jones, W. D., McLean, C. A., Barnham, K. J., Volitakis, I., Fraser, F. W., Kim, Y., et al. 2001. Treatment with a copper-zinc chelator markedly and rapidly inhibits beta-amyloid accumulation in Alzheimer's disease transgenic mice. *Neuron* 30, 665-676.
- Chiba, T., Suzuki, E., Yuki, K., Zen, Y., Oshima, M., Miyagi, S., Saraya, A., Koide, S., Motoyama, T., Ogasawara, S., et al. 2014. Disulfiram Eradicates Tumor-Initiating Hepatocellular Carcinoma Cells in ROS-p38 MAPK Pathway-Dependent and -Independent Manners. *PLoS One* 9, e84807.
- Chitambar, C. R. 2004. Gallium compounds as antineoplastic agents. *Curr Opin Oncol* 16, 547-552.
- Chitambar, C. R. 2010. Medical applications and toxicities of gallium compounds. *Int J Environ Res Public Health* 7, 2337-2361.
- Christiansen, J. J. & Rajasekaran, A. K. 2006. Reassessing epithelial to mesenchymal transition as a prerequisite for carcinoma invasion and metastasis. *Cancer Res* 66, 8319-8326.
- Chua, M. S., Bernstein, L. R., Li, R. & So, S. K. 2006. Gallium maltolate is a promising chemotherapeutic agent for the treatment of hepatocellular carcinoma. *Anticancer Res* 26, 1739-1743.
- Ciechanover, A. 1998. The ubiquitin-proteasome pathway: on protein death and cell life. *EMBO J* 17, 7151-7160.
- Ciechanover, A. 2006. The ubiquitin proteolytic system: from a vague idea, through basic mechanisms, and onto human diseases and drug targeting. *Neurology* 66, S7-19.
- Ciechanover, A., Orian, A. & Schwartz, A. L. 2000. Ubiquitin-mediated proteolysis: biological regulation via destruction. *Bioessays* 22, 442-451.

- Ciehanover, A., Hod, Y. & Hershko, A. 1978. A heat-stable polypeptide component of an ATP-dependent proteolytic system from reticulocytes. *Biochem Biophys Res Commun* 81, 1100-1105.
- Clark, R. C., Lee, S. Y. & Boger, D. L. 2008. Total synthesis of chlorofusin, its seven chromophore diastereomers, and key partial structures. *J Am Chem Soc* 130, 12355-12369.
- Collery, P., Keppler, B., Madoulet, C. & Desoize, B. 2002. Gallium in cancer treatment. *Crit Rev Oncol Hematol* 42, 283-296.
- Collery, P., Lechenault, F., Cazabat, A., Juvin, E., Khassanova, L., Evangelou, A. & Keppler, B. 2000. Inhibitory effects of gallium chloride and tris (8-quinolinolato) gallium III on A549 human malignant cell line. *Anticancer Res* 20, 955-958.
- Collins, G. A. & Tansey, W. P. 2006. The proteasome: a utility tool for transcription? *Curr Opin Genet Dev* 16, 197-202.
- Costello, L. C. & Franklin, R. B. 2006. The clinical relevance of the metabolism of prostate cancer; zinc and tumor suppression: connecting the dots. *Mol Cancer* 5, 17.
- Coux, O., Tanaka, K. & Goldberg, A. L. 1996. Structure and functions of the 20S and 26S proteasomes. *Annu Rev Biochem* 65, 801-847.
- Craiu, A., Gaczynska, M., Akopian, T., Gramm, C. F., Fenteany, G., Goldberg, A. L. & Rock, K. L. 1997. Lactacystin and clasto-lactacystin beta-lactone modify multiple proteasome beta-subunits and inhibit intracellular protein degradation and major histocompatibility complex class I antigen presentation. *J Biol Chem* 272, 13437-13445.
- Crawford, L. J., Walker, B., Ovaa, H., Chauhan, D., Anderson, K. C., Morris, T. C. & Irvine, A. E. 2006. Comparative selectivity and specificity of the proteasome inhibitors BzLLLCOCHO, PS-341, and MG-132. *Cancer Res* 66, 6379-6386.

- Cvek, B., Milacic, V., Taraba, J. & Dou, Q. P. 2008. Ni(II), Cu(II), and Zn(II) diethyldithiocarbamate complexes show various activities against the proteasome in breast cancer cells. *J Med Chem* 51, 6256-6258.
- D'Arcy, P. & Linder, S. 2012. Proteasome deubiquitinases as novel targets for cancer therapy. *Int J Biochem Cell Biol* 44, 1729-1738.
- da Fonseca, P. C. & Morris, E. P. 2008. Structure of the human 26S proteasome: subunit radial displacements open the gate into the proteolytic core. *J Biol Chem* 283, 23305-23314.
- Dalla Via, L., Nardon, C. & Fregona, D. 2012. Targeting the ubiquitin-proteasome pathway with inorganic compounds to fight cancer: a challenge for the future. *Future Med Chem* 4, 525-543.
- Daniel, K. G., Chen, D., Orlu, S., Cui, Q. C., Miller, F. R. & Dou, Q. P. 2005. Clioquinol and pyrrolidine dithiocarbamate complex with copper to form proteasome inhibitors and apoptosis inducers in human breast cancer cells. *Breast Cancer Res* 7, R897-908.
- Daniel, K. G., Gupta, P., Harbach, R. H., Guida, W. C. & Dou, Q. P. 2004. Organic copper complexes as a new class of proteasome inhibitors and apoptosis inducers in human cancer cells. *Biochem Pharmacol* 67, 1139-1151.
- de Gramont, A., Figer, A., Seymour, M., Homerin, M., Hmissi, A., Cassidy, J., Boni, C., Cortes-Funes, H., Cervantes, A., Freyer, G., et al. 2000. Leucovorin and fluorouracil with or without oxaliplatin as first-line treatment in advanced colorectal cancer. *J Clin Oncol* 18, 2938-2947.
- DeMartino, G. N. & Slaughter, C. A. 1999. The proteasome, a novel protease regulated by multiple mechanisms. *J Biol Chem* 274, 22123-22126.

- Deveraux, Q., Ustrell, V., Pickart, C. & Rechsteiner, M. 1994. A 26 S protease subunit that binds ubiquitin conjugates. *J Biol Chem* 269, 7059-7061.
- Deveraux, Q. L., Leo, E., Stennicke, H. R., Welsh, K., Salvesen, G. S. & Reed, J. C. 1999. Cleavage of human inhibitor of apoptosis protein XIAP results in fragments with distinct specificities for caspases. *EMBO J* 18, 5242-5251.
- Di Vaira, M., Bazzicalupi, C., Orioli, P., Messori, L., Bruni, B. & Zatta, P. 2004. Clioquinol, a drug for Alzheimer's disease specifically interfering with brain metal metabolism: structural characterization of its zinc(II) and copper(II) complexes. *Inorg Chem* 43, 3795-3797.
- Dick, L. R., Cruikshank, A. A., Grenier, L., Melandri, F. D., Nunes, S. L. & Stein, R. L. 1996. Mechanistic studies on the inactivation of the proteasome by lactacystin: a central role for clasto-lactacystin beta-lactone. *J Biol Chem* 271, 7273-7276.
- Diez, M., Arroyo, M., Cerdan, F. J., Munoz, M., Martin, M. A. & Balibrea, J. L. 1989. Serum and tissue trace metal levels in lung cancer. *Oncology* 46, 230-234.
- Ding, W. Q., Liu, B., Vaught, J. L., Yamauchi, H. & Lind, S. E. 2005. Anticancer activity of the antibiotic clioquinol. *Cancer Res* 65, 3389-3395.
- Dou, Q. P. & Li, B. 1999. Proteasome inhibitors as potential novel anticancer agents. *Drug Resist Updat* 2, 215-223.
- Du, T., Filiz, G., Caragounis, A., Crouch, P. J. & White, A. R. 2008. Clioquinol promotes cancer cell toxicity through tumor necrosis factor alpha release from macrophages. *J Pharmacol Exp Ther* 324, 360-367.
- Duncan, S. J., Gruschow, S., Williams, D. H., McNicholas, C., Purewal, R., Hajek, M., Gerlitz, M., Martin, S., Wrigley, S. K. & Moore, M. 2001. Isolation and structure elucidation of

- Chlorofusin, a novel p53-MDM2 antagonist from a *Fusarium* sp. *J Am Chem Soc* 123, 554-560.
- Eckelman, B. P., Salvesen, G. S. & Scott, F. L. 2006. Human inhibitor of apoptosis proteins: why XIAP is the black sheep of the family. *EMBO Rep* 7, 988-994.
- Eckhardt, S. 2002. Recent progress in the development of anticancer agents. *Curr Med Chem Anticancer Agents* 2, 419-439.
- Elsasser, S., Gali, R. R., Schwickart, M., Larsen, C. N., Leggett, D. S., Muller, B., Feng, M. T., Tubing, F., Dittmar, G. A. & Finley, D. 2002. Proteasome subunit Rpn1 binds ubiquitin-like protein domains. *Nat Cell Biol* 4, 725-730.
- Etlinger, J. D., Li, S. X., Guo, G. G. & Li, N. 1993. Phosphorylation and ubiquitination of the 26S proteasome complex. *Enzyme Protein* 47, 325-329.
- Federico, A., Iodice, P., Federico, P., Del Rio, A., Mellone, M. C., Catalano, G. & Federico, P. 2001. Effects of selenium and zinc supplementation on nutritional status in patients with cancer of digestive tract. *Eur J Clin Nutr* 55, 293-297.
- Feinman, R., Koury, J., Thames, M., Barlogie, B., Epstein, J. & Siegel, D. S. 1999. Role of NF-kappaB in the rescue of multiple myeloma cells from glucocorticoid-induced apoptosis by bcl-2. *Blood* 93, 3044-3052.
- Fenteany, G., Standaert, R. F., Lane, W. S., Choi, S., Corey, E. J. & Schreiber, S. L. 1995. Inhibition of proteasome activities and subunit-specific amino-terminal threonine modification by lactacystin. *Science* 268, 726-731.
- Figueiredo-Pereira, M. E., Berg, K. A. & Wilk, S. 1994. A new inhibitor of the chymotrypsin-like activity of the multicatalytic proteinase complex (20S proteasome) induces accumulation of ubiquitin-protein conjugates in a neuronal cell. *J Neurochem* 63, 1578-1581.

- Finley, D. 2009. Recognition and processing of ubiquitin-protein conjugates by the proteasome. *Annu Rev Biochem* 78, 477-513.
- Forestier, J. 1935. Rheumatoid arthritis and its treatment with gold salts - results of six years' experience. *J Lab Clin Med.* 20, 827-840.
- Foster, B. J., Clagett-Carr, K., Hoth, D. & Leyland-Jones, B. 1986. Gallium nitrate: the second metal with clinical activity. *Cancer Treat Rep* 70, 1311-1319.
- Frangoulis, M., Georgiou, P., Chrisostomidis, C., Perrea, D., Dontas, I., Kavantzas, N., Kostakis, A. & Papadopoulos, O. 2007. Rat epigastric flap survival and VEGF expression after local copper application. *Plast Reconstr Surg* 119, 837-843.
- Frankel, A., Man, S., Elliott, P., Adams, J. & Kerbel, R. S. 2000. Lack of multicellular drug resistance observed in human ovarian and prostate carcinoma treated with the proteasome inhibitor PS-341. *Clin Cancer Res* 6, 3719-3728.
- Franklin, R. B. & Costello, L. C. 2007. Zinc as an anti-tumor agent in prostate cancer and in other cancers. *Arch Biochem Biophys* 463, 211-217.
- Franklin, R. B. & Costello, L. C. 2009. The important role of the apoptotic effects of zinc in the development of cancers. *J Cell Biochem* 106, 750-757.
- Fregona, D., Ronconi, L., Formaggio, F., Dou, Q. P. & Aldinucci, D. 2010. Gold (III) complexes with oligopeptides functionalized with sulfur donors and use thereof as antitumor agents. *Ed PI Appl.*
- Frezza, M., Hindo, S. S., Tomco, D., Allard, M. M., Cui, Q. C., Heeg, M. J., Chen, D., Dou, Q. P. & Verani, C. N. 2009. Comparative activities of nickel(II) and zinc(II) complexes of asymmetric [NN'O] ligands as 26S proteasome inhibitors. *Inorg Chem* 48, 5928-5937.

- Fribley, A. & Wang, C. Y. 2006. Proteasome inhibitor induces apoptosis through induction of endoplasmic reticulum stress. *Cancer Biol Ther* 5, 745-748.
- Fribley, A., Zeng, Q. & Wang, C. Y. 2004. Proteasome inhibitor PS-341 induces apoptosis through induction of endoplasmic reticulum stress-reactive oxygen species in head and neck squamous cell carcinoma cells. *Mol Cell Biol* 24, 9695-9704.
- Fu, H., Doelling, J. H., Rubin, D. M. & Vierstra, R. D. 1999. Structural and functional analysis of the six regulatory particle triple-A ATPase subunits from the Arabidopsis 26S proteasome. *Plant J* 18, 529-539.
- Galanski, M., Arion, V. B., Jakupec, M. A. & Keppler, B. K. 2003. Recent developments in the field of tumor-inhibiting metal complexes. *Curr Pharm Des* 9, 2078-2089.
- Galanski, M., Jakupec, M. A. & Keppler, B. K. 2005. Update of the preclinical situation of anticancer platinum complexes: novel design strategies and innovative analytical approaches. *Curr Med Chem* 12, 2075-2094.
- Ganoth, D., Leshinsky, E., Eytan, E. & Hershko, A. 1988. A multicomponent system that degrades proteins conjugated to ubiquitin. Resolution of factors and evidence for ATP-dependent complex formation. *J Biol Chem* 263, 12412-12419.
- Gholz, L. M. & Arons, W. L. 1964. Prophylaxis and Therapy of Amebiasis and Shigellosis with Iodochlorhydroxyquin. *Am J Trop Med Hyg* 13, 396-401.
- Ghosh, S. K., Kim, P., Zhang, X. A., Yun, S. H., Moore, A., Lippard, S. J. & Medarova, Z. 2010. A novel imaging approach for early detection of prostate cancer based on endogenous zinc sensing. *Cancer Res* 70, 6119-6127.
- Gil-Gomez, G., Berns, A. & Brady, H. J. 1998. A link between cell cycle and cell death: Bax and Bcl-2 modulate Cdk2 activation during thymocyte apoptosis. *EMBO J* 17, 7209-7218.

- Glas, R., Bogyo, M., McMaster, J. S., Gaczynska, M. & Ploegh, H. L. 1998. A proteolytic system that compensates for loss of proteasome function. *Nature* 392, 618-622.
- Goldberg, A. L., Cascio, P., Saric, T. & Rock, K. L. 2002. The importance of the proteasome and subsequent proteolytic steps in the generation of antigenic peptides. *Mol Immunol* 39, 147-164.
- Grassilli, E., Benatti, F., Dansi, P., Giammarioli, A. M., Malorni, W., Franceschi, C. & Desiderio, M. A. 1998. Inhibition of proteasome function prevents thymocyte apoptosis: involvement of ornithine decarboxylase. *Biochem Biophys Res Commun* 250, 293-297.
- Gregory, R. C., Taniguchi, T. & D'Andrea, A. D. 2003. Regulation of the Fanconi anemia pathway by monoubiquitination. *Semin Cancer Biol* 13, 77-82.
- Groll, M., Ditzel, L., Lowe, J., Stock, D., Bochtler, M., Bartunik, H. D. & Huber, R. 1997. Structure of 20S proteasome from yeast at 2.4 Å resolution. *Nature* 386, 463-471.
- Groll, M., Heinemeyer, W., Jager, S., Ullrich, T., Bochtler, M., Wolf, D. H. & Huber, R. 1999. The catalytic sites of 20S proteasomes and their role in subunit maturation: a mutational and crystallographic study. *Proc Natl Acad Sci U S A* 96, 10976-10983.
- Groll, M., Koguchi, Y., Huber, R. & Kohno, J. 2001. Crystal structure of the 20 S proteasome:TMC-95A complex: a non-covalent proteasome inhibitor. *J Mol Biol* 311, 543-548.
- Gross, A., McDonnell, J. M. & Korsmeyer, S. J. 1999. BCL-2 family members and the mitochondria in apoptosis. *Genes Dev* 13, 1899-1911.
- Grover, P., Rekhadevi, P. V., Danadevi, K., Vuyyuri, S. B., Mahboob, M. & Rahman, M. F. 2010. Genotoxicity evaluation in workers occupationally exposed to lead. *Int J Hyg Environ Health* 213, 99-106.

- Guo, G. G., Gu, M. & Etlinger, J. D. 1994. 240-kDa proteasome inhibitor (CF-2) is identical to delta-aminolevulinic acid dehydratase. *J Biol Chem* 269, 12399-12402.
- Gupta, S. K., Singh, S. P. & Shukla, V. K. 2005. Copper, zinc, and Cu/Zn ratio in carcinoma of the gallbladder. *J Surg Oncol* 91, 204-208.
- Guzzi, G. & La Porta, C. A. 2008. Molecular mechanisms triggered by mercury. *Toxicology* 244, 1-12.
- Habib, F. K., Dembinski, T. C. & Stitch, S. R. 1980. The zinc and copper content of blood leucocytes and plasma from patients with benign and malignant prostates. *Clin Chim Acta* 104, 329-335.
- Hall, M. D., Failes, T. W., Yamamoto, N. & Hambley, T. W. 2007. Bioreductive activation and drug chaperoning in cobalt pharmaceuticals. *Dalton Trans* 3983-3990.
- Halling-Brown, M. D., Bulusu, K. C., Patel, M., Tym, J. E. & Al-Lazikani, B. 2012. canSAR: an integrated cancer public translational research and drug discovery resource. *Nucleic Acids Res* 40, D947-956.
- Hamazaki, J., Iemura, S., Natsume, T., Yashiroda, H., Tanaka, K. & Murata, S. 2006. A novel proteasome interacting protein recruits the deubiquitinating enzyme UCH37 to 26S proteasomes. *EMBO J* 25, 4524-4536.
- Hanahan, D. & Weinberg, R. A. 2000. The hallmarks of cancer. *Cell* 100, 57-70.
- Hanahan, D. & Weinberg, R. A. 2011. Hallmarks of cancer: the next generation. *Cell* 144, 646-674.
- Harrap, K. R. 1985. Preclinical studies identifying carboplatin as a viable cisplatin alternative. *Cancer Treat Rev* 12 Suppl A, 21-33.

- Hartertinger, C. G., Jakupiec, M. A., Zorbas-Seifried, S., Groessl, M., Egger, A., Berger, W., Zorbas, H., Dyson, P. J. & Keppler, B. K. 2008. KP1019, a new redox-active anticancer agent--preclinical development and results of a clinical phase I study in tumor patients. *Chem Biodivers* 5, 2140-2155.
- Hartmann-Petersen, R., Tanaka, K. & Hendil, K. B. 2001. Quaternary structure of the ATPase complex of human 26S proteasomes determined by chemical cross-linking. *Arch Biochem Biophys* 386, 89-94.
- Hashemi, M., Ghavami, S., Eshraghi, M., Booy, E. P. & Los, M. 2007. Cytotoxic effects of intra and extracellular zinc chelation on human breast cancer cells. *Eur J Pharmacol* 557, 9-19.
- He, H., Qi, X. M., Grossmann, J. & Distelhorst, C. W. 1998. c-Fos degradation by the proteasome. An early, Bcl-2-regulated step in apoptosis. *J Biol Chem* 273, 25015-25019.
- Hernberg, S., Nikkanen, J., Mellin, G. & Lilius, H. 1970. Delta-aminolevulinic acid dehydrase as a measure of lead exposure. *Arch Environ Health* 21, 140-145.
- Hershko, A., Ciechanover, A., Heller, H., Haas, A. L. & Rose, I. A. 1980. Proposed role of ATP in protein breakdown: conjugation of protein with multiple chains of the polypeptide of ATP-dependent proteolysis. *Proc Natl Acad Sci U S A* 77, 1783-1786.
- Hideshima, T., Ikeda, H., Chauhan, D., Okawa, Y., Raje, N., Podar, K., Mitsiades, C., Munshi, N. C., Richardson, P. G., Carrasco, R. D., et al. 2009. Bortezomib induces canonical nuclear factor-kappaB activation in multiple myeloma cells. *Blood* 114, 1046-1052.
- Hideshima, T., Richardson, P., Chauhan, D., Palombella, V. J., Elliott, P. J., Adams, J. & Anderson, K. C. 2001. The proteasome inhibitor PS-341 inhibits growth, induces apoptosis, and overcomes drug resistance in human multiple myeloma cells. *Cancer Res* 61, 3071-3076.

- Hindo, S. S., Frezza, M., Tomco, D., Heeg, M. J., Hryhorczuk, L., McGarvey, B. R., Dou, Q. P. & Verani, C. N. 2009. Metals in anticancer therapy: copper(II) complexes as inhibitors of the 20S proteasome. *Eur J Med Chem* 44, 4353-4361.
- Hirsch, C. & Ploegh, H. L. 2000. Intracellular targeting of the proteasome. *Trends Cell Biol* 10, 268-272.
- Hong, Y., Yang, J., Wu, W., Wang, W., Kong, X., Wang, Y., Yun, X., Zong, H., Wei, Y., Zhang, S., et al. 2008. Knockdown of BCL2L12 leads to cisplatin resistance in MDA-MB-231 breast cancer cells. *Biochim Biophys Acta* 1782, 649-657.
- Hoyt, M. A. & Coffino, P. 2004. Ubiquitin-free routes into the proteasome. *Cell Mol Life Sci* 61, 1596-1600.
- Hoyt, M. A., Zhang, M. & Coffino, P. 2003. Ubiquitin-independent mechanisms of mouse ornithine decarboxylase degradation are conserved between mammalian and fungal cells. *J Biol Chem* 278, 12135-12143.
- Hu, G. F. 1998. Copper stimulates proliferation of human endothelial cells under culture. *J Cell Biochem* 69, 326-335.
- Huang, Y. L., Sheu, J. Y. & Lin, T. H. 1999. Association between oxidative stress and changes of trace elements in patients with breast cancer. *Clin Biochem* 32, 131-136.
- Isasa, M., Katz, E. J., Kim, W., Yugo, V., Gonzalez, S., Kirkpatrick, D. S., Thomson, T. M., Finley, D., Gygi, S. P. & Crosas, B. 2010. Monoubiquitination of RPN10 regulates substrate recruitment to the proteasome. *Mol Cell* 38, 733-745.
- Ivanov, V. N. & Nikolic-Zugic, J. 1998. Biochemical and kinetic characterization of the glucocorticoid-induced apoptosis of immature CD4+CD8+ thymocytes. *Int Immunol* 10, 1807-1817.

- Iwafune, Y., Kawasaki, H. & Hirano, H. 2002. Electrophoretic analysis of phosphorylation of the yeast 20S proteasome. *Electrophoresis* 23, 329-338.
- Jaffe, E. K., Martins, J., Li, J., Kervinen, J. & Dunbrack, R. L., Jr. 2001. The molecular mechanism of lead inhibition of human porphobilinogen synthase. *J Biol Chem* 276, 1531-1537.
- Jaffe, E. K. & Stith, L. 2007. ALAD porphyria is a conformational disease. *Am J Hum Genet* 80, 329-337.
- Jakupec, M. A., Arion, V. B., Kapitza, S., Reisner, E., Eichinger, A., Pongratz, M., Marian, B., Graf von Keyserlingk, N. & Keppler, B. K. 2005. KP1019 (FFC14A) from bench to bedside: preclinical and early clinical development--an overview. *Int J Clin Pharmacol Ther* 43, 595-596.
- Jakupec, M. A. & Keppler, B. K. 2004. Gallium and other main group metal compounds as antitumor agents. *Met Ions Biol Syst* 42, 425-462.
- Jariel-Encontre, I., Bossis, G. & Piechaczyk, M. 2008. Ubiquitin-independent degradation of proteins by the proteasome. *Biochim Biophys Acta* 1786, 153-177.
- Jeffery, E. H. 1995. Biochemical Mechanisms of Aluminum Toxicity. In *Handbook of Experimental Pharmacology*, pp 139-161.
- Jiang, H., Taggart, J. E., Zhang, X., Benbrook, D. M., Lind, S. E. & Ding, W. Q. 2011. Nitroxoline (8-hydroxy-5-nitroquinoline) is more a potent anti-cancer agent than clioquinol (5-chloro-7-iodo-8-quinoline). *Cancer Lett* 312, 11-17.
- Johansson, B. 1992. A review of the pharmacokinetics and pharmacodynamics of disulfiram and its metabolites. *Acta Psychiatr Scand Suppl* 369, 15-26.

- Johnson, D. E., Gastman, B. R., Wieckowski, E., Wang, G. Q., Amoscato, A., Delach, S. M. & Rabinowich, H. 2000. Inhibitor of apoptosis protein hILP undergoes caspase-mediated cleavage during T lymphocyte apoptosis. *Cancer Res* 60, 1818-1823.
- Johnson, E. S. 2002. Ubiquitin branches out. *Nat Cell Biol* 4, E295-298.
- Kane, R. C., Bross, P. F., Farrell, A. T. & Pazdur, R. 2003. Velcade: U.S. FDA approval for the treatment of multiple myeloma progressing on prior therapy. *Oncologist* 8, 508-513.
- Kelada, S. N., Shelton, E., Kaufmann, R. B. & Khoury, M. J. 2001. Delta-aminolevulinic acid dehydratase genotype and lead toxicity: a HuGE review. *Am J Epidemiol* 154, 1-13.
- Kikuchi, J., Iwafune, Y., Akiyama, T., Okayama, A., Nakamura, H., Arakawa, N., Kimura, Y. & Hirano, H. 2010. Co- and post-translational modifications of the 26S proteasome in yeast. *Proteomics* 10, 2769-2779.
- Kimura, Y., Takaoka, M., Tanaka, S., Sassa, H., Tanaka, K., Plevoda, B., Sherman, F. & Hirano, H. 2000. N(alpha)-acetylation and proteolytic activity of the yeast 20 S proteasome. *J Biol Chem* 275, 4635-4639.
- Koguchi, Y., Kohno, J., Nishio, M., Takahashi, K., Okuda, T., Ohnuki, T. & Komatsubara, S. 2000. TMC-95A, B, C, and D, novel proteasome inhibitors produced by *Apiospora montagnei* Sacc. TC 1093. Taxonomy, production, isolation, and biological activities. *J Antibiot (Tokyo)* 53, 105-109.
- Kona, F. R., Buac, D. & Burger, A. M. 2011. Disulfiram, and disulfiram derivatives as novel potential anticancer drugs targeting the ubiquitin-proteasome system in both preclinical and clinical studies. *Curr Cancer Drug Targets* 11, 338-346.

- Krogan, N. J., Lam, M. H., Fillingham, J., Keogh, M. C., Gebbia, M., Li, J., Datta, N., Cagney, G., Buratowski, S., Emili, A., et al. 2004. Proteasome involvement in the repair of DNA double-strand breaks. *Mol Cell* 16, 1027-1034.
- Kukreja, A., Hutchinson, A., Mazumder, A., Vesole, D., Angitapalli, R., Jagannath, S., O'Connor O, A. & Dhodapkar, M. V. 2007. Bortezomib disrupts tumour-dendritic cell interactions in myeloma and lymphoma: therapeutic implications. *Br J Haematol* 136, 106-110.
- Kumatori, A., Tanaka, K., Inamura, N., Sone, S., Ogura, T., Matsumoto, T., Tachikawa, T., Shin, S. & Ichihara, A. 1990. Abnormally high expression of proteasomes in human leukemic cells. *Proc Natl Acad Sci U S A* 87, 7071-7075.
- Kuo, H. W., Chen, S. F., Wu, C. C., Chen, D. R. & Lee, J. H. 2002. Serum and tissue trace elements in patients with breast cancer in Taiwan. *Biol Trace Elem Res* 89, 1-11.
- Laine, A., Topisirovic, I., Zhai, D., Reed, J. C., Borden, K. L. & Ronai, Z. 2006. Regulation of p53 localization and activity by Ubc13. *Mol Cell Biol* 26, 8901-8913.
- Larregle, E. V. & Ferranola, M. L. 2010. Molecular Mechanisms of Cadmium Toxicity in Mammals. In *Metals in Biological Systems*, pp 163-185. Ed MS Gimenez.
- LeBlanc, R., Catley, L. P., Hideshima, T., Lentzsch, S., Mitsiades, C. S., Mitsiades, N., Neuberg, D., Goloubeva, O., Pien, C. S., Adams, J., et al. 2002. Proteasome inhibitor PS-341 inhibits human myeloma cell growth in vivo and prolongs survival in a murine model. *Cancer Res* 62, 4996-5000.
- Lee, D. H. & Goldberg, A. L. 1996. Selective inhibitors of the proteasome-dependent and vacuolar pathways of protein degradation in *Saccharomyces cerevisiae*. *J Biol Chem* 271, 27280-27284.

- Lee, K., Briehl, M. M., Mazar, A. P., Batinic-Haberle, I., Reboucas, J. S., Glinsmann-Gibson, B., Rimsza, L. M. & Tome, M. E. 2013. The copper chelator ATN-224 induces peroxynitrite-dependent cell death in hematological malignancies. *Free Radic Biol Med* 60, 157-167.
- Lemire, J. & Appanna, V. D. 2011. Aluminum toxicity and astrocyte dysfunction: a metabolic link to neurological disorders. *J Inorg Biochem* 105, 1513-1517.
- Levkau, B., Garton, K. J., Ferri, N., Kloke, K., Nofer, J. R., Baba, H. A., Raines, E. W. & Breithardt, G. 2001. xIAP induces cell-cycle arrest and activates nuclear factor-kappaB : new survival pathways disabled by caspase-mediated cleavage during apoptosis of human endothelial cells. *Circ Res* 88, 282-290.
- Li, B. & Dou, Q. P. 2000. Bax degradation by the ubiquitin/proteasome-dependent pathway: involvement in tumor survival and progression. *Proc Natl Acad Sci U S A* 97, 3850-3855.
- Li, L., Yang, H., Chen, D., Cui, C. & Dou, Q. P. 2008. Disulfiram promotes the conversion of carcinogenic cadmium to a proteasome inhibitor with pro-apoptotic activity in human cancer cells. *Toxicol Appl Pharmacol* 229, 206-214.
- Li, M., Zhang, Y., Liu, Z., Bharadwaj, U., Wang, H., Wang, X., Zhang, S., Liuzzi, J. P., Chang, S. M., Cousins, R. J., et al. 2007. Aberrant expression of zinc transporter ZIP4 (SLC39A4) significantly contributes to human pancreatic cancer pathogenesis and progression. *Proc Natl Acad Sci U S A* 104, 18636-18641.
- Li, X. C., Gu, M. Z. & Etlinger, J. D. 1991. Isolation and characterization of a novel endogenous inhibitor of the proteasome. *Biochemistry* 30, 9709-9715.
- Li, X. S. & Etlinger, J. D. 1992. Ubiquitinated proteasome inhibitor is a component of the 26 S proteasome complex. *Biochemistry* 31, 11964-11967.

- Lim, H. S., Archer, C. T. & Kodadek, T. 2007a. Identification of a peptoid inhibitor of the proteasome 19S regulatory particle. *J Am Chem Soc* 129, 7750-7751.
- Lim, H. S., Cai, D., Archer, C. T. & Kodadek, T. 2007b. Periodate-triggered cross-linking reveals Sug2/Rpt4 as the molecular target of a peptoid inhibitor of the 19S proteasome regulatory particle. *J Am Chem Soc* 129, 12936-12937.
- Lim, H. W. & Sassa, S. 1993. The Porphyrins. . In *Clinical Photomedicine*, pp 241-267. Eds HW Lim & NA Scoter. New York, NY: Marcel Dekker, Inc.
- Lioni, M., Noma, K., Snyder, A., Klein-Szanto, A., Diehl, J. A., Rustgi, A. K., Herlyn, M. & Smalley, K. S. 2008. Bortezomib induces apoptosis in esophageal squamous cell carcinoma cells through activation of the p38 mitogen-activated protein kinase pathway. *Mol Cancer Ther* 7, 2866-2875.
- Liston, P., Fong, W. G. & Korneluk, R. G. 2003. The inhibitors of apoptosis: there is more to life than Bcl2. *Oncogene* 22, 8568-8580.
- Loda, M., Cukor, B., Tam, S. W., Lavin, P., Fiorentino, M., Draetta, G. F., Jessup, J. M. & Pagano, M. 1997. Increased proteasome-dependent degradation of the cyclin-dependent kinase inhibitor p27 in aggressive colorectal carcinomas. *Nat Med* 3, 231-234.
- Lopes, U. G., Erhardt, P., Yao, R. & Cooper, G. M. 1997. p53-dependent induction of apoptosis by proteasome inhibitors. *J Biol Chem* 272, 12893-12896.
- Lowe, J., Stock, D., Jap, B., Zwickl, P., Baumeister, W. & Huber, R. 1995. Crystal structure of the 20S proteasome from the archaeon *T. acidophilum* at 3.4 Å resolution. *Science* 268, 533-539.
- Lowndes, S. A. & Harris, A. L. 2005. The role of copper in tumour angiogenesis. *J Mammary Gland Biol Neoplasia* 10, 299-310.

- Ma, M. H., Yang, H. H., Parker, K., Manyak, S., Friedman, J. M., Altamirano, C., Wu, Z. Q., Borad, M. J., Frantzen, M., Roussos, E., et al. 2003. The proteasome inhibitor PS-341 markedly enhances sensitivity of multiple myeloma tumor cells to chemotherapeutic agents. *Clin Cancer Res* 9, 1136-1144.
- Makhov, P., Golovine, K., Uzzo, R. G., Rothman, J., Crispen, P. L., Shaw, T., Scoll, B. J. & Kolenko, V. M. 2008. Zinc chelation induces rapid depletion of the X-linked inhibitor of apoptosis and sensitizes prostate cancer cells to TRAIL-mediated apoptosis. *Cell Death Differ* 15, 1745-1751.
- Malaguarnera, L., Pilastro, M. R., DiMarco, R., Scifo, C., Renis, M., Mazzarino, M. C. & Messina, A. 2003. Cell death in human acute myelogenous leukemic cells induced by pyrrolidinedithiocarbamate. *Apoptosis* 8, 539-545.
- Manning, D. L., Robertson, J. F., Ellis, I. O., Elston, C. W., McClelland, R. A., Gee, J. M., Jones, R. J., Green, C. D., Cannon, P., Blamey, R. W., et al. 1994. Oestrogen-regulated genes in breast cancer: association of pLIV1 with lymph node involvement. *Eur J Cancer* 30A, 675-678.
- Mao, X., Li, X., Sprangers, R., Wang, X., Venugopal, A., Wood, T., Zhang, Y., Kuntz, D. A., Coe, E., Trudel, S., et al. 2009. Clioquinol inhibits the proteasome and displays preclinical activity in leukemia and myeloma. *Leukemia* 23, 585-590.
- Maret, W., Jacob, C., Vallee, B. L. & Fischer, E. H. 1999. Inhibitory sites in enzymes: zinc removal and reactivation by thionein. *Proc Natl Acad Sci U S A* 96, 1936-1940.
- Margalioth, E. J., Schenker, J. G. & Chevion, M. 1983. Copper and zinc levels in normal and malignant tissues. *Cancer* 52, 868-872.

- Marikovsky, M., Nevo, N., Vadai, E. & Harris-Cerruti, C. 2002. Cu/Zn superoxide dismutase plays a role in angiogenesis. *Int J Cancer* 97, 34-41.
- McAuslan, B. R. & Reilly, W. 1980. Endothelial cell phagokinesis in response to specific metal ions. *Exp Cell Res* 130, 147-157.
- Messori, L., Marcon, G. & Orioli, P. 2003. Gold(III) compounds as new family of anticancer drugs. *Bioinorg Chem Appl* 177-187.
- Meyer, R. E. 1989. Prospects for a rational pharmacotherapy of alcoholism. *J Clin Psychiatry* 50, 403-412.
- Michaelis, M., Fichtner, I., Behrens, D., Haider, W., Rothweiler, F., Mack, A., Cinatl, J., Doerr, H. W. & Cinatl, J., Jr. 2006. Anti-cancer effects of bortezomib against chemoresistant neuroblastoma cell lines in vitro and in vivo. *Int J Oncol* 28, 439-446.
- Milacic, V., Chen, D., Giovagnini, L., Diez, A., Fregona, D. & Dou, Q. P. 2008a. Pyrrolidine dithiocarbamate-zinc(II) and -copper(II) complexes induce apoptosis in tumor cells by inhibiting the proteasomal activity. *Toxicol Appl Pharmacol* 231, 24-33.
- Milacic, V., Chen, D., Ronconi, L., Landis-Piwowar, K. R., Fregona, D. & Dou, Q. P. 2006. A novel anticancer gold(III) dithiocarbamate compound inhibits the activity of a purified 20S proteasome and 26S proteasome in human breast cancer cell cultures and xenografts. *Cancer Res* 66, 10478-10486.
- Milacic, V., Fregona, D. & Dou, Q. P. 2008b. Gold complexes as prospective metal-based anticancer drugs. *Histol Histopathol* 23, 101-108.
- Mirabelli, C. K., Johnson, R. K., Hill, D. T., Faucette, L. F., Girard, G. R., Kuo, G. Y., Sung, C. M. & Crooke, S. T. 1986. Correlation of the in vitro cytotoxic and in vivo antitumor activities of gold(I) coordination complexes. *J Med Chem* 29, 218-223.

- Mitsiades, N., Mitsiades, C. S., Poulaki, V., Chauhan, D., Fanourakis, G., Gu, X., Bailey, C., Joseph, M., Libermann, T. A., Treon, S. P., et al. 2002. Molecular sequelae of proteasome inhibition in human multiple myeloma cells. *Proc Natl Acad Sci U S A* 99, 14374-14379.
- Molineaux, S. M. 2012. Molecular pathways: targeting proteasomal protein degradation in cancer. *Clin Cancer Res* 18, 15-20.
- Moreau, P., Richardson, P. G., Cavo, M., Orłowski, R. Z., San Miguel, J. F., Palumbo, A. & Harousseau, J. L. 2012. Proteasome inhibitors in multiple myeloma: 10 years later. *Blood* 120, 947-959.
- Moriguchi, M., Nakajima, T., Kimura, H., Watanabe, T., Takashima, H., Mitsumoto, Y., Katagishi, T., Okanoue, T. & Kagawa, K. 2002. The copper chelator trientine has an antiangiogenic effect against hepatocellular carcinoma, possibly through inhibition of interleukin-8 production. *Int J Cancer* 102, 445-452.
- Morizane, Y., Honda, R., Fukami, K. & Yasuda, H. 2005. X-linked inhibitor of apoptosis functions as ubiquitin ligase toward mature caspase-9 and cytosolic Smac/DIABLO. *J Biochem* 137, 125-132.
- Moulis, J. M. 2010. Cellular mechanisms of cadmium toxicity related to the homeostasis of essential metals. *Biometals* 23, 877-896.
- Mufti, A. R., Burstein, E., Csomos, R. A., Graf, P. C., Wilkinson, J. C., Dick, R. D., Challa, M., Son, J. K., Bratton, S. B., Su, G. L., et al. 2006. XIAP Is a copper binding protein deregulated in Wilson's disease and other copper toxicosis disorders. *Mol Cell* 21, 775-785.
- Murakami, K. & Etlinger, J. D. 1986. Endogenous inhibitor of nonlysosomal high molecular weight protease and calcium-dependent protease. *Proc Natl Acad Sci U S A* 83, 7588-7592.

- Murakami, M. & Hirano, T. 2008. Intracellular zinc homeostasis and zinc signaling. *Cancer Sci* 99, 1515-1522.
- Nakahashi, A., Miura, N., Monde, K. & Tsukamoto, S. 2009. Stereochemical studies of hexylitaconic acid, an inhibitor of p53-HDM2 interaction. *Bioorg Med Chem Lett* 19, 3027-3030.
- Nalepa, G., Rolfe, M. & Harper, J. W. 2006. Drug discovery in the ubiquitin-proteasome system. *Nat Rev Drug Discov* 5, 596-613.
- Nandi, D., Tahiliani, P., Kumar, A. & Chandu, D. 2006. The ubiquitin-proteasome system. *J Biosci* 31, 137-155.
- Nardon, C., Schmitt, S. M., Yang, H., Zuo, J., Fregona, D. & Dou, Q. P. 2014. Gold(III)-Dithiocarbamate Peptidomimetics in the Forefront of the Targeted Anticancer Therapy: Preclinical Studies against Human Breast Neoplasia. *PLoS One* 9, e84248.
- Nasulewicz, A., Mazur, A. & Opolski, A. 2004. Role of copper in tumour angiogenesis--clinical implications. *J Trace Elem Med Biol* 18, 1-8.
- Nawrocki, S. T., Bruns, C. J., Harbison, M. T., Bold, R. J., Gotsch, B. S., Abbruzzese, J. L., Elliott, P., Adams, J. & McConkey, D. J. 2002. Effects of the proteasome inhibitor PS-341 on apoptosis and angiogenesis in orthotopic human pancreatic tumor xenografts. *Mol Cancer Ther* 1, 1243-1253.
- Nayak, S. B., Bhat, V. R., Upadhyay, D. & Udupa, S. L. 2003. Copper and ceruloplasmin status in serum of prostate and colon cancer patients. *Indian J Physiol Pharmacol* 47, 108-110.
- Neelam, S., Kakhniashvili, D. G., Wilkens, S., Levene, S. D. & Goodman, S. R. 2011. Functional 20S proteasomes in mature human red blood cells. *Exp Biol Med (Maywood)* 236, 580-591.

- Neslund-Dudas, C., Mitra, B., Kandegedara, A., Chen, D., Schmitt, S., Shen, M., Cui, Q., Rybicki, B. A. & Dou, Q. P. 2012. Association of metals and proteasome activity in erythrocytes of prostate cancer patients and controls. *Biol Trace Elem Res* 149, 5-9.
- Neustadt, J. & Pieczenik, S. 2007. Heavy-metal toxicity—with emphasis on mercury. *Integr Med* 6, 26-32.
- Nguyen, T., Hamby, A. & Massa, S. M. 2005. Clioquinol down-regulates mutant huntingtin expression in vitro and mitigates pathology in a Huntington's disease mouse model. *Proc Natl Acad Sci U S A* 102, 11840-11845.
- Nickeleit, I., Zender, S., Sasse, F., Geffers, R., Brandes, G., Sorensen, I., Steinmetz, H., Kubicka, S., Carlomagno, T., Menche, D., et al. 2008. Argyrin a reveals a critical role for the tumor suppressor protein p27(kip1) in mediating antitumor activities in response to proteasome inhibition. *Cancer Cell* 14, 23-35.
- Nickell, S., Beck, F., Scheres, S. H., Korinek, A., Forster, F., Lasker, K., Mihalache, O., Sun, N., Nagy, I., Sali, A., et al. 2009. Insights into the molecular architecture of the 26S proteasome. *Proc Natl Acad Sci U S A* 106, 11943-11947.
- Nikiforov, M. A., Riblett, M., Tang, W. H., Gratchouck, V., Zhuang, D., Fernandez, Y., Verhaegen, M., Varambally, S., Chinnaiyan, A. M., Jakubowiak, A. J., et al. 2007. Tumor cell-selective regulation of NOXA by c-MYC in response to proteasome inhibition. *Proc Natl Acad Sci U S A* 104, 19488-19493.
- Oda, E., Ohki, R., Murasawa, H., Nemoto, J., Shibue, T., Yamashita, T., Tokino, T., Taniguchi, T. & Tanaka, N. 2000. Noxa, a BH3-only member of the Bcl-2 family and candidate mediator of p53-induced apoptosis. *Science* 288, 1053-1058.

- Omura, S., Matsuzaki, K., Fujimoto, T., Kosuge, K., Furuya, T., Fujita, S. & Nakagawa, A. 1991. Structure of lactacystin, a new microbial metabolite which induces differentiation of neuroblastoma cells. *J Antibiot (Tokyo)* 44, 117-118.
- Ooi, M. G., Hayden, P. J., Kotoula, V., McMillin, D. W., Charalambous, E., Daskalaki, E., Raje, N. S., Munshi, N. C., Chauhan, D., Hideshima, T., et al. 2009. Interactions of the Hdm2/p53 and proteasome pathways may enhance the antitumor activity of bortezomib. *Clin Cancer Res* 15, 7153-7160.
- Orlowski, R. Z. & Kuhn, D. J. 2008. Proteasome inhibitors in cancer therapy: lessons from the first decade. *Clin Cancer Res* 14, 1649-1657.
- Pan, Q., Klee, C. G., van Golen, K. L., Irani, J., Bottema, K. M., Bias, C., De Carvalho, M., Mesri, E. A., Robins, D. M., Dick, R. D., et al. 2002. Copper deficiency induced by tetrathiomolybdate suppresses tumor growth and angiogenesis. *Cancer Res* 62, 4854-4859.
- Paranjpe, A., Zhang, R., Ali-Osman, F., Bobustuc, G. C. & Srivenugopal, K. S. 2013. Disulfiram is a direct and potent inhibitor of human O6-methylguanine-DNA methyltransferase (MGMT) in brain tumor cells and mouse brain and markedly increases the alkylating DNA damage. *Carcinogenesis*.
- Pelletier, C., Prognon, P., Latrache, H., Villart, L. & Bourlioux, P. 1994. [Microbiological consequences of chelation of bivalent metal cations by nitroxoline]. *Pathol Biol (Paris)* 42, 406-411.
- Peters, J. M., Cejka, Z., Harris, J. R., Kleinschmidt, J. A. & Baumeister, W. 1993. Structural features of the 26 S proteasome complex. *J Mol Biol* 234, 932-937.

- Prasad, A. S., Beck, F. W., Doerr, T. D., Shamsa, F. H., Penny, H. S., Marks, S. C., Kaplan, J., Kucuk, O. & Mathog, R. H. 1998. Nutritional and zinc status of head and neck cancer patients: an interpretive review. *J Am Coll Nutr* 17, 409-418.
- Provinciali, M., Di Stefano, G. & Fabris, N. 1995. Dose-dependent opposite effect of zinc on apoptosis in mouse thymocytes. *Int J Immunopharmacol* 17, 735-744.
- Qin, J. Z., Ziffra, J., Stennett, L., Bodner, B., Bonish, B. K., Chaturvedi, V., Bennett, F., Pollock, P. M., Trent, J. M., Hendrix, M. J., et al. 2005. Proteasome inhibitors trigger NOXA-mediated apoptosis in melanoma and myeloma cells. *Cancer Res* 65, 6282-6293.
- Qiu, X. B., Ouyang, S. Y., Li, C. J., Miao, S., Wang, L. & Goldberg, A. L. 2006. hRpn13/ADRM1/GP110 is a novel proteasome subunit that binds the deubiquitinating enzyme, UCH37. *EMBO J* 25, 5742-5753.
- Radhakrishnan, S. K., Lee, C. S., Young, P., Beskow, A., Chan, J. Y. & Deshaies, R. J. 2010. Transcription factor Nrf1 mediates the proteasome recovery pathway after proteasome inhibition in mammalian cells. *Mol Cell* 38, 17-28.
- Rajaraman, P., Schwartz, B. S., Rothman, N., Yeager, M., Fine, H. A., Shapiro, W. R., Selker, R. G., Black, P. M. & Inskip, P. D. 2005. Delta-aminolevulinic acid dehydratase polymorphism and risk of brain tumors in adults. *Environ Health Perspect* 113, 1209-1211.
- Rajaraman, P., Stewart, P. A., Samet, J. M., Schwartz, B. S., Linet, M. S., Zahm, S. H., Rothman, N., Yeager, M., Fine, H. A., Black, P. M., et al. 2006. Lead, genetic susceptibility, and risk of adult brain tumors. *Cancer Epidemiol Biomarkers Prev* 15, 2514-2520.
- Regland, B., Lehmann, W., Abedini, I., Blennow, K., Jonsson, M., Karlsson, I., Sjogren, M., Wallin, A., Xilinas, M. & Gottfries, C. G. 2001. Treatment of Alzheimer's disease with clioquinol. *Dement Geriatr Cogn Disord* 12, 408-414.

- Reymond, J. C. 1950. [Fight against alcoholism; a new product: antabuse]. *J Prat Rev Gen Clin Ther* 64, 64-66.
- Ritchie, C. W., Bush, A. I., Mackinnon, A., Macfarlane, S., Mastwyk, M., MacGregor, L., Kiers, L., Cherny, R., Li, Q. X., Tammer, A., et al. 2003. Metal-protein attenuation with iodochlorhydroxyquin (clioquinol) targeting Abeta amyloid deposition and toxicity in Alzheimer disease: a pilot phase 2 clinical trial. *Arch Neurol* 60, 1685-1691.
- Ritchie, C. W., Bush, A. I. & Masters, C. L. 2004. Metal-protein attenuating compounds and Alzheimer's disease. *Expert Opin Investig Drugs* 13, 1585-1592.
- Rivett, A. J. 1998. Intracellular distribution of proteasomes. *Curr Opin Immunol* 10, 110-114.
- Rizk, S. L. & Sky-Peck, H. H. 1984. Comparison between concentrations of trace elements in normal and neoplastic human breast tissue. *Cancer Res* 44, 5390-5394.
- Rock, K. L., Gramm, C., Rothstein, L., Clark, K., Stein, R., Dick, L., Hwang, D. & Goldberg, A. L. 1994. Inhibitors of the proteasome block the degradation of most cell proteins and the generation of peptides presented on MHC class I molecules. *Cell* 78, 761-771.
- Ronconi, L. & Fregona, D. 2009. The Midas touch in cancer chemotherapy: from platinum- to gold-dithiocarbamate complexes. *Dalton Trans* 10670-10680.
- Ronconi, L., Marzano, C., Zanello, P., Corsini, M., Miolo, G., Macca, C., Trevisan, A. & Fregona, D. 2006. Gold(III) dithiocarbamate derivatives for the treatment of cancer: solution chemistry, DNA binding, and hemolytic properties. *J Med Chem* 49, 1648-1657.
- Rubin, D. M., Glickman, M. H., Larsen, C. N., Dhruvakumar, S. & Finley, D. 1998. Active site mutants in the six regulatory particle ATPases reveal multiple roles for ATP in the proteasome. *EMBO J* 17, 4909-4919.

- Rudnev, A. V., Foteeva, L. S., Kowol, C., Berger, R., Jakupec, M. A., Arion, V. B., Timerbaev, A. R. & Keppler, B. K. 2006. Preclinical characterization of anticancer gallium(III) complexes: solubility, stability, lipophilicity and binding to serum proteins. *J Inorg Biochem* 100, 1819-1826.
- Ruschak, A. M., Slassi, M., Kay, L. E. & Schimmer, A. D. 2011. Novel proteasome inhibitors to overcome bortezomib resistance. *J Natl Cancer Inst* 103, 1007-1017.
- Ryan, D. P., Appleman, L. J., Lynch, T., Supko, J. G., Fidas, P., Clark, J. W., Fishman, M., Zhu, A. X., Enzinger, P. C., Kashala, O., et al. 2006a. Phase I clinical trial of bortezomib in combination with gemcitabine in patients with advanced solid tumors. *Cancer* 107, 2482-2489.
- Ryan, D. P., O'Neil, B. H., Supko, J. G., Rocha Lima, C. M., Dees, E. C., Appleman, L. J., Clark, J., Fidas, P., Orłowski, R. Z., Kashala, O., et al. 2006b. A Phase I study of bortezomib plus irinotecan in patients with advanced solid tumors. *Cancer* 107, 2688-2697.
- Sadoul, K., Wang, J., Diagouraga, B. & Khochbin, S. 2011. The tale of protein lysine acetylation in the cytoplasm. *J Biomed Biotechnol* 2011, 970382.
- Salvesen, G. S. & Duckett, C. S. 2002. IAP proteins: blocking the road to death's door. *Nat Rev Mol Cell Biol* 3, 401-410.
- Sartore-Bianchi, A., Gasparri, F., Galvani, A., Nici, L., Darnowski, J. W., Barbone, D., Fennell, D. A., Gaudino, G., Porta, C. & Mutti, L. 2007. Bortezomib inhibits nuclear factor-kappaB dependent survival and has potent in vivo activity in mesothelioma. *Clin Cancer Res* 13, 5942-5951.
- Sasse, F., Steinmetz, H., Schupp, T., Petersen, F., Memmert, K., Hofmann, H., Heusser, C., Brinkmann, V., von Matt, P., Hofle, G., et al. 2002. Argyrins, immunosuppressive cyclic

- peptides from myxobacteria. I. Production, isolation, physico-chemical and biological properties. *J Antibiot (Tokyo)* 55, 543-551.
- Satoh, K., Sasajima, H., Nyomura, K. I., Yokosawa, H. & Sawada, H. 2001. Assembly of the 26S proteasome is regulated by phosphorylation of the p45/Rpt6 ATPase subunit. *Biochemistry* 40, 314-319.
- Sava, G., Pacor, S., Bergamo, A., Cocchietto, M., Mestroni, G. & Alessio, E. 1995. Effects of ruthenium complexes on experimental tumors: irrelevance of cytotoxicity for metastasis inhibition. *Chem Biol Interact* 95, 109-126.
- Sava, G., Pacor, S., Mestroni, G. & Alessio, E. 1992. Na[trans-RuCl₄(DMSO)Im], a metal complex of ruthenium with antimetastatic properties. *Clin Exp Metastasis* 10, 273-280.
- Schieber, C., Howitt, J., Putz, U., White, J. M., Parish, C. L., Donnelly, P. S. & Tan, S. S. 2011. Cellular up-regulation of Nedd4 family interacting protein 1 (Ndfip1) using low levels of bioactive cobalt complexes. *J Biol Chem* 286, 8555-8564.
- Schile, A. J., Garcia-Fernandez, M. & Steller, H. 2008. Regulation of apoptosis by XIAP ubiquitin-ligase activity. *Genes Dev* 22, 2256-2266.
- Schimmer, A. D. & Dalili, S. 2005. Targeting the IAP family of caspase inhibitors as an emerging therapeutic strategy. *Hematology Am Soc Hematol Educ Program* 215-219.
- Schimmer, A. D., Dalili, S., Batey, R. A. & Riedl, S. J. 2006. Targeting XIAP for the treatment of malignancy. *Cell Death Differ* 13, 179-188.
- Schreck, R., Meier, B., Mannel, D. N., Droge, W. & Baeuerle, P. A. 1992. Dithiocarbamates as potent inhibitors of nuclear factor kappa B activation in intact cells. *J Exp Med* 175, 1181-1194.

- Schwartz, A. E., Leddicotte, G. W., Fink, R. W. & Friedman, E. W. 1974. Trace elements in normal and malignant human breast tissue. *Surgery* 76, 325-329.
- Sekizawa, R., Ikeno, S., Nakamura, H., Naganawa, H., Matsui, S., Iinuma, H. & Takeuchi, T. 2002. Panepophenanthrin, from a mushroom strain, a novel inhibitor of the ubiquitin-activating enzyme. *J Nat Prod* 65, 1491-1493.
- Sen, C. K., Khanna, S., Venojarvi, M., Trikha, P., Ellison, E. C., Hunt, T. K. & Roy, S. 2002. Copper-induced vascular endothelial growth factor expression and wound healing. *Am J Physiol Heart Circ Physiol* 282, H1821-1827.
- Shah, S. A., Potter, M. W., McDade, T. P., Ricciardi, R., Perugini, R. A., Elliott, P. J., Adams, J. & Callery, M. P. 2001. 26S proteasome inhibition induces apoptosis and limits growth of human pancreatic cancer. *J Cell Biochem* 82, 110-122.
- Shaik, A. P., Khan, M. & Jamil, K. 2009. Phylogenetic analysis of ALAD and MGP genes related to lead toxicity. *Toxicol Ind Health* 25, 403-409.
- Shakya, R., Peng, F., Liu, J., Heeg, M. J. & Verani, C. N. 2006. Synthesis, structure, and anticancer activity of gallium(III) complexes with asymmetric tridentate ligands: growth inhibition and apoptosis induction of cisplatin-resistant neuroblastoma cells. *Inorg Chem* 45, 6263-6268.
- Shi, G., Chen, D., Zhai, G., Chen, M. S., Cui, Q. C., Zhou, Q., He, B., Dou, Q. P. & Jiang, G. 2009. The proteasome is a molecular target of environmental toxic organotins. *Environ Health Perspect* 117, 379-386.
- Shim, J. S., Matsui, Y., Bhat, S., Nacev, B. A., Xu, J., Bhang, H. E., Dhara, S., Han, K. C., Chong, C. R., Pomper, M. G., et al. 2010. Effect of nitroxoline on angiogenesis and growth of human bladder cancer. *J Natl Cancer Inst* 102, 1855-1873.

- Siegel, R. 2014. American Cancer Society Cancer Statistics, 2014. *CA Cancer Journal for Clinicians*.
- Smith, L., Lind, M. J., Drew, P. J. & Cawkwell, L. 2007. The putative roles of the ubiquitin/proteasome pathway in resistance to anticancer therapy. *Eur J Cancer* 43, 2330-2338.
- Souza, E. T., Castro, L. C., Castro, F. A., do Canto Visentin, L., Pinheiro, C. B., Pereira, M. D., de Paula Machado, S. & Scarpellini, M. 2009. Synthesis, characterization and biological activities of mononuclear Co(III) complexes as potential bioreductively activated prodrugs. *J Inorg Biochem* 103, 1355-1365.
- Speiser, S. & Etlinger, J. D. 1983. ATP stimulates proteolysis in reticulocyte extracts by repressing an endogenous protease inhibitor. *Proc Natl Acad Sci U S A* 80, 3577-3580.
- Srinivasula, S. M. & Ashwell, J. D. 2008. IAPs: what's in a name? *Mol Cell* 30, 123-135.
- Strauss, S. J., Higginbottom, K., Juliger, S., Maharaj, L., Allen, P., Schenkein, D., Lister, T. A. & Joel, S. P. 2007. The proteasome inhibitor bortezomib acts independently of p53 and induces cell death via apoptosis and mitotic catastrophe in B-cell lymphoma cell lines. *Cancer Res* 67, 2783-2790.
- Sunwoo, J. B., Chen, Z., Dong, G., Yeh, N., Crowl Bancroft, C., Sausville, E., Adams, J., Elliott, P. & Van Waes, C. 2001. Novel proteasome inhibitor PS-341 inhibits activation of nuclear factor-kappa B, cell survival, tumor growth, and angiogenesis in squamous cell carcinoma. *Clin Cancer Res* 7, 1419-1428.
- Tanaka, K., Kumatori, A., Ii, K. & Ichihara, A. 1989. Direct evidence for nuclear and cytoplasmic colocalization of proteasomes (multiprotease complexes) in liver. *J Cell Physiol* 139, 34-41.

- Taylor, K. M., Morgan, H. E., Smart, K., Zahari, N. M., Pumford, S., Ellis, I. O., Robertson, J. F. & Nicholson, R. I. 2007. The emerging role of the LIV-1 subfamily of zinc transporters in breast cancer. *Mol Med* 13, 396-406.
- Teicher, B. A., Ara, G., Herbst, R., Palombella, V. J. & Adams, J. 1999. The proteasome inhibitor PS-341 in cancer therapy. *Clin Cancer Res* 5, 2638-2645.
- Theophanides, T. & Anastassopoulou, J. 2002. Copper and carcinogenesis. *Crit Rev Oncol Hematol* 42, 57-64.
- Thompson, J., Jones, D. D. & Beasley, W. H. 1977. The effect of metal ions on the activity of delta-aminolevulinic acid dehydratase. *Br J Ind Med* 34, 32-36.
- Tomco, D., Schmitt, S., Heeg, M. J., Dou, Q. P. & Verani, C. N. 2014. Inhibition of the 26S proteasome as a possible mechanism for toxicity of heavy metal species. *J Inorg Biochem*.
- Tomco, D., Schmitt, S., Ksebati, B., Heeg, M. J., Dou, Q. P. & Verani, C. N. 2011. Effects of tethered ligands and of metal oxidation state on the interactions of cobalt complexes with the 26S proteasome. *J Inorg Biochem* 105, 1759-1766.
- Tomco, D., Xavier, F. R., Allard, M. M. & Verani, C. N. 2012. Probing chemical reduction in a cobalt(III) complex as a viable route for the inhibition of the 20S proteasome. *Inorg Chim Acta* 393, 269-275.
- Tsukamoto, I., Yoshinaga, T. & Sano, S. 1979. The role of zinc with special reference to the essential thiol groups in delta-aminolevulinic acid dehydratase of bovine liver. *Biochim Biophys Acta* 570, 167-178.
- Tsukamoto, S., Hirota, H., Imachi, M., Fujimuro, M., Onuki, H., Ohta, T. & Yokosawa, H. 2005. Himeic acid A: a new ubiquitin-activating enzyme inhibitor isolated from a marine-derived fungus, *Aspergillus* sp. *Bioorg Med Chem Lett* 15, 191-194.

- Tsukamoto, S., Takeuchi, T., Rotinsulu, H., Mangindaan, R. E., van Soest, R. W., Ukai, K., Kobayashi, H., Namikoshi, M., Ohta, T. & Yokosawa, H. 2008. Leucettamol A: a new inhibitor of Ubc13-Uev1A interaction isolated from a marine sponge, *Leucetta aff. microrhaphis*. *Bioorg Med Chem Lett* 18, 6319-6320.
- Tsukamoto, S., Yoshida, T., Hosono, H., Ohta, T. & Yokosawa, H. 2006. Hexylitaconic acid: a new inhibitor of p53-HDM2 interaction isolated from a marine-derived fungus, *Arthrinium* sp. *Bioorg Med Chem Lett* 16, 69-71.
- Turecky, L., Kalina, P., Uhlikova, E., Namerova, S. & Krizko, J. 1984. Serum ceruloplasmin and copper levels in patients with primary brain tumors. *Klin Wochenschr* 62, 187-189.
- Uhlen, M., Oksvold, P., Fagerberg, L., Lundberg, E., Jonasson, K., Forsberg, M., Zwahlen, M., Kampf, C., Wester, K., Hober, S., et al. 2010. Towards a knowledge-based Human Protein Atlas. *Nat Biotechnol* 28, 1248-1250.
- Vallari, R. C. & Pietruszko, R. 1982. Human aldehyde dehydrogenase: mechanism of inhibition of disulfiram. *Science* 216, 637-639.
- van Bommel, D. M., Boffetta, P., Liao, L. M., Berndt, S. I., Menashe, I., Yeager, M., Chanock, S., Karami, S., Zaridze, D., Matteev, V., et al. 2011. Comprehensive analysis of 5-aminolevulinic acid dehydrogenase (ALAD) variants and renal cell carcinoma risk among individuals exposed to lead. *PLoS One* 6, e20432.
- van Golen, K. L., Bao, L., Brewer, G. J., Pienta, K. J., Kamradt, J. M., Livant, D. L. & Merajver, S. D. 2002. Suppression of tumor recurrence and metastasis by a combination of the PHSCN sequence and the antiangiogenic compound tetrathiomolybdate in prostate carcinoma. *Neoplasia* 4, 373-379.
- Vassilev, L. T. 2007. MDM2 inhibitors for cancer therapy. *Trends Mol Med* 13, 23-31.

- Vassilev, L. T., Vu, B. T., Graves, B., Carvajal, D., Podlaski, F., Filipovic, Z., Kong, N., Kammlott, U., Lukacs, C., Klein, C., et al. 2004. In vivo activation of the p53 pathway by small-molecule antagonists of MDM2. *Science* 303, 844-848.
- Vaux, D. L. & Silke, J. 2005. IAPs, RINGs and ubiquitylation. *Nat Rev Mol Cell Biol* 6, 287-297.
- Verani, C. N. 2012. Metal complexes as inhibitors of the 26S proteasome in tumor cells. *J Inorg Biochem* 106, 59-67.
- Verma, R., Peters, N. R., D'Onofrio, M., Tochtrop, G. P., Sakamoto, K. M., Varadan, R., Zhang, M., Coffino, P., Fushman, D., Deshaies, R. J., et al. 2004. Ubistatins inhibit proteasome-dependent degradation by binding the ubiquitin chain. *Science* 306, 117-120.
- Westhoff, M. A., Zhou, S., Nonnenmacher, L., Karpel-Massler, G., Jennewein, C., Schneider, M., Halatsch, M. E., Carragher, N. O., Baumann, B., Krause, A., et al. 2013. Inhibition of NF-kappaB Signaling Ablates the Invasive Phenotype of Glioblastoma. *Mol Cancer Res* 11, 1611-1623.
- Williams, S., Pettaway, C., Song, R., Papandreou, C., Logothetis, C. & McConkey, D. J. 2003. Differential effects of the proteasome inhibitor bortezomib on apoptosis and angiogenesis in human prostate tumor xenografts. *Mol Cancer Ther* 2, 835-843.
- Wilson, R., Goyal, L., Ditzel, M., Zachariou, A., Baker, D. A., Agapite, J., Steller, H. & Meier, P. 2002. The DIAP1 RING finger mediates ubiquitination of Dronc and is indispensable for regulating apoptosis. *Nat Cell Biol* 4, 445-450.
- Wojcik, C. & DeMartino, G. N. 2003. Intracellular localization of proteasomes. *Int J Biochem Cell Biol* 35, 579-589.

- Wolfgang, M. & Jean-Marc, M. 2013. The Bioinorganic Chemistry of Cadmium in the Context of Its Toxicity,. In *Cadmium: From Toxicology to Essentiality Metal Ions in Life Sciences*, pp 1-30.
- Wong, E. & Giandomenico, C. M. 1999. Current status of platinum-based antitumor drugs. *Chem Rev* 99, 2451-2466.
- Xu, G. W., Ali, M., Wood, T. E., Wong, D., Maclean, N., Wang, X., Gronda, M., Skrtic, M., Li, X., Hurren, R., et al. 2010. The ubiquitin-activating enzyme E1 as a therapeutic target for the treatment of leukemia and multiple myeloma. *Blood* 115, 2251-2259.
- Yang, D. Y., Chen, Y. W., Gunn, J. M. & Belzile, N. 2008. Selenium and mercury in organisms: interactions and mechanisms. *Environ Res* 16, 71-92.
- Yang, H., Chen, D., Cui, Q. C., Yuan, X. & Dou, Q. P. 2006. Celastrol, a triterpene extracted from the Chinese "Thunder of God Vine," is a potent proteasome inhibitor and suppresses human prostate cancer growth in nude mice. *Cancer Res* 66, 4758-4765.
- Yang, H., Zonder, J. A. & Dou, Q. P. 2009. Clinical development of novel proteasome inhibitors for cancer treatment. *Expert Opin Investig Drugs* 18, 957-971.
- Yang, Y., Fang, S., Jensen, J. P., Weissman, A. M. & Ashwell, J. D. 2000. Ubiquitin protein ligase activity of IAPs and their degradation in proteasomes in response to apoptotic stimuli. *Science* 288, 874-877.
- Yang, Y., Kitagaki, J., Dai, R. M., Tsai, Y. C., Lorick, K. L., Ludwig, R. L., Pierre, S. A., Jensen, J. P., Davydov, I. V., Oberoi, P., et al. 2007. Inhibitors of ubiquitin-activating enzyme (E1), a new class of potential cancer therapeutics. *Cancer Res* 67, 9472-9481.
- Yang, Y. L. & Li, X. M. 2000. The IAP family: endogenous caspase inhibitors with multiple biological activities. *Cell Res* 10, 169-177.

- Yao, T., Song, L., Xu, W., DeMartino, G. N., Florens, L., Swanson, S. K., Washburn, M. P., Conaway, R. C., Conaway, J. W. & Cohen, R. E. 2006. Proteasome recruitment and activation of the Uch37 deubiquitinating enzyme by Adrm1. *Nat Cell Biol* 8, 994-1002.
- Yasuhiro, S. & Toshiyuki, K. 2012. Cellular Defense Mechanisms against Lead Toxicity in the Vascular System. *Biol Pharm Bull* 35, 1885-1891.
- Yoshii, J., Yoshiji, H., Kuriyama, S., Ikenaka, Y., Noguchi, R., Okuda, H., Tsujinoue, H., Nakatani, T., Kishida, H., Nakae, D., et al. 2001. The copper-chelating agent, trientine, suppresses tumor development and angiogenesis in the murine hepatocellular carcinoma cells. *Int J Cancer* 94, 768-773.
- Zhai, S., Yang, L., Cui, Q. C., Sun, Y., Dou, Q. P. & Yan, B. 2010. Tumor cellular proteasome inhibition and growth suppression by 8-hydroxyquinoline and clioquinol requires their capabilities to bind copper and transport copper into cells. *J Biol Inorg Chem* 15, 259-269.
- Zhang, F., Su, K., Yang, X., Bowe, D. B., Paterson, A. J. & Kudlow, J. E. 2003. O-GlcNAc modification is an endogenous inhibitor of the proteasome. *Cell* 115, 715-725.
- Zhang, X., Frezza, M., Milacic, V., Ronconi, L., Fan, Y., Bi, C., Fregona, D. & Dou, Q. P. 2010. Inhibition of tumor proteasome activity by gold-dithiocarbamate complexes via both redox-dependent and -independent processes. *J Cell Biochem* 109, 162-172.
- Zhang, Z., Bi, C., Buac, D., Fan, Y., Zhang, X., Zuo, J., Zhang, P., Zhang, N., Dong, L. & Dou, Q. P. 2013. Organic cadmium complexes as proteasome inhibitors and apoptosis inducers in human breast cancer cells. *J Inorg Biochem* 123, 1-10.
- Zhao, H. & Eide, D. 1996. The yeast ZRT1 gene encodes the zinc transporter protein of a high-affinity uptake system induced by zinc limitation. *Proc Natl Acad Sci U S A* 93, 2454-2458.

Zheng, J., Payne, K., Taggart, J. E., Jiang, H., Lind, S. E. & Ding, W. Q. 2012. Trolox enhances curcumin's cytotoxicity through induction of oxidative stress. *Cell Physiol Biochem* 29, 353-360.

ABSTRACT**MOLECULAR STUDIES ON METAL-BASED COMPLEXES: EFFECTS ON THE UBIQUITIN-PROTEASOME SYSTEM AND APOPTOTIC PATHWAY**

by

SARA M. SCHMITT

May 2014

Advisor: Q. Ping Dou, Ph.D.**Major:** Cancer Biology**Degree:** Doctor of Philosophy

The ubiquitin-proteasome pathway is crucial to normal cellular function, and as such, has been extensively investigated as a potential target for cancer therapeutics. Many compounds have been tested for their proteasome inhibitory ability, including various small peptide aldehydes, and, following the success of cisplatin, several metal-containing complexes. The efficacy of these compounds in preclinical studies ultimately resulted in the development and approval of the first-in-class proteasome inhibitor bortezomib, the use of which, unfortunately, has been hindered by toxicity and resistance. These limitations have led to a massive push toward designing and developing new, less toxic proteasome inhibitors for clinical use.

The discovery more than twenty years ago that the heme-synthesis enzyme δ -aminolevulinic acid dehydratase (ALAD) possesses proteasome inhibitory activity revealed another potential approach for targeting the UPP in cancer. However, this discovery predated the initial investigation into proteasome inhibition as a therapeutic strategy, so a surprising lack of research into the relationship between ALAD and the proteasome exists. Therefore, further investigation into this relationship is necessary.

Taken together, these observations validate the proteasome as a viable chemotherapeutic target. Additionally, novel agents that target not only the proteasomal core, but also other factors involved in the pathway, including E3s like XIAP which are also critical components of the apoptotic cascade, as well as potential endogenous inhibitors like ALAD. The data presented in this dissertation suggest a novel interaction between the 20S proteasomal core and ALAD, which results in proteasome inhibition and tumor cell growth suppression, suggesting that targeting this relationship is a promising approach for cancer treatment. Additionally, a series of new metal-based complexes with various metal centers, including cobalt, gold, gallium and the copper chelator nitroxoline were shown to be potent inhibitors of the proteasome in several cancer cell lines and tumor xenograft models. Furthermore, proteasome inhibition was also revealed as a secondary mechanism of cell death for mercury-containing species. Finally, zinc chelation was explored as a strategy for inducing apoptosis via degradation of the E3 ligase X-linked inhibitor of apoptosis (XIAP). Collectively, these data confirm the potential of the UPP as an anticancer target and substantiate several factors within the pathway as viable druggable targets.

PUBLICATIONS

- Frezza, M., Hindo, S., Chen, D., Davenport, A., **Schmitt, S.**, Tomco, D. & Dou, Q. P. 2010. Novel metals and metal complexes as platforms for cancer therapy. *Curr Pharm Des* 16, 1813-1825.
- Lu, L., Kanwar, J., **Schmitt, S.**, Cui, Q. C., Zhang, C., Zhao, C. & Dou, Q. P. 2011. Inhibition of tumor cellular proteasome activity by triptolide extracted from the Chinese medicinal plant 'thunder god vine'. *Anticancer Res* 31, 1-10.
- Chen, D., Frezza, M., **Schmitt, S.**, Kanwar, J. & Dou, Q. P. 2011. Bortezomib as the first proteasome inhibitor anticancer drug: current status and future perspectives. *Curr Cancer Drug Targets* 11, 239-253.
- Jackson, C. S., **Schmitt, S.**, Dou, Q. P. & Kodanko, J. J. 2011. Synthesis, Characterization and Reactivity of the Stable Iron Carbonyl Complex $[\text{Fe}(\text{CO})(\text{N4Py})](\text{ClO}_4)_2$: Photoactivated Carbon Monoxide Release, Growth Inhibitory Activity and Peptide Ligation. *Inorg Chem* 50, 5336-5338.
- Frezza, M., **Schmitt, S.** & Dou, Q. P. 2011. Targeting the Ubiquitin-Proteasome Pathway: An Emerging Concept in Cancer Therapy. *Curr Top Med Chem* 11, 2888-2905.
- Tomco, D., **Schmitt, S. M.**, Ksebati, B., Heeg, M. J., Dou, Q.P. & Verani, C. N. 2011. Effects of tethered ligands and of metal oxidation state on the interactions of cobalt complexes with the 26S proteasome. *J Inorg Biochem* 105, 1759-1766.
- Schmitt, S.**, Lu, L. & Dou, Q. P. 2011. Use of Proteasome Inhibitors in Anticancer Therapy. *Reviews in Healthcare* 2(4).
- Frezza, M., **Schmitt, S.**, Tomco, D., Chen, D., Verani, C. N.* & Dou, Q. P.* 2012. Inhibition of the 26S Proteasome Activity by Gallium(III) Complexes. *The Encyclopedia of*

Metalloproteins, edited by Professors Robert Kreitsinger, Eugene Permyakov and Vladimir Uversky and published by Springer.

Schmitt, S., Frezza, M. & Dou, Q. P. 2012. New applications of old metal-binding drugs in the treatment of human cancer. *Front Bioscience* 4, 375-391.

Prakash, J., **Schmitt, S.**, Dou, Q. P. & Kodanko, J. J. 2012. Inhibition of the purified 20S proteasome by non-heme iron complexes. *Metallomics* 4, 174-178.

Zuo, J.,* **Schmitt, S.M.**,* Zhang, Z., Prakash, J., Fan, Y., Bi, C., Kodanko, J. J. & Dou, Q. P. 2012. Novel polypyridyl chelators deplete cellular zinc and destabilize the X-linked inhibitor of apoptosis protein (XIAP) prior to induction of apoptosis in human prostate and breast cancer cells. *J Cell Biochem* 113, 2567-2575. *Equal Contribution.

Neslund-Dudas, C., Mitra, B., Kandegedara, A., Chen, D., **Schmitt, S.**, Shen, M., Cui, C., Rybicki, B. A. & Dou, Q. P. 2012. Association of Metals and Proteasome Activity in Erythrocytes of Prostate Cancer Patients and Controls. *Biol Trace Elem Res* 149, 5-9.

Buac, D., **Schmitt, S.**, Ventro, G., Kona, F. R. & Dou, Q. P. 2012. Dithiocarbamate-Based Coordination Compounds as Potent Proteasome Inhibitors in Human Cancer Cells. *Mini Rev Med Chem* 12, 1193-1201.

Zhang, Z., Bi, C., **Schmitt, S. M.**, Fan, Y., Dong, L., Zuo, J. & Dou, Q. P. 2012. 1, 10-Phenanthroline promotes copper complexes into tumor cells and induces apoptosis by inhibiting the proteasome activity. *J Biol Inorg Chem* 17, 1257-1267.

Buac, D., Shen, M., **Schmitt, S.**, Kona, F. R., Deshmukh, R., Zhang, Z., Neslund-Dudas, C., Mitra, B. & Dou, Q. P. 2012. From Bortezomib to Other Inhibitors of the Proteasome and Beyond. *Curr Pharm Des* 19, 4025-4038.

- Shen, M., **Schmitt, S.**, Buac, D. & Dou, Q. P. 2013. Targeting the ubiquitin-proteasome system for cancer therapy. *Expert Opin Ther Targets* 17, 1091-1108.
- Schmitt, S. M.** & Dou, Q. P. 2013. Editorial: Metal-Based Compounds as Proteasome-Inhibitory Anti-Cancer Drugs. *J Pharmacovigilance* 1(1).
- Nardon, C., **Schmitt, S. M.**, Yang, H., Zuo, J., Fregona, D. & Dou, Q. P. 2014. The cutting-edge Au(III)-peptidomimetics may revolutionize the anticancer therapy: preclinical studies against human breast neoplasia. *PLoS One* 9, e84248.
- Tomco, D., **Schmitt, S. M.**, Heeg, M. J., Dou, Q. P. & Verani, C. N. 2014. Inhibition of the 26S Proteasome as a Possible Mechanism for Toxicity of Heavy Metal Species. *J Inorg Biochem* 132, 96-103.
- Deshmukh, R. R., **Schmitt, S. M.**, Hwang, C. & Dou, Q. P. 2014. Chemotherapeutic inhibitors in the treatment of prostate cancer. *Expert Opin Pharmacother* 15, 11-22.
- Schmitt, S. M.**, Deshmukh, R. R. & Dou, Q. P. 2014. The ubiquitin proteasome pathway as a chemotherapeutic target. Resistance to Proteasome Inhibitors in Cancer, edited by Q. Ping Dou.

AUTOBIOGRAPHICAL STATEMENT

SARA M. SCHMITT

Sara was born in Neenah, WI and grew up in Beaver Dam, WI. Sara graduated from Beaver Dam High School, where she participated in cross country and marching band, in 2004. She received her Bachelor of Arts degree from Ripon College with a double major in Chemistry-Biology and German in 2008. At Ripon, Sara ran cross country and played in the band, as well as tutoring students and working as an EMT. Sara also spent a semester abroad at the University of Bonn, Germany, where she also worked for an ambulance service. She joined the Graduate Program in Cancer Biology at the Wayne State University School of Medicine in fall 2009 and began her dissertation work in the lab of Q. Ping Dou, Ph.D. in spring 2010. Sara participated in many projects within the lab, including studying the effects of metal-based complexes on the tumor proteasome as well as clarifying the relationship between the proteasome and its reported endogenous inhibitor, ALAD.